Finance and Economics Discussion Series

Federal Reserve Board, Washington, D.C.
ISSN 1936-2854 (Print)
ISSN 2767-3898 (Online)

United States of U-Star

Hie Joo Ahn and Jeremy Rudd

2026-060

Please cite this paper as:
Ahn, Hie Joo, and Jeremy Rudd (2026). "United States of U-Star," Finance and Economics Discussion Series 2026-060. Washington: Board of Governors of the Federal Reserve System, https://doi.org/10.17016/FEDS.2026.060.

United States of U-Star*

Hie Joo Ahn† Jeremy B. Rudd‡

Federal Reserve Board Federal Reserve Board

July 25, 2026

Abstract

This paper estimates state-level trend unemployment rates (trend U-star) based on the trend components of unemployment inflows and outflows across unemployment durations. The estimated trend U-stars, particularly the portions attributable to long-term unemployment, have levels and dynamics that vary substantially across states. Long-term unemployment makes a relatively small contribution to trend U-star in agricultural states, but takes a larger share for Rust Belt states and several states in the Sun Belt. While higher educational attainment and population aging put downward pressure on U-star, the effects of industrial structure and labor-market rigidities are mixed. Using the estimates of state-level trend U-star, we revisit previous work on state-level Phillips curves and find that the estimated slopes of forward-looking inflation equations are driven by movements in trend U-star rather than by cyclical variation in the unemployment rate.

JEL classification: C41, C53, E24, E27, E32, J21

Keywords: trend unemployment rate, natural rate of unemployment, unemployment duration, duration dependence, trend-cycle decomposition, nonlinear state space model, extended Kalman filter, Nelson–Siegel model, new-Keynesian Phillips curve.

---

*All errors are our own. The views expressed herein are those of the authors, and do not reflect the views of the Federal Reserve Board or any person associated with the Federal Reserve System.

†Federal Reserve Board of Governors, 20th Street and Constitution Avenue NW, Washington, DC 20551, U.S.A. Email: hiejoo.ahn@frb.gov

‡Federal Reserve Board of Governors, 20th Street and Constitution Avenue NW, Washington, DC 20551, U.S.A. Email: jeremy.rudd@frb.gov

1 Introduction

A growing body of research exploits regional heterogeneity to understand the cyclical dynamics of the macroeconomy and the effectiveness of macroeconomic policy.[1] In order to do so correctly, however, it is important to account for structural differences across regional economies. One key structural difference is labor-market functioning, as captured by a region-specific natural rate of unemployment. But despite its importance, this feature of regional heterogeneity is not well understood. This paper estimates the natural rate of unemployment for U.S. states (the "NRU" or "U-star," henceforth). We explore the determinants of the natural rate and demonstrate that the presence of regional heterogeneity carries significant implications for empirical Phillips curves fit to state-level data.

We associate the U-star with the noncyclical component of the unemployment rate, as measured using a trend-cycle decomposition. As is well known, identifying and estimating the NRU at the aggregate level became increasingly challenging from the 1990s on because the link between inflation and labor-market slack weakened dramatically (a phenomenon often referred to as the flattening—or even the "death –of the Phillips curve). In response, researchers began using the noncyclical or "trend" components of unemployment stocks or flows to recover estimates of the NRU.[2]

In related work, Ahn (2023) further decomposes unemployment outflows by the duration of unemployment and uses these variables' trend components, along with low-frequency changes in unemployment inflows, to estimate the NRU. By exploiting information from changes in the unemployment–duration distribution, Ahn's approach decomposes the NRU into short-term and long-term components, which can be interpreted as frictional and structural unemployment, respectively. In this paper, we estimate Ahn's model using unemployment levels and distributions across all 50 states and the District of Columbia in order to recover an NRU, which we refer to as *trend U-star*. By combining microdata from the Local Area Unemployment Statistics (LAUS) and

[1] For examples, see Nakamura and Steinsson (2014); Hazell, Herreño, Nakamura and Steinsson (2020); and Jo and Zubairy (2025).

[2] For examples, see Tasci (2012); Barnichon and Mesters (2018); Crump, Eusepi, Giannoni and Şahin (2019); and Hornstein and Kudlyak (2019). An alternative approach is to employ a structural model, such as a DSGE or new-Keynesian framework (see, for example, Crump, Eusepi, Giannoni and Şahin, 2024; and Hall and Kudlyak, 2023).

the Current Population Survey (CPS), our approach produces *state-level trend U-star* estimates that consistently aggregate to a national trend U-star estimate.

These state-level U-star estimates deepen our understanding of both local labor-market conditions and the cyclical position of the aggregate economy. The state-level estimates reflect regional heterogeneity in low-frequency movements in labor-market flows and in the distributions of unemployment durations. This regional heterogeneity provides additional information about labor-market functioning that helps us infer the aggregate NRU, which can be difficult to identify using aggregate data alone and especially when the NRU is time-varying. In addition, using a large number of states sharpens inference and helps make the NRU estimates more robust, given that idiosyncratic variation, including measurement errors, can wash out to some degree in the aggregate.[3] Rich regional information embedded in the disaggregated estimates also helps evaluate the role of structural factors—such as demographics, migration, and changes in industrial structure—in determining the natural rate. Finally, the regional estimates can uncover pockets of economic slack that are not apparent in the national-level data, which permits national and place-based stabilization policies to be coordinated.

The state-level estimates reveal substantial cross-state variation in trend U-star. Over the period 1978:Q1–2025:Q1, average levels of trend U-star range from 3.3 percent in Nebraska and South Dakota to 7.5 percent in Alaska, with agricultural states in the Midwest disproportionately represented in the bottom quartile and states in the Rust Belt and Sun Belt in the top quartile. In addition, the state-level estimates exhibit significant heterogeneity in their contours. For example, unemployment inflows in Nebraska and Nevada remain relatively flat over the sample period, while those in many other states exhibit downward trends. Although a number of states experience increases in the portion of trend U-star that reflects long-term unemployment (defined as unemployment durations that are longer than 6 months), others—such as Iowa and North Dakota—exhibit little discernible change in their long-term components. As a result, in many states declining unemployment inflows and rising long-term components partially offset each other, producing net downward trajectories with varying slopes.

These findings suggest that the secular decline seen in trend U-star at the national level is not uniform across states. Approximately twenty states show more pronounced reductions,

[3] See chapter 1 of Forni and Lippi (1997) for a related example.

while twenty-five states exhibit a slower pace of decline. In four states, trend U-star does not change or even rises. In addition, structural forces commonly associated with reductions in the NRU—such as declining labor-market dynamism, population aging, and rising educational attainment——have not been felt uniformly across regions. That said, cross-state dispersion in trend U-star has narrowed over time, largely because the components attributable to short-term unemployment spells have converged across states.

The duration composition of trend U-star also varies substantially across states, with the long-term share ranging from about 10 percent in Wyoming to roughly 25 percent in the District of Columbia. This heterogeneity indicates that the relative contributions of frictional and structural unemployment to U-star differ markedly across states. For example, the U-stars for Rust Belt states tend to reflect a relatively larger share of longer-term (structural) unemployment, suggesting the presence of hysteresis effects in which job losers remain unemployed for extended periods, become increasingly detached from the labor market, and face reduced reemployment prospects. By contrast, agricultural states generally display lower shares of structural unemployment in their trend U-star estimates, reflecting the relatively high worker churn that is associated with the nature of production in the agricultural sector.

We use the state-level estimates to examine how demographics, industry mix, labor-market institutions, and other economic fundamentals shape cross-state variation in trend U-star. Educational composition matters, with higher average educational attainment associated with a net decline in trend U-star. Population aging also reduces trend U-star, as younger workers are associated with higher frictional unemployment. However, we find little evidence that either the share of women in employment or a state's industry structure matter for trend U-star. Likewise, labor-market rigidities and institutional factors such as unionization, tax burdens, and downward nominal wage rigidity have mixed effects on trend U-star, as do stronger fundamentals (in the form of higher labor force participation and labor productivity).

Finally, we use our estimates of U-star to revisit the results of well-cited studies of the Phillips curve that use state-level data (e.g., McLeay and Tenreyro, 2020; Hazell et al., 2020; and Fitzgerald, Jones, Kulish and Nicolini, 2020).[4] In these studies, time and state fixed effects are included in the

[4]The main specification of Fitzgerald et al. (2020) uses MSA-level data, but these authors also consider state-level specifications as robustness checks.

empirical model to recover the slope of the Phillips curve under two maintained assumptions: first, that the state-level natural rate is either constant (and so captured by state fixed effects) or varies over time but is perfectly correlated with the aggregate trend (and so captured by time fixed effects that can also control for changes in monetary policy regimes and inflation expectations); and second, that aggregate demand shocks are uncorrelated with the NRU. Our state-level trend U-star estimates indicate that these assumptions are not empirically supported, which biases previous estimates of the Phillips curve's slope obtained using state-level data.

In particular, Hazell et al. (2020) find a small but statistically significant Phillips curve slope based on a new-Keynesian specification where the slope is the coefficient on a discounted forward sum of future unemployment rates. Under their assumptions regarding state-level natural rates, the forward sum of the unemployment rate can be interpreted as the forward sum of the unemployment gap. However, our finding of substantial regional heterogeneity in the time paths of U-star calls their assumptions into question. Moreover, because the unemployment-rate gap is mean-zero and stationary, the forward sum of the unemployment *rate* will essentially be a forward sum of the natural rate, implying that the statistically significant association that they find between the forward sum of unemployment and inflation is instead a relationship between inflation and the natural rate. Taken together, these considerations suggest that Hazell et al.'s model is likely to be misspecified, and when we repeat their estimation procedure using state-specific unemployment gaps, we no longer obtain a statistically significant Phillips curve slope.

Hazell et al. (2020) also consider a specification that uses the lagged unemployment rate in place of the discounted forward sum. We find that the estimated coefficient on the lagged unemployment rate increases in magnitude and remains statistically significant once state-level trend U-star is taken into account. This result suggests that controlling for idiosyncratic variation in state-level U-star values permits better identification of the margin of labor-market slack that is relevant for inflation, and also suggests that a traditional Phillips curve specification does a better job than the new-Keynesian Phillips curve in characterizing inflation dynamics.

Importantly, our paper contributes to the literature on the natural rate of unemployment and unemployment dynamics. As inflation lost power to identify the natural rate, economists have paid greater attention to the trend unemployment rate as a proxy for the natural rate (see for example, (including Fleischman and Roberts, 2011; Tasci, 2012; Barnichon and Mesters, 2018; Crump et al., 2019; Ahn and Rudd, 2024; Hornstein and Kudlyak, 2026)).[5] Our paper is related to this approach, but distinguishes itself from the previous literature in three ways. First, we estimate state-level trend unemployment rate, and aggregate them up to recover the aggregate natural rate, which none of the previous studies attempted to do so. Second, the paper makes a methodological contribution by integrating nonlinear state-space estimation, duration-structure accounting, and Bayesian trend–cycle decomposition into a unified framework for measuring regional trend unemployment. For this, the model allows unemployment exit probabilities to vary with unemployment duration—an important extension relative to the previous literature, which decomposes the natural rate by the duration of unemployment. Third, our paper connects to research on heterogeneity in cyclical labor-market dynamics (such as Blanchard and Katz, 1992; Aaronson, Daly, Wascher and Wilcox, 2019; Cajner, Coglianese and Montes, 2025) by examining regional differences in labor-market functioning.

In the following section, we discuss how we construct our dataset. Section 3 introduces the duration-structure model and describes our estimation procedure, and Section 4 reports estimation results for the model parameters across states. Section 5 presents a decomposition of changes in trend unemployment rates and discusses regional patterns and their implications for aggregate U-star, and Section 6 explores implications for the Phillips curve. Section 7 concludes.

2 Data

For each U.S. state and the District of Columbia, we use CPS microdata to construct the number of individuals unemployed for 1 month (less than 5 weeks), 2–3 months (5–14 weeks), 4–6 months (15–26 weeks), 7–12 months (27–52 weeks), and 13 months or more (53 weeks and

[5] Tasci (2012) established a foundational framework based on an unobserved component model for analyzing long-term labor market dynamics by decomposing the aggregate unemployment rate into underlying job-finding (outflow) and job-separation (inflow) rates. Barnichon and Mesters (2018) utilized a dynamic factor model for the flows data to capture heterogeneous group-specific cyclical responses, overcoming the restrictive assumptions of standard shift-share models. Crump et al. (2019) consider both the flows-based statistical approach inspired by the two studies and the DSGE model with the Phillips curve. The authors attributed this structural decline in the natural rate primarily to the joint aging of both the civilian workforce and active business firms. Hornstein and Kudlyak (2026) estimate a state-space model across 44 distinct age-gender-education groups to identify the contributions of latent cohort, age, and education effects to the natural rate. While rising educational attainment historically buoyed aggregate labor force participation, 21st-century population aging has overtaken it as the dominant structural driver pushing trends downward.

over). The monthly counts are aggregated from individual-level CPS responses based on the reported duration of unemployment and the respondent's state of residence. We also construct the number of individuals in the civilian labor force and total employment by state. All series are seasonally adjusted using the X-13-ARIMA procedure.[6] The sample period spans January 1976 to March 2025.

To ensure consistency with official statistics, we scale CPS-based unemployment counts to match published state-level unemployment totals from the BLS Local Area Unemployment Statistics (LAUS). We also use the seasonally adjusted LAUS labor force to compute state-level unemployment rates. Because LAUS does not provide information on the distribution of unemployment duration at the local level, our adjustment preserves each state's distribution of unemployment durations from the CPS while aligning aggregate unemployment and labor force levels with the LAUS data. As a result, for each state and in each month, the sum of unemployment across duration categories equals the total number of unemployed persons reported in the LAUS data.

All of the CPS-based counts are computed using the individual sampling weights to ensure that the state-level estimates are representative of the civilian noninstitutional population. For the early part of the sample, we harmonize state identifiers to ensure consistent geographic definitions over time. These harmonized, population-weighted series are used to estimate a dynamic accounting identity between unemployment duration and subsequent state-level trend unemployment rates. The data thus combine the detailed duration information from the CPS micro data with the comprehensive coverage and benchmarking of the LAUS series, ensuring both internal consistency and cross-state comparability.

3 Estimating State-Level Trend Unemployment

We use the methodology derived in Ahn (2023) to estimate the trend unemployment rate of each state.[7] Section 3.1 describes the dynamic accounting identity that we employ as our measurement equation, and Section 3.2 discusses how we model the duration structure of

[6]We use the X-13 filter in EVIEWS for our seasonal adjustment.

[7]Our notation closely follows Ahn (2023).

unemployment hazards. Section 3.3 describes the state-space representation of our model and discusses how we identify the time-varying parameters that we estimate; finally, Section 3.4 describes how we handle the Covid-19 pandemic period.

3.1 A dynamic accounting identity

The model characterizes changes in the number of unemployed individuals in state s using unemployment inflows and unemployment hazards by duration. For each state, we use the observed counts of unemployed workers whose unemployment duration falls into five bins: less than 5 weeks, 5–14 weeks, 15–26 weeks, 27–52 weeks, and longer than 1 year. Let

$$y_{st} = [U_{st}^{1}, U_{st}^{2.3}, U_{st}^{4.6}, U_{st}^{7.12}, U_{st}^{13.+}]'$$

be the vector of these duration categories in month t.

The number of newly unemployed individuals, or unemployment inflows, in month t is denoted by w_{st}, which satisfies

$$U_{st}^{1} = w_{st}. \tag{3.1}$$

The notation $P_{st}(\tau)$ denotes the fraction of individuals in state s who were unemployed for one month or less at time $t-\tau$ and who are still unemployed and searching at time t. For example, the number of unemployed individuals with unemployment durations between 5 and 14 weeks can be written as:

$$U_{st}^{2.3} = w_{s,t-1}P_{st}(1) + w_{s,t-2}P_{st}(2). \tag{3.2}$$

Analogously,

$$U_{st}^{4.6} = \sum_{\tau=3}^{5} w_{s,t-\tau}P_{st}(\tau), \tag{3.3}$$

$$U_{st}^{7.12} = \sum_{\tau=6}^{11} w_{s,t-\tau}P_{st}(\tau), \tag{3.4}$$

$$U_{st}^{13.+} = \sum_{\tau=12}^{47} w_{s,t-\tau}P_{st}(\tau). \tag{3.5}$$

We assume a maximum unemployment duration of four years, consistent with Hornstein (2012).

The survival probability $P_{st}(\tau)$ can be expressed as:

$$P_{st}(\tau) = \prod_{h=1}^{\tau} p_{s,t-\tau+h}(h),$$

where $p_{st}(\tau)$ is the monthly probability that an unemployed individual with duration τ in state s remains unemployed one more month.

3.2 Duration structure of unemployment hazards

We express the time-varying parameter $p_{st}(\tau)$ as

$$p_{st}(\tau) = \exp[-\exp(x_{st}(\tau))], \tag{3.6}$$

where $x_{st}(\tau)$ follows a Laguerre polynomial expansion in level, slope, and curvature components:

$$x_{st}(\tau) = \begin{bmatrix} \beta^0_{st} \\ \beta^1_{st} \\ \beta^2_{st} \end{bmatrix}' \begin{bmatrix} 1 \\ e^{-(N-\tau)/\lambda_s} \\ ((N-\tau)/\lambda_{st})e^{-(N-\tau)/\lambda_s} \end{bmatrix}. \tag{3.7}$$

Each parameter captures a distinct feature of the duration profile: β^0_{st} governs the level (the exit probability for newly unemployed individuals), β^1_{st} the slope (the overall deterioration in unemployment hazards), and β^2_{st} the curvature (nonlinearity in hazards). The location parameter λ_{st} controls where in the duration profile the non-monotonicity arises.

For estimation, we assume the continuation probabilities flatten beyond 12 months of unemployment:

$$x_{st}(\tau) = \begin{cases} \beta^0_{st} + \beta^1_{st}e^{-(12-\tau)/\lambda_s} + \beta^2_{st}((12-\tau)/\lambda_s)e^{-(12-\tau)/\lambda_s}, & 1 \leq \tau < 12, \\ \beta^0_{st} + \beta^1_{st}, & \tau \geq 12. \end{cases}$$

3.3 State-space representation and identification

Our goal is to estimate the four time-varying parameters w_{st}, $\beta^0_{st}, \beta^1_{st}$, and β^2_{st}, along with the constant λ_s. Since the dynamic accounting identity is a nonlinear function of the four dynamic latent variables, our model is cast into nonlinear state-space form.

The dynamic accounting identity serves as the basis for the measurement equation. Let $\mathbf{H}(\cdot)$ denote the right-hand-side of equations (3.1) – (3.5) and let y_{st} denote the vector of five data points $[U^1_{st}, U^{2.3}_{st}, U^{4.6}_{st}, U^{7.12}_{st}, U^{13.+}_{st}]'$. The measurement equation is:

$$y_{st} = \mathbf{H}(\Xi_{st}) + r_{st},$$

where Ξ_{st} is the vector capturing the history of latent variables between t and $t-47$,

$$\begin{aligned} \Xi_{st} &= [\xi'_{st}, \xi'_{s,t-1}, \cdots, \xi'_{s,t-47}]', \\ \xi_{st} &= [w_{st}, \beta^0_{st}, \beta^1_{st}, \beta^2_{st}]', \end{aligned}$$

and $r_{st} = [r^1_{st}, r^{2.3}_{st}, r^{4.6}_{st}, r^{7.12}_{st}, r^{13.+}_{st}]'$ is the vector of measurement errors for each data point in y_{it}. We assume that r_{st} is drawn independently from the normal distribution with a diagonal covariance matrix R_i,

$$r_{st} \sim N(0, R_s).$$

For the state equation, we assume ξ_{st} evolves according to an independent random walk:

$$\underbrace{\xi_{st}}_{4\times 1} = \xi_{s,t-1} + \underbrace{\epsilon_{st}}_{4\times 1},$$

where the vector innovation, $\epsilon_{st} = [\epsilon^w_{st}, \epsilon^{\beta_0}_{st}, \epsilon^{\beta_1}_{st}, \epsilon^{\beta_2}_{st}]'$ is drawn from a normal distribution with a diagonal covariance matrix Σ_i,

$$\underbrace{\epsilon_{st}}_{4\times 1} \sim N(\underbrace{0}_{4\times 1}, \underbrace{\Sigma_s}_{4\times 4}).$$

The full state vector Ξ_{st} evolves according to

$$\Xi_{st} = F\,\Xi_{s,t-1} + \underline{\epsilon_{st}},$$

where $\underline{\epsilon_{st}}$ stacks the ϵ_{st} vectors.

For each state the model has 10 parameters that need to be estimated: the diagonal terms in the variance matrices Σ_s and R_s along with λ_s. Because the measurement equation is nonlinear in the latent variables, the extended Kalman filter is used to form the likelihood function for the observed data $\{y_{s1}, ..., y_{sT}\}$ and to infer the unobserved latent variables $\{\xi_{s1}, ..., \xi_{sT}\}$. For the rest of the paper, we report the full-sample smoothed estimates, $\{\xi_{s1|T}, \xi_{s2|T}, ..., \xi_{sT|T}\}$.

The intuition for how the latent variables are identified is as follows. Suppose the economy is in a steady state, with the number of unemployed individuals distributed across five duration categories: $[U_s^1, U_s^{2.3}, U_s^{4.6}, U_s^{7.12}, U_s^{13.+}]$. Given the dynamic accounting identity and assuming zero measurement error, we can identify five steady-state values of $[w_s, \beta_s^0, \beta_s^1, \beta_s^2, \lambda_s]$ that exactly match the five data points. In this setup, w_s is identified from U_s^1, while the remaining four duration categories inform the average unemployment continuation probability for each group. The model fits these implied continuation probabilities by duration using a profile of unemployment-exit probabilities, characterized by Laguerre polynomials that capture the level, slope, and curvature and that are parameterized by the four coefficients β_s^0, β_s^1, β_s^2, and λ_s.

In a dynamic setting, changes in the five data points reflect shifts in w_{st} as well as in the implied average unemployment exit probabilities for each duration category. To capture these changes, four of the five parameters—$[w_s, \beta_s^0, \beta_s^1, \beta_s^2]$—are assumed to evolve over time as a random walk. The overall difference in unemployment exit probabilities between the 2–3 month and 13+ month duration categories identifies β_s^1, while the exit probability for the 2–3 month category identifies β_s^0. The exit probabilities for the 4–6 month and 7–12 month categories pin down β_s^2 and λ_s, respectively. Note that we assume λ_s to be constant.

The assumption regarding the measurement errors implies that the model targets the smoothed component of the observed data, interpreting high-frequency fluctuations as largely transitory noise.

3.4 Covid-19 treatment

The data exhibit extraordinarily large swings during the pandemic, and fitting the model without special treatment of the Covid-19 outliers runs the risk of distorting the estimates. Following recent approaches used to deal with pandemic-period outliers (for example, Lenza and Primiceri, 2022 and Ng, 2021), we estimate the model parameters using data through December 2019 and filter the latent variables through March 2025 after excluding observations with unusually large swings. This approach prevents dramatic swings in the data from distorting the model parameters; without it, the model will allow the parameters to change abruptly so as to fit the pandemic outliers (see Lenza and Primiceri, 2022). However, this approach by itself cannot prevent the two-sided inference in a state-space model from changing significantly, as the model carries information from the pandemic observations backward and allows it to influence the smoothed estimates of the latent variables. Changes in the history of the latent variables that arise from large transitory outliers like these can be problematic if our goal is to estimate the trend components of the latent variables.

To mitigate this problem, we follow Ng (2021) and exclude the period with extreme transitory swings from our dataset. Specifically, we pre-treat the data by removing observations between March 2020 and June 2022 and setting the missing observations to the average value of March 2020 and June 2022.[8] This approach prevents the observations with extreme transitory swings from influencing the two-sided inference over history, thereby enhancing the robustness of the trend estimates.[9]

3.5 Estimated time-varying parameters by state

Appendix B displays the estimates of $\hat{w}_{s,t|T}$, $\hat{\beta}^0_{s,t|T}$, and $\hat{\beta}^2_{s,t|T}$ for each of the 50 U.S. states and the District of Columbia.[10] The estimates reveal common cyclical patterns as well as important heterogeneity across states. States with more cyclically sensitive labor markets (such as Nevada, Michigan, and Florida) exhibit sharper fluctuations in $\hat{w}_{s,t|T}$, while states with larger shares of employment in the public sector or in the technology sector (for example, D.C., Washington state, and Massachusetts) display smoother inflows.

Notably, $\hat{\beta}^0_{s,t|T}$—which captures the exit probability of newly unemployed workers—has declined across nearly all states since the 1980s, with particularly pronounced declines in states

[8] Linearly interpolating the missing observations does not change the results.

[9] We also estimated the model without truncating the data. Overall, the estimated trend unemployment rates remain robust, even though the smoothed estimates of unemployment flows and related parameters are influenced by the COVID-19 outliers.

[10] See Figures B.1 – B.5.

undergoing structural employment shifts, such as the manufacturing-intensive states of the Midwest. In contrast, $\hat{\beta}^2_{s,t|T}$—which captures changes in the relative decline in unemployment exit hazards for short-term unemployed workers relative to the long-term unemployed—fell sharply after the Great Recession, reflecting a rise in long-term unemployment across regions.

4 State-Level Trend U-Star Estimates

In this section, we recover trend U-star estimates for each state based on the trend components of the parameter estimates described in the previous section. We start with a Bayesian trend-cycle decomposition of the four time-varying parameters. We then recover estimates of trend U-star by feeding these trend components into the dynamic accounting identity.

4.1 Trend-cycle decomposition

We decompose each state's smoothed parameters into trend and cyclical components by applying a Bayesian trend-cycle decomposition to the quarterly averages of $\hat{w}_{s,t|T}$, $\hat{\beta}^0_{s,t|T}$, $\hat{\beta}^1_{s,t|T}$, and $\hat{\beta}^2_{s,t|T}$.[11] The model that is typically employed in the literature uses data at quarterly frequencies (see, for example, Stock and Watson, 1998 or Grant and Chan, 2017), so we first convert our monthly smoothed estimates into quarterly values by taking averages within the quarter. We use an integrated random walk to characterize the stochastic trend of each estimate as a smooth curve, which is an appropriate way to model time-varying trends in two-sided (smoothed) estimates.[12]

We denote $\hat{w}_{sq|T}$ as the average of the smoothed estimates $\hat{w}_{st|T}$ in quarter q. The term $\hat{w}_{sq|T}$ is composed of the trend, ψ^w_{sq}, and a transitory deviation from the trend, c^w_{sq},

$$\hat{w}_{sq|T} = \psi^w_{sq} + c^w_{sq}. \tag{4.1}$$

[11]See Chan, Koop, Poirier and Tobias (2019).

[12]Integrated random-walk models are commonly used to extract underlying trends in macroeconomic variables; for example, Chan et al. (2019) use an integrated random-walk specification for their trend-cycle decomposition of quarterly U.S. real GDP growth.

The cyclical component is modeled as a zero-mean stationary AR(2) process:

$$c^w_{sq} = \phi^w_1 c^w_{s,q-1} + \phi^w_2 c^w_{s,q-2} + \epsilon^{cw}_{sq}, \tag{4.2}$$

where $\epsilon^{cw}_{sq} \sim N(0, (\sigma^{cw}_s)^2)$.[13] We express the trend, ψ^w_{sq}, as

$$\begin{aligned} \psi^w_{sq} &= \mu^w_{sq} + \psi^w_{s,q-1}, \\ \mu^w_{sq} &= \mu^w_{s,q-1} + \epsilon^{\psi w}_{sq}, \end{aligned} \tag{4.3}$$

where $\epsilon^{\psi w}_{sq} \sim N(0, (\sigma^{\psi w}_s)^2)$. Note that equation (4.3) is equivalent to

$$\triangle\psi^w_{sq} = \triangle\psi^w_{s,q-1} + \epsilon^{\psi w}_{sq}. \tag{4.4}$$

Similar specifications are used to estimate the trend components of $\hat{\beta}^0_{iq|T}, \hat{\beta}^1_{sq|T}$, and $\hat{\beta}^2_{sq|T}$, which we denote by $\psi^{\beta 0}_{sq}$, $\psi^{\beta 1}_{sq}$, and $\psi^{\beta 2}_{sq}$, respectively.

To recover the trend unemployment rate for each state we also estimate each state's trend labor force, ψ^{LF}_{sq}. We again use an integrated random walk model because it provides a good way to capture the I(2) dynamics of the civilian labor force. (As it turns out, the estimates of trend U-star are relatively insensitive to the priors used for the trend-cycle decomposition of the labor force.) Details on the priors and the derivation of the Gibbs sampler can be found in the appendix.

We then feed the relevant trend estimates back into the dynamic accounting identity with the measurement errors set equal to zero. To do this, we convert the quarterly trend estimates into monthly series, $\hat{\psi}^w_{st|T}$, $\hat{\psi}^{\beta 0}_{st|T}$, $\hat{\psi}^{\beta 1}_{st|T}$, $\hat{\psi}^{\beta 2}_{st|T}$, and $\hat{\psi}^{LF}_{st|T}$, under the assumption that the monthly values for a given quarter are the same.[14] The trend U-star for state s in month t is therefore defined as:

$$U^*_{st} = 100 \times \frac{\mathbf{1}' h(\hat{\psi}_{st|T}, \hat{\psi}_{s,t-1|T}, \hat{\psi}_{s,t-2|T}, \ldots, \hat{\psi}_{s,t-47|T}, \hat{\lambda}_s)}{\hat{\psi}^{LF}_{st|T}},$$

where $\mathbf{1}$ is a (5×1) vector of ones, $h(\cdot)$ denotes the system of equations (3.1)-(3.5) with measure-

[13]This way of implementing a trend-cycle decomposition is relatively standard; see Stock and Watson (1998) and Fleischman and Roberts (2011) for other examples.

[14]We obtain essentially the same quarterly trend unemployment rates if we instead interpolate the monthly observations from the quarterly series.

ment errors set to zero, and $\hat{\psi}_{st|T}$ is the vector $[\hat{\psi}^{w}_{st|T}, \hat{\psi}^{\beta 0}_{st|T}, \hat{\psi}^{\beta 1}_{st|T}, \hat{\psi}^{\beta 2}_{st|T}]'$. The quarterly trend U-star is computed by taking the quarterly average of the monthly estimates.

5 Key Features of State-Level Trend Unemployment Rates

5.1 Changes in the overall distribution

Figure 1 presents estimates of trend U-star together with the portions of the trend that reflect short-term unemployment (defined as unemployment spells that last six months or less) and longer-term unemployment (more than six months). Panel A plots the aggregate estimate (solid blue line) and its 68% credible interval, together with the actual unemployment rate (black line). Overall, the aggregate trend exhibits a decline from the 1980s through the 1990s, flattens during the 2000s, and then resumes its downward movement after the Great Recession. This downward trajectory primarily reflects demographic forces—including population aging, rising educational attainment, and reduced labor-market dynamism—which result in declining inflows into unemployment and a steady reduction in the short-term component of trend U-star. Notably, the aggregate long-term component remains roughly flat through 2000, edges upward between 2000 and 2010, and then declines modestly thereafter; this increase in the long-term component is responsible for the 2000–2010 upturn in the aggregate U-star estimate. Apparently, then, the factors pushing down the short-term component had no effect on the long-term component (or other factors impeded a simultaneous decline in the long-term component).

Panels B through D also display the 51 state-level estimates of total, short-term, and long-term U-star, with each estimate shown as a thin light-blue line. The solid black lines in the panels represent the mean estimate weighted by population, and the dashed black lines represent the median estimate. Overall, states share a common downward trend in the total and short-term components, but both the pace of decline and the level of U-star vary substantially across states, as shown by the wide dispersion of cross-state estimates in Panels B and C. A similar pattern emerges for the long-term component (Panel D), though the dispersion of these estimates is smaller. These patterns highlight the pronounced cross-state heterogeneity in both the level and dynamics of trend U-star.

Figure 1: The Trend Unemployment Rate and Its Distribution by State and Duration

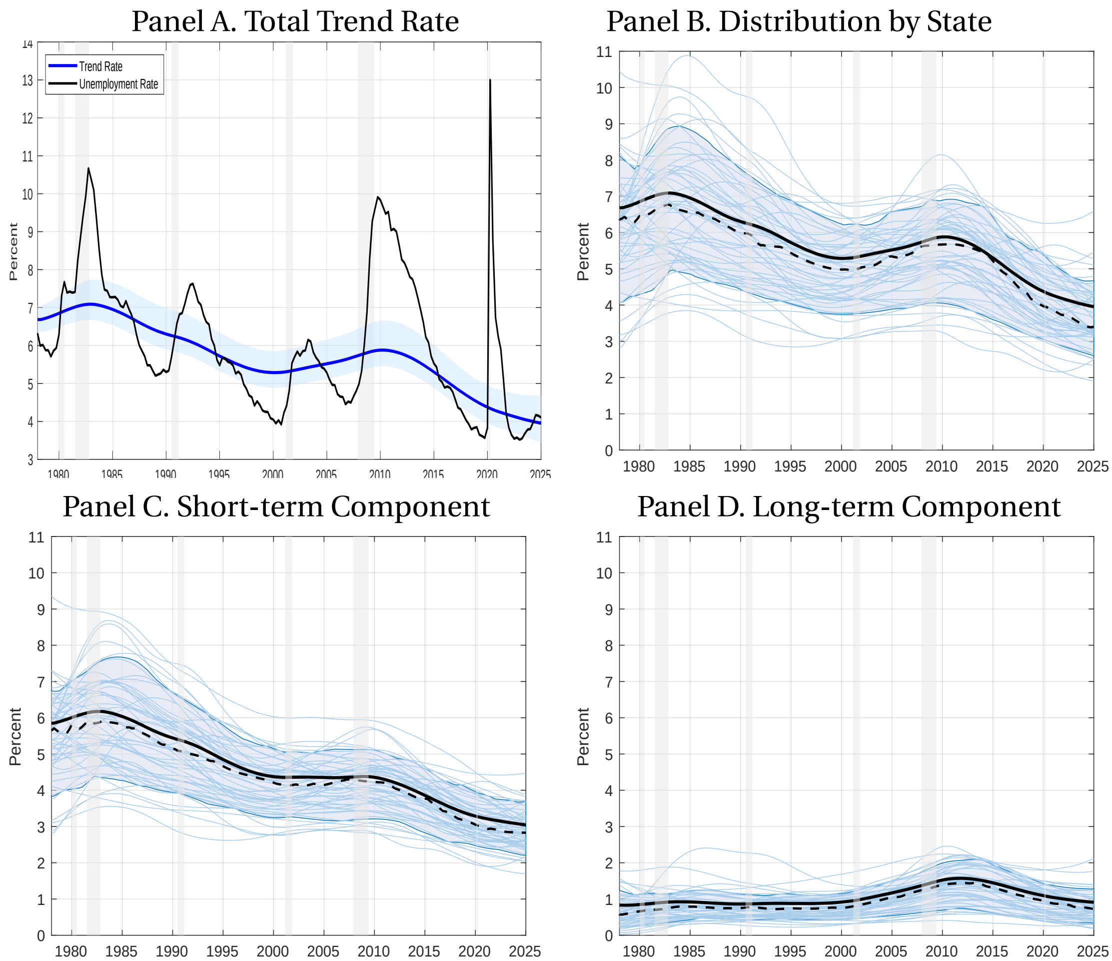

Notes to figure: Panel A displays the aggregate unemployment rate (black line) and the trend U-star (blue line), with the 68% posterior interval shown as a light-blue shaded region. Panel B shows the total trend unemployment rates for the 50 states and the District of Columbia (thin lines), along with the labor-force-weighted mean (solid line) and median (dashed line); the grey shaded band represents the 90% cross-state distribution. Panels C and D present analogous figures for the short-term and long-term components—defined as unemployment spells of six months or less and longer than six months, respectively. The vertical shaded bars denote periods of recession as defined by the NBER. **Source**: Authors' calculation.

Figure 2: OVERALL CHANGES IN TREND U-STAR BY STATE

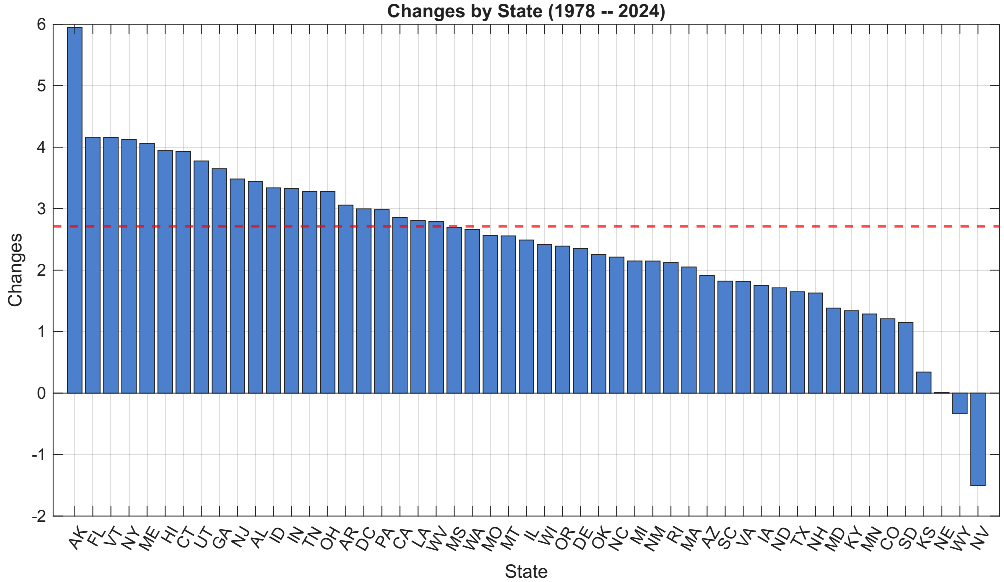

Notes to figure: This figure displays changes in trend U-star between the average values in 1978 and those in the five-quarter period 2024:Q1–2025:Q1. The red dashed line is the corresponding national average. **Source**: Authors' calculation.

Figure 2 summarizes state-level changes in trend U-star between the 1978 and 2024:Q1–2025:Q1 averages. This figure highlights significant heterogeneity in secular declines in state-level unemployment rates. In particular, about twenty states show larger declines than the national-level estimate; twenty-five states exhibit slower declines; and four states' trend U-star did not change or even rose.

Figure 3 shows the evolution of cross-state dispersion, measured using both the interquartile range and the standard deviation of the state-level estimates. As Panel A illustrates, cross-state dispersion declines from the mid-1980s through the mid-2000s before then stabilizing. This pattern is driven primarily by the short-term component (Panel B), with the dispersion of the long-term component remaining relatively constant over time. (Note that the convergence of the estimates does not imply that state-level estimates are becoming more synchronized, only that they are moving in a narrower range.)

5.2 Features of state-level estimates

Figure 4 presents the mean level of each state's trend U-star (Panel A) and the share that is accounted for by the long-term component (Panel B). The trend U-stars are highly heterogeneous

Figure 3: Evolution of Cross-State Dispersion in Trend Unemployment

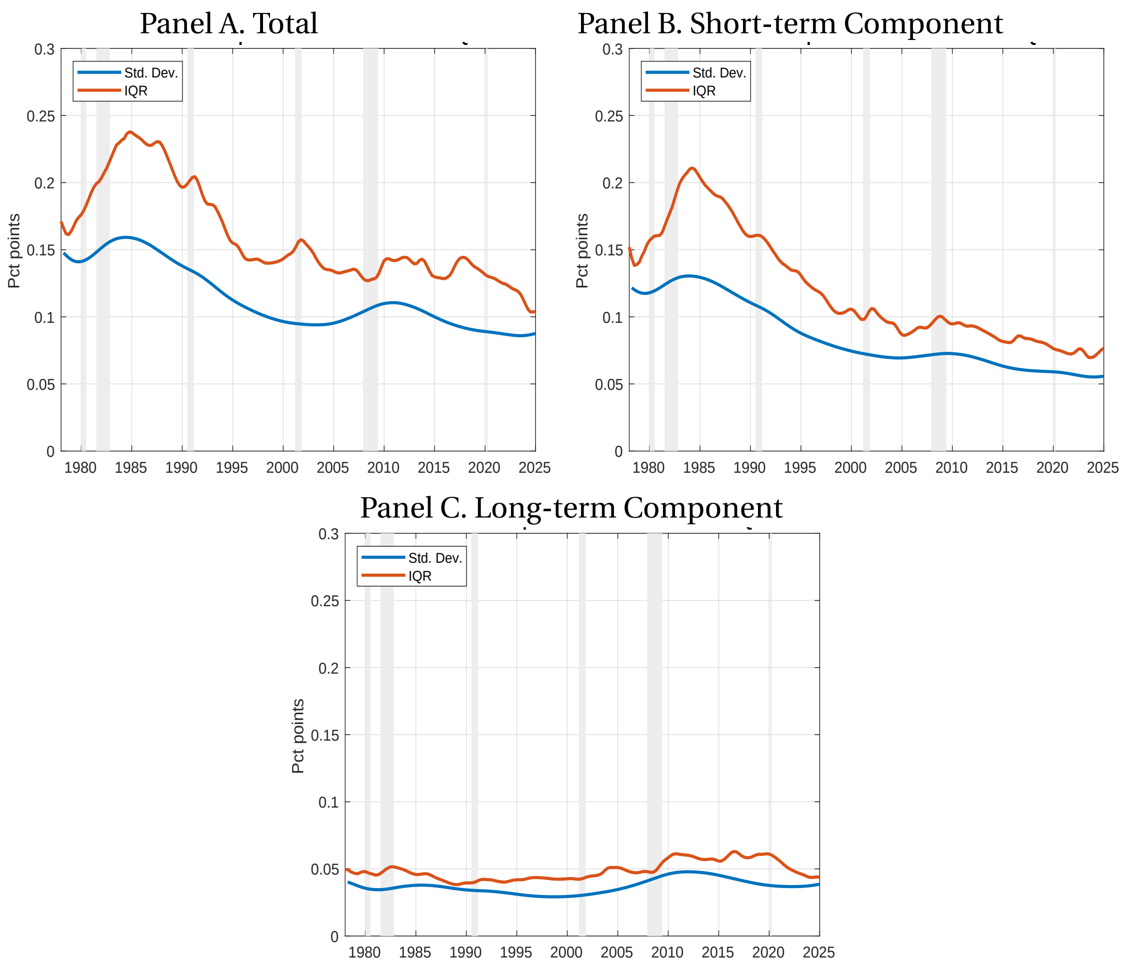

Notes to figure: The panels show the standard deviation (blue line) and interquartile range (IQR) of the state-level trend unemployment rate estimates at each point in time. Panel A uses the estimates of total trend unemployment, while Panels B and C use the short- and long-term components, respectively. **Source**: Authors' calculation.

Figure 4: AVERAGE LEVEL OF TREND U-STAR AND THE RELATIVE IMPORTANCE OF ITS LONG-TERM COMPONENT ACROSS STATES

Panel A: Average Level of Trend U-star (1978:Q1-2025:Q1, %)

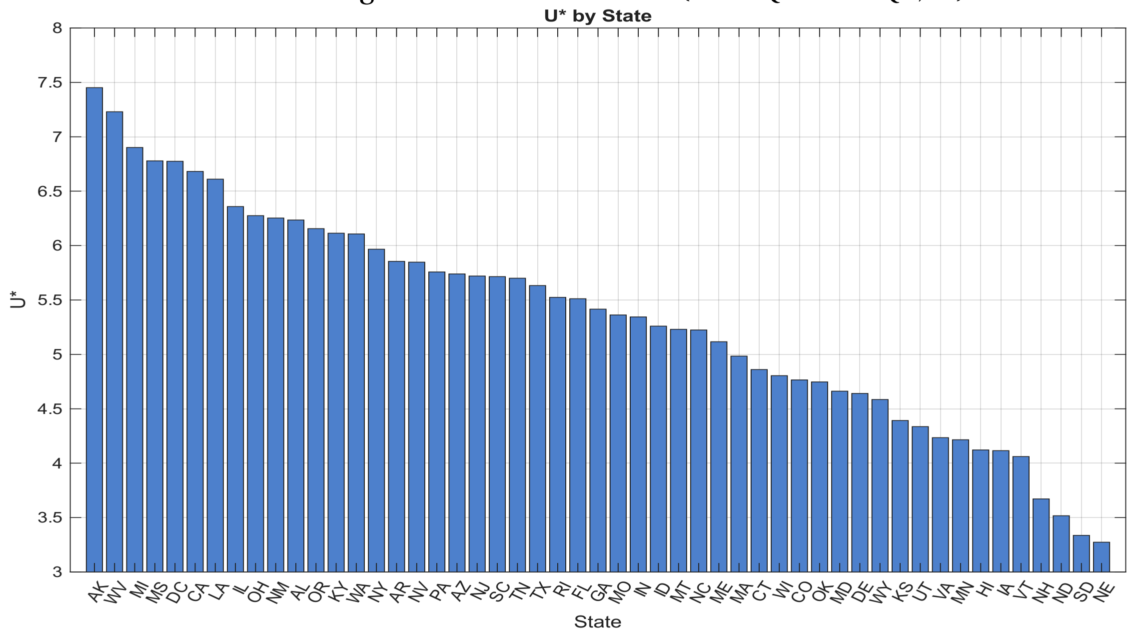

Panel B: Long-term Share (1978:Q1-2025:Q1, %)

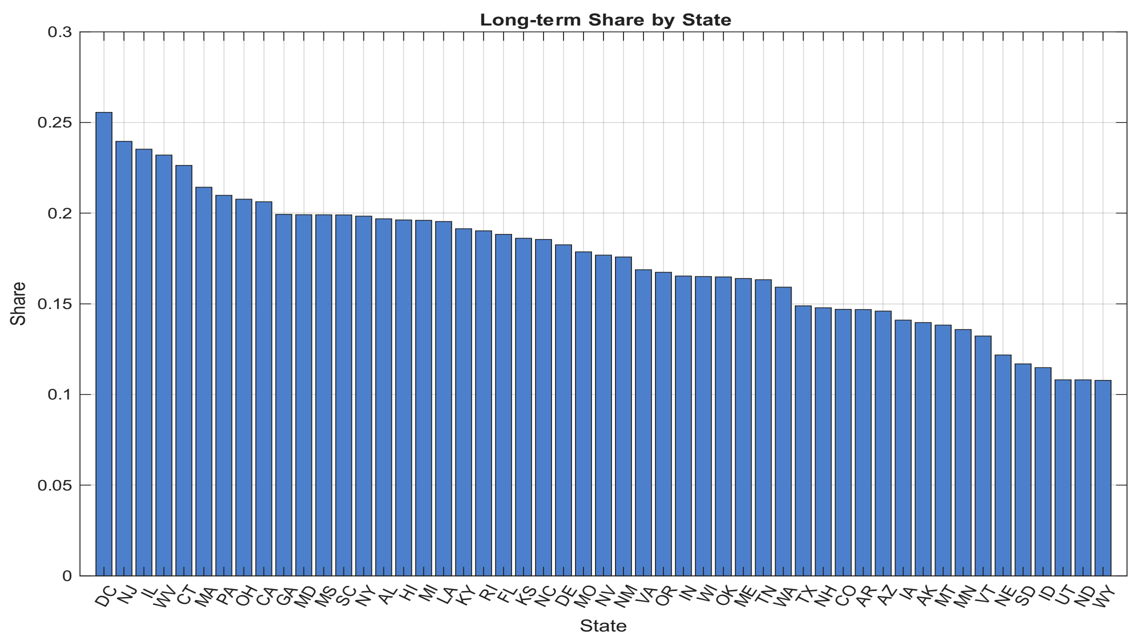

Note to figure: Panel A displays the average level of trend U-star for U.S. states (in %). Panel B displays the share of each state's total trend U-star that is accounted for by its long-term component (also in %). The sample period is 1978:Q1-2025:Q1.

Source: Authors' calculation.

Figure 5: TREND U-STAR LEVELS AND LONG-TERM SHARES

Panel A: Average Level of Trend U-star

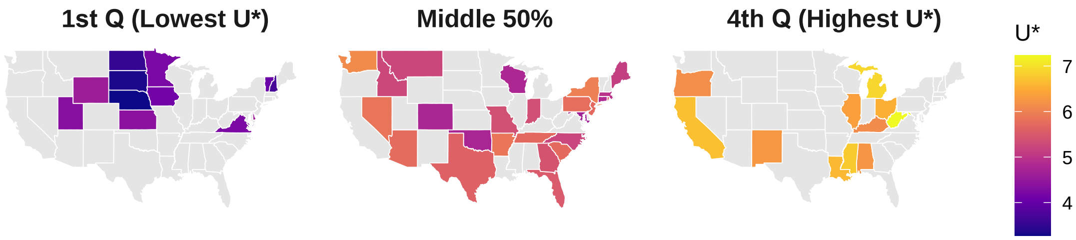

Panel B: Long-term Share

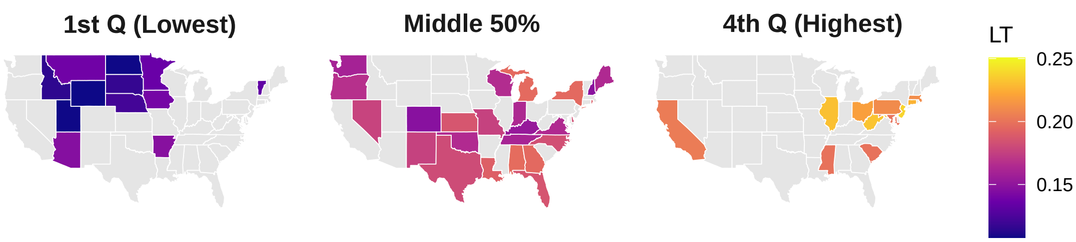

Note to figure: This figure displays U-star quartile groupings (Panel A) and the long-term share groupings (Panel B) across states. The left column shows states in the lowest quartile ("1st Q"); the center column shows the middle two quartiles, and the right figure shows the highest quartile ("4th Q"). Colors correspond to the scales shown on the right. The sample period is 1978:Q1-2025:Q1.
Source: Authors' calculation.

across states, ranging from about 3.25% in Nebraska to roughly 7.5% in Alaska. The long-term shares also vary substantially, from just above 10% in Wyoming to around 25% in the District of Columbia. Taken together, these observations suggest considerable cross-state heterogeneity in labor-market functioning, and particularly in the relative importance of structural versus frictional unemployment.

Figure 5 shows the geography of trend U-star and its long-term share. Panel A displays states with the lowest trend U-star (the bottom 25%, left), those in the middle 50% of the trend U-star distribution (middle 50%), and states with the highest trend U-star (the top 25%, right). States in the bottom 25% are clustered in the Upper Midwest and the mountain plains, including Nebraska, North Dakota, South Dakota, Iowa, and Montana, which appear in dark purple (left figure in Panel A). These states have strong agricultural as well as manufacturing bases and have high labor force participation rates. In these states, the long-term share also tends to be low, as can be seen by comparing this map to the corresponding map in Panel B. The top 25% includes states from the industrial Midwest and deep South, as well as California. The higher U-star levels and larger long-term shares in this group imply that workers in these states are more likely to experience structural unemployment.

The positive association between the level of trend U-star and its long-term share is confirmed by the scatterplots in Figure 6, as well as by the Spearman rank correlation between the level of U-star and its long-term share, which is 0.53.[15] A positive association is also evident within each Census region (Panel B), and is quantitatively strongest in the Northeast and Midwest.

5.3 Drivers of trend U-star

This section investigates the role of state-level factors in shaping variation in trend U-star. Consider the following model:

$$U^*_{st} = a_s + \sum_i b_i X^i_{st} + \varepsilon_{st}, \tag{5.1}$$

where U^*_{st} denotes trend U-star for state s in quarter t; a_s is a state fixed effect; X^i_{st} denotes attribute i of state s in quarter t, which receives coefficient b_i; and ε_{st} is the error term. We consider four broad categories of state-level attributes: demographics, industry structure, labor-market rigidity, and state-specific labor force participation and labor productivity. As demographic variables, we include the population shares of high-school dropouts and the share of college graduates out of population aged 25 and over; the shares of individuals aged 16–24 and 55-plus among those aged 16 and older; and men's share of total state employment. Industry structure is captured by the employment shares of manufacturing, professional and business services, and finance, as well as with an indicator for oil-producing states. Measures of labor-market rigidity include the union membership share, the employment share of large firms (defined as firms with 500 or more employees), the tax-to-income ratio, the level of the minimum wage, and the share of nominal wage changes that are zero.[16] Finally, we include state-specific labor force participation rates and average labor productivity to capture broad conditions of labor supply and labor demand.

The estimation period runs from 1980:Q1 to 2018:Q4 and excludes Washington, D.C. because

[15] The Kendall rank correlation is 0.38.

[16] The state-level tax-to-income ratio is computed from total tax receipts from the Annual Survey of State Government Tax Collections (Census) and total income from the Personal Income By State report (BEA); it is available yearly from 1960 to 2022.

Figure 6: TREND U-STAR AND ITS LONG-TERM SHARE

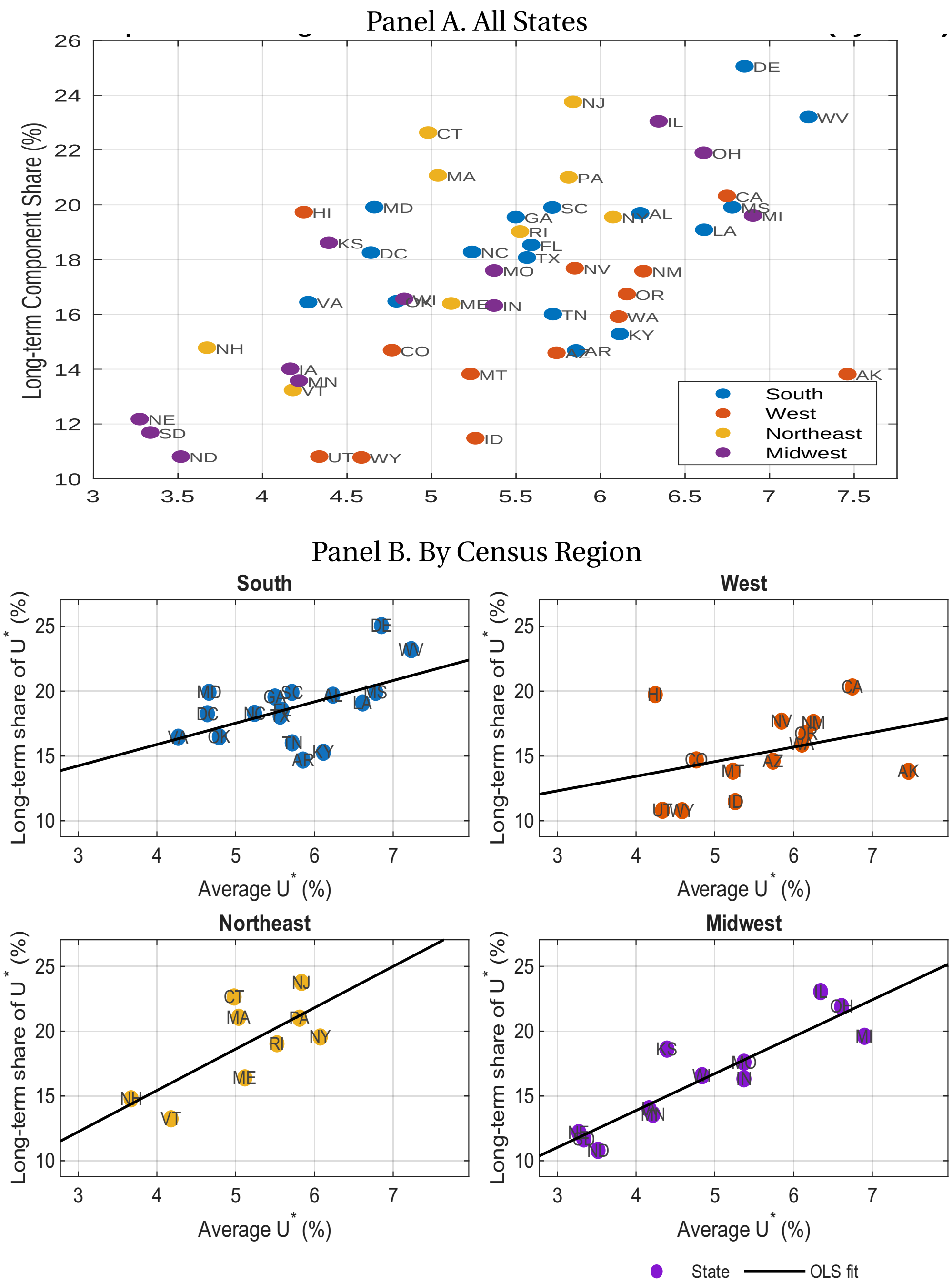

Notes to figure: The charts plot the share of U-star that is accounted for by its long-term component (y-axis) against the average level of U-star (x-axis) for each state. The black lines in panel B are OLS regression lines.
Source: Authors' calculation.

of data constraints. (Excluding Washington, D.C., the downward nominal wage rigidity measure is available from 1978 until 2020, while labor productivity is available from 1976 until 2018.) New Mexico and South Dakota are omitted from 2002 onward because data on the financial employment shares in those states are unavailable. The standard errors are clustered by state.

Table 1: Coefficient Estimates from Equation (5.1)

	(1) Total	(2) Short-term	(3) Long-term	(4) LT share
1. High-school dropouts	0.048**	0.050***	-0.002	-0.001**
	(0.021)	(0.018)	(0.006)	(0.001)
2. College graduates	0.031	0.051*	-0.021	-0.000
	(0.038)	(0.029)	(0.013)	(0.001)
3. Age 16-24	0.083**	0.074***	0.009	-0.000
	(0.032)	(0.026)	(0.010)	(0.001)
4. Age 55+	-0.034	-0.017	-0.017*	-0.001
	(0.027)	(0.022)	(0.009)	(0.001)
5. Manufacturing	-0.026	-0.008	-0.017	-0.001
	(0.031)	(0.023)	(0.011)	(0.001)
6. Professional Services	-0.009	-0.042***	0.033***	0.005***
	(0.020)	(0.015)	(0.008)	(0.001)
7. Finance Share	0.044	0.043	0.001	-0.001
	(0.058)	(0.060)	(0.015)	(0.002)
8. Union Share	0.020	0.018	0.003	0.000
	(0.014)	(0.012)	(0.005)	(0.001)
9. Large-Firm Share	-0.020	-0.019	-0.001	0.000
	(0.023)	(0.021)	(0.006)	(0.001)
10. Tax-Income Ratio	0.035*	0.036**	-0.000	-0.001
	(0.018)	(0.014)	(0.008)	(0.001)
11. Minimum Wage	-0.092**	-0.135***	0.042**	0.005**
	(0.046)	(0.035)	(0.019)	(0.002)
12. Oil Production	-1.042***	-0.777***	-0.265***	-0.029***
	(0.118)	(0.097)	(0.038)	(0.005)
13. DNWR	0.037***	0.026***	0.010***	0.001***
	(0.007)	(0.005)	(0.002)	(0.000)
14. Male Share in EPOP	0.034	0.051	-0.017	-0.002*
	(0.047)	(0.036)	(0.014)	(0.001)
15. LFPR	-0.091***	-0.036	-0.056***	-0.007***
	(0.034)	(0.023)	(0.013)	(0.001)
16. Labor Productivity	0.574	0.302	0.273	0.053**
	(0.592)	(0.484)	(0.202)	(0.024)
No of Obs.	6,864	6,864	6,864	6,864
R^2	.836	.875	.833	.918

Note: This table reports the coefficient estimates from equation (5.1). Standard errors (in parentheses) are clustered by state. * p<0.10, ** p<0.05, *** p<0.01.
Source: Author's calculation.

Table 1 reports the coefficient estimates. Starting with educational attainment, a higher share of high-school dropouts (row 1) has a statistically significant positive effect on trend U-star through its effect on the short-term component (column 2), possibly because less-educated workers tend to have higher job-separation rates. The overall effect of a higher share of college graduates (row 2) is smaller and insignificant, reflecting a modest negative effect on the long-term component (column 3) that appears to offset a counterintuitive (but barely significant) positive effect on the short-term component. Overall, because the boost to aggregate U-star is larger for high-school dropouts than for college graduates, rising educational attainment would appear to lower trend U-star on net.

As shown in rows 3 and 4, a larger share of young workers (aged 16–24) raises trend U-star, while the effect of a larger share of older workers (aged 55 or more) is negative but not statistically significant. The population share of young workers primarily raises the short-term component of U-star, while the share of older workers has a marginally significant negative effect on the long-term component, indicating that population aging puts downward pressure on U-star. Finally, the effect on U-star of a higher relative share of men in employment (row 14) is insignificant.

We find little evidence that industry structure plays an important role in determining trend U-star. In the aggregate, a higher employment share in professional and business services (row 6) does not have a statistically significant effect on aggregate U-star, but this is because it has opposite effects on the duration components. Specifically, a larger employment share for professional services lowers the short-term component of U-star, but *raises* its long-term component, with both effects statistically significant at the 1% level. Here, two opposing forces are likely at work: Job-specific human capital in this high-skilled sector enhances short-term employment stability, but displaced workers face longer unemployment spells, thereby raising the long-term component. This pattern could obtain because these workers are more selective about job offers, have more financial resources to engage in an extended job search, or maintain relatively high reservation wages. This result suggests that the increased employment share of professional and business services over time has likely raised the long-term share of U-star, but left its aggregate level little changed. Finally, a greater role of oil production in a state (row 12) tends to lower both the short-term and long-term components of U-star (columns 2 and 3), while the employment shares of the manufacturing and finance industries do not exhibit statistically significant effects.

Labor-market rigidities and institutional factors have mixed effects on U-star. A higher tax-to-income ratio (row 10) and greater downward nominal wage rigidity (row 13) exert upward pressure on U-star. While we would expect (and find) that a higher tax burden reduces labor demand and restrains job creation (all else equal), its effect on U-star comes through the short-term component (column 2), which is perhaps surprising. Greater downward nominal wage rigidity raises both duration components of U-star (row 13), which is intuitive, while minimum wages have distinct, heterogeneous effects across the duration components of U-star (row 11). A higher minimum wage significantly lowers both the aggregate and short-term components, a finding consistent with the view that higher minimum wages reduce voluntary separations and enhance job attachment. At the same time, however, a higher minimum wage significantly raises the long-term component (column 3) and the long-term share (column 4). This result suggests that higher minimum wages may discourage firms from hiring low-productivity job seekers, thereby prolonging these workers' unemployment spells and increasing their risk of long-term unemployment. Finally, the effects of higher unionization rates (row 8) and a larger employment share in large firms (row 9) have intuitive signs, but are not statistically significant.

A higher labor force participation rate (LFPR) in a state (row 15) is associated with a reduction in U-star, mostly through its long-term component (including the long-term share, column 4). Because the LFPR reflects the interaction of labor supply and labor demand, a higher participation rate suggests the presence of robust labor demand that effectively draws individuals into the workforce. This alignment between demand and supply could in turn be associated with improved long-term labor-market matching and functioning, thereby reducing prolonged unemployment spells. In contrast, higher labor productivity (row 16) does not exhibit a statistically significant effect, aside from a positive association with the long-term share (column 4). This association might reflect the fact that higher productivity driven by restructuring or by the exit of less-productive sectors can lengthen search durations for displaced workers whose skills have become obsolete, thus raising the long-term share in U-star.

6 Implications for the Phillips Curve

It is now clear that state-level estimates of U-star differ substantially in terms of both their levels and their evolution over time. We next show that this heterogeneity has important implications for identifying the slope of the Phillips curve using state-level data. Previous research on the Phillips curve based on state-level data (e.g., Hazell et al., 2020; Fitzgerald et al., 2020; and McLeay and Tenreyro, 2020) employed time and state fixed effects in their empirical models. State fixed effects are designed to capture differences in the levels of state-specific natural rates and other time-invariant state-specific attributes. Conversely, time fixed effects account for national-level economic conditions, such as shifts in monetary policy regimes, movements in inflation expectations, and changes in the aggregate natural rate of unemployment. Implicit in this approach is the assumption that changes in state-level natural rates are perfectly correlated with the national aggregate. Finally, the last assumption made by these studies is that aggregate demand shocks are uncorrelated with the natural rate. The presence of significant and persistent heterogeneity in state-level U-stars calls each of these assumptions into question.

For example, in Hazell et al. (2020)'s two-way fixed-effects specification, their instrument capturing heterogeneous state-level responses to changes in aggregate demand may not adequately isolate the structural relationship between the state-level unemployment-rate gap and (nontradables) price inflation—that is, the slope of the Phillips curve. Using our state-level U-star estimates, we revisit Hazell et al. (2020) and re-estimate the Phillips curve, replacing state-level unemployment rates with the corresponding state-level unemployment-rate gaps (while maintaining all the other features of their empirical framework).[17]

6.1 Estimating state-level Phillips curves

Hazell et al. (2020) estimate the following forward-looking new-Keynesian Phillips curve in order to recover the slope κ of the aggregate Phillips curve:

$$\pi_{it}^N = \alpha_i + \gamma_t - \kappa \sum_{j=0}^{T} \beta^j u_{i,t+j} - \lambda \sum_{j=0}^{T} \beta^j \hat{p}_{i,t+j}^N + \tilde{\omega}_{it}^N + \eta_{it}^N, \tag{6.1}$$

[17]Throughout this section, we use the notation and terminology of Hazell et al. (2020).

where π^N_{it} is the four-quarter percent change in nontradable goods prices for state i at time t, α_i is a state fixed effect, γ_t is a time fixed effect, $u_{i,t+j}$ is the unemployment rate of state i at time $t+j$, $\hat{p}^N_{i,t+j}$ is the relative price of nontradables in state i at time $t+j$, $\tilde{\omega}^N_{it}$ is an error term that is related to supply shocks in the nontradable goods sector of state i, and η^N_{it} is an error term that includes an expectation error that is orthogonal to information known at time t along with a truncation error that results from using a finite T in equation (6.1).[18] The parameter β denotes a discount factor, which is set equal to 0.99.

Equation (6.1) can be estimated using standard GMM methods by instrumenting for the two forward sums. Hazell et al. (2020) consider two ways to do this. The first approach is to instrument for the two forward sums using four-quarter lagged unemployment, $u_{i,t-4}$, and the four-quarter lagged relative price of nontradables, $\hat{p}^N_{i,t-4}$. Assuming rational expectations, these lagged variables are uncorrelated with the expectations error in $\eta^N_{i,t}$. The second approach involves constructing a Bartik instrument that captures the idea that demand for nontradables in state i will rise relatively more when there is a national increase in demand for the types of *tradable* goods that state i produces relatively more of. The instrument that captures tradable-demand spillovers is given by

$$\text{tradable Demand}_{i,t} = \sum_k \tilde{S}_{k,i} \times \Delta_{3Y} \log S_{-i,k,t}, \tag{6.2}$$

where $\tilde{S}_{k,i}$ is the average employment share of industry k in state i over time, and $\Delta_{3Y} \log S_{-i,k,t}$ is the three-year growth in national employment of industry k at time t excluding state i.[19]

Hazell et al. (2020) set $T = 20$ quarters in the forward sums in equation (6.1), which implies that five years' worth of observations at the end of the sample are discarded. To minimize the effect of this reduction in sample size, they use a two-sample two-stage least squares (2SLS) regression where the first-stage regression is estimated on a sample that omits the most-recent five years and the second stage is estimated on the full sample. (Standard errors are clustered at the state level, and are corrected using the method developed by Chodorow-Reich and Wieland,

[18] Equation (6.1) corresponds to equation (17) in Hazell et al. Note that, following their notation, κ is a positively signed parameter.

[19] Hazell et al. (2020), p. 1328 discuss the identifying assumptions under which the demand spillover variable is an appropriate instrument.

2020.)

If we are willing to assume that u_{it} and p^N_{it} follow AR(1) processes, then the time-t expected forward sums in equation (6.1) can be expressed in terms of the AR parameters, the discount factor β, and the time-t values of u_{it} and p^N_{it}. This motivates a second specification that Hazell et al. (2020) consider:

$$\pi^N_{it} = \alpha_i + \gamma_t - \psi u_{i,t} - \delta p^N_{i,t} + \varepsilon_{it}, \tag{6.3}$$

where ε_{it} is an error term.[20] Because inflation is defined as a four-quarter change, Hazell et al. (2020) actually estimate equation (6.3) using $u_{i,t-4}$ and $p^N_{i,t-4}$,

$$\pi^N_{it} = \alpha_i + \gamma_t - \psi u_{i,t-4} - \delta p^N_{i,t-4} + \varepsilon_{it}, \tag{6.4}$$

so that inflation over the next four quarters represents the outcome of the current-quarter values of u and p^N. Equation (6.4) can be estimated by OLS; alternatively, we can instrument for the lagged unemployment rate using the tradable demand variable defined in equation (6.2).

The assumption that is being made about the natural rate with the two-way fixed effects is that the state-level natural rate is either constant over time—and therefore captured by state fixed effects—or co-moves perfectly with the aggregate natural rate, and so can be captured by time fixed effects. Under these assumptions, Hazell et al. interpret the forward sum of the unemployment rate as the forward sum of the unemployment-rate *gap*, and similarly interpret the lagged unemployment rate in equation (6.4) as the lagged unemployment-rate gap. However, if state-level trend unemployment is not constant or does not closely track the aggregate trend, both equations (6.1) and (6.4) are misspecified and their estimated coefficients are likely biased. As we have seen, our state-level estimates indicate that trend U-star is generally neither constant nor perfectly aligned with its aggregate counterpart. We would therefore expect the estimated Phillips curve coefficients to change when the state-level unemployment rate is replaced with the corresponding state-level unemployment-rate gap, defined as the difference between a state's unemployment rate and its trend U-star.

[20] This is equation (15) in Hazell et al. (2020). Note that if the autoregressive parameters for u_{it} and p^N_{it} are ρ_1 and ρ_2, respectively, then $\psi = \kappa/(1-\beta\rho_1)$ and $\delta = \lambda/(1-\beta\rho_2)$, where κ and λ are the same as in equation (6.1). If the autoregressive parameter for u_{it} is positive and less than one, then ψ will be a scaled-up multiple of κ. (It is not clear why we would want to assume that the autoregressive parameters are the same across states, but this is the assumption that Hazell et al. make in motivating equation 6.3.)

The original sample period used in Hazell et al. (2020) is 1978–2018. In Hazell et al.'s dataset, some states do not have unemployment rate data after 2017; we therefore restrict our sample period to 1978–2017, which implies that unemployment rates and U-star estimates are available for every state in each period. As we will show, doing so yields estimates that are quite close to Hazell et al.'s original results.[21]

[21] Hazell et al.'s original dataset ends in 2018:Q3 and does not have the unemployment rate and the Bartik instrument for 10 states in 2018 (Arkansas, Georgia, Illinois, Mississippi, Missouri, South Carolina, Tennessee, Texas, Washington, and Wisconsin). In addition, Hazell et al. (2020) note a 26-month gap in 1986–1988 due to missing micro-data in their dataset. We use the Local Area Unemployment Statistics (LAUS) to obtain state-level data on seasonally adjusted monthly unemployment rates, employment and unemployment levels, and the labor force rather than the state-level unemployment rates provided in Hazell et al. (2020)'s replication package; in some cases, the latter differ from the LAUS values for reasons that we cannot determine.

Table 2: ESTIMATION RESULTS

1. Unempl. Rate (κ)	(1) No FE	(2) No TE	(3) SE&TE	(4) Bartik (SE&TE)
U-sum	-0.00388***	-0.000176	0.00521*	0.00547**
	(0.00132)	(0.00184)	(0.00276)	(0.00217)
No. of Obs.	4,460	4,460	4,460	4,059
2. Eq. (6.4) with UR (ψ)	(1)	(2)	(3)	(4)
Lagged UR	-0.110***	0.0113	0.0995*	0.349**
	(0.0364)	(0.0279)	(0.0597)	(0.140)
No. of Obs.	4,460	4,460	4,460	4,059
3. UR-gap (κ)	(1)	(2)	(3)	(4)
U-sum	0.00476	0.00505	0.00503	0.0103**
	(0.00342)	(0.00840)	(0.00447)	(0.00488)
No. of Obs.	4,460	4,460	4,460	4,059
4. Eq. (6.4) with UR-gap (ψ)	(1)	(2)	(3)	(4)
Lagged UR gap	0.0544*	0.0411	0.0690	0.650**
	(0.0315)	(0.0326)	(0.0687)	(0.278)
No. of Obs.	4,460	4,460	4,460	4,059

Note: This table presents estimates of κ and ψ from regression specifications (6.1) and (6.4), respectively. The outcome variable is the four-quarter change in nontradable prices (in percent). The estimates in the first three columns use the fourth lags of quarterly state unemployment and the relative price of nontradables as instruments (this corresponds to OLS for ψ). "No FE" denotes specifications with no fixed effects included; "No TE" denotes specifications that include state but not time fixed effects; "SE&TE" denotes specifications with both state and time fixed effects. In the fourth column, "Bartik (SE&TE)," we replace lagged unemployment in the instrument set with the tradeable-demand (Bartik) instrument and include both state and time fixed effects. Standard errors, clustered by state and corrected using the procedure from Chodorow-Reich and Wieland (2020), are reported. Standard errors are in parentheses * p<0.10, ** p<0.05, *** p<0.01.

Source: Authors' calculation.

Table 2 compares the estimation results that we obtain using either the unemployment rate or the unemployment-rate gap. Panels 1 and 2 use the unemployment rate to replicate the results in Hazell et al. (2020). As in Hazell et al. (2020), the slope of the Phillips curve (κ in equation 6.1) has the "wrong" sign when the fixed effects are omitted (panel 1, columns 1 and 2). Using both state and time fixed effects (columns 3 and 4) yields a Phillips curve slope that is statistically significant but extremely flat; this conclusion is robust when we instrument for the unemployment rate with the Bartik instrument (column 4). As shown in panel 2, if we estimate ψ from equation (6.4), the coefficients become much larger in absolute magnitude. Note that the role of the unemployment rate in equation (6.4) is fully consistent with a conventional Phillips curve, in which inflation is determined by excess supply or demand in labor and product markets, and where the unemployment rate serves as a proxy for the degree of resource utilization rather than as a predictor of future real marginal costs. Hence, these results do not rule out that the conventional interpretation of the unemployment–inflation relationship provides a better description of inflation dynamics than the new-Keynesian model.[22] Leaving that aside, we would point out that all of the results we obtain are very similar to what Hazell et al. report.

Replacing the unemployment rate with its gap (panel 3) causes the results to change in several interesting ways. First, the slope estimate from the specification without fixed effects (column 1) receives the expected (positive) sign. Second, whether fixed effects are included has essentially no effect on the slope—the estimates with and without fixed effects (columns 1 to 3) are roughly equal in magnitude—but the slopes are no longer statistically significant. When the two-way fixed effects specification with the Bartik instrument is used (column 4), the coefficient on κ becomes statistically significant and is approximately twice as large as the other estimates that use the gap, and is also roughly twice as large as the corresponding estimate obtained using the unemployment rate. The results for ψ—the slope coefficient from equation (6.4)—are broadly similar (panel 4).

These findings suggest a different interpretation of the results in Hazell et al. (2020). First, the fact that we no longer obtain a statistically significant estimate of κ when we use the gap

[22] Hazell et al. (2020) explain the larger coefficients in the equation (6.4) specification as stemming from the unemployment rate's serving as a proxy for the discounted sum; under the assumption that u_{it} follows an AR(1) process with a positive autoregressive parameter that is less than one, that sum will be a multiple of the unemployment rate that is greater than one (see note 20, above).

specification (column 3) likely reflects the fact that variations in state-level U-star have predictive power for state-level nontradables price inflation. By smoothing through any cyclical variation, the discounted forward sum of the unemployment rate will approximate the discounted forward sum of U-star—that is, the trend component will dominate the forward sum.[23] On average, both U-star and inflation trend lower over the sample period. Hence, rather than recovering a Phillips curve correlation, the specifications in panel 1 are capturing this low-frequency co-movement between inflation and the natural rate.

In addition, our finding that the gap-based estimate of κ increases when we use the Bartik instrument has two implications. First, in contrast to Hazell et al.'s claim (p. 1331), inclusion of two-way fixed effects is apparently not sufficient to capture relevant supply shocks (such as shocks to the natural rate of unemployment).[24] Second, the larger value of κ that obtains in the gap-based specification when the Bartik instrument is used suggests that we are not recovering a structural estimate of the slope. As Hazell et al. note, the Bartik demand instrument is more persistent than the unemployment rate itself; they use this fact to explain why the "reduced-form" parameter ψ receives a larger coefficient when the Bartik instrument is used. Specifically, Hazell et al. argue that the size of ψ could be lower if (for example) a demand shock is attributable to a temporary policy change, while κ should be policy invariant, as it represents a structural parameter (p. 1332). (Put differently, ψ embeds both the structural parameter κ as well as the average persistence of unemployment rate movements, but this persistence can vary depending on the source and nature of the shock to unemployment.) However, under the gap-based specification we obtain an estimate of κ that is nearly twice as large when the Bartik instrument is used, suggesting that we are not in fact recovering a structural estimate of the slope.[25]

[23] Recall that our trend-cycle decomposition implies that the cyclical component of the unemployment rate is stationary and mean zero.

[24] Because the Bartik instrument should do a better job isolating purely demand-related changes in the unemployment rate, Hazell et al. (2020), p. 1331, argue that finding a similar estimate of κ across specifications that instrument with the lagged unemployment rate or the Bartik term is evidence that the fixed effects are fully capturing any supply shocks. When we use a gap-based specification that explicitly controls for changes in the natural rate of unemployment, however, the point estimate of κ doubles when the Bartik instrument is used.

[25] This increase in the size of κ could reflect an interaction between the greater persistence of the Bartik instrument and the low-frequency movement between U-star and inflation—see the discussion in the previous paragraph—or the hysteresis mechanism we discuss below.

Table 3: ESTIMATION RESULTS WITH SHORT- AND LONG-TERM UNEMPLOYMENT

	(1) No FE	(2) No TE	(3) SE&TE	(4) Instrument (SE&TE)
1. UR $<$ 7 **months**				
U-sum (κ)	-0.00783***	0.00771	0.00912**	0.0119**
	(0.00185)	(0.00482)	(0.00414)	(0.00467)
Obs.	4,460	4,460	4,460	4,059
2. Eqn. (6.4)				
Lagged UR (ψ)	-0.295***	0.105**	0.141**	0.782**
	(0.0659)	(0.0528)	(0.0655)	(0.315)
Obs.	4,460	4,460	4,460	4,059
3. U-gap $<$ 7 **months**				
U-gap-sum (κ)	0.00198	0.0464	0.0105	0.0273*
	(0.00761)	(0.0647)	(0.00928)	(0.0142)
Obs.	4,460	4,460	4,460	4,059
4. Eqn. (6.4)				
Lagged U-gap (ψ)	0.0228	0.109*	0.0866	1.994**
	(0.0723)	(0.0590)	(0.0803)	(0.934)
Obs.	4,460	4,460	4,460	4,059
5. UR $>$ 6 **months**				
U-sum (κ)	0.00507**	-0.00864**	0.00602	0.0101**
	(0.00243)	(0.00375)	(0.00526)	(0.00421)
Obs.	4,460	4,460	4,460	4,059
6. Eqn. (6.4)				
Lagged UR (ψ)	0.110**	-0.0832	0.0970	0.632**
	(0.0555)	(0.0517)	(1.111)	(0.262)
Obs.	4,460	4,460	4,460	4,059
7. U-gap $>$ 6 **months**				
U-gap-sum (κ)	0.0169***	-0.00477	0.00718	0.0167**
	(0.00646)	(0.0148)	(0.00857)	(0.00800)
Obs.	4,460	4,460	4,460	4,059
8. Eqn. (6.4)				
Lagged U-gap (ψ)	0.147***	0.0162	0.0749	0.964**
	(0.0475)	(0.0581)	(0.111)	(0.422)

Note: See Table 2. **Source:** Authors' calculation.

Next, we assess whether the Phillips curve slope differs by unemployment duration by replacing the state-level unemployment rates and unemployment-rate gaps with their short-term and long-term components. Across many states, the trends in these duration components have moved in opposite directions since the 2000s; their cyclical dynamics also differ, which suggests it might be informative to estimate separate Phillips curves for short-term and long-term unemployment. Table 3, which mirrors the structure of Table 2, reports these estimation results.

The first noteworthy finding is that the slope coefficients from the models with two-way fixed effects (column 3) are all statistically insignificant when the unemployment gap is used. In contrast, both the short-term and long-term gaps receive statistically significant coefficients in the model that uses the Bartik instrument (panels 3 and 7, column 4), which is consistent with the aggregate results. However, the coefficient on each individual gap is larger than the coefficient on the aggregate gap (in the case of the short-term gap, the coefficient is more than 2.5 times larger than its aggregate counterpart). Similarly, the coefficients on the short- and long-term lagged unemployment rate gap (ψ) obtained using the Bartik instrument are significantly larger than the corresponding coefficient on the aggregate gap (compare column 4 of panels 4 and 8 with column 4 of panel 4 in Table 2). Together, these results suggest that differences in the cyclicality of the short-term and long-term unemployment components partially offset each other in the aggregate, resulting in a more-muted overall cyclical response.

The statistically significant coefficient on the long-term gap is also noteworthy inasmuch as it points to a possible role for hysteresis in inflation dynamics. The long-term unemployed are likely to include workers prone to scarring effects and labor force detachment, which are the core mechanisms of unemployment hysteresis. Changes in the long-term component of the gap that result from changes in local demand (as captured by the Bartik instrument) receive a significant coefficient in the Phillips curve, which in turn suggests a potential interaction between demand shocks and structural unemployment. Finally, comparing panel 1 of Table 3 with panel 1 of Table 2 suggests that the original results of Hazell et al. are largely driven by the short-term unemployment rate. Given that the overall trend in the unemployment rate was predominantly influenced by its short-term component during the sample period, this finding further supports the conclusion that those results reflect an association between U-star and inflation.

We next repeat Hazell et al.'s exercise that looks at the stability of the slope coefficients before and after 1990. Table 4 shows results for the models with two-way fixed effects (columns 1 and 2 give the slope estimates when lagged unemployment is used as an instrument, and columns 3 and 4 give the estimates when the Bartik instrument is used). For the gap-based models, neither estimate of κ is statistically significant after 1990 (columns 2 and 4); in both subsamples, we again find the result that the gap-based estimates of κ increase noticeably (though not significantly) when the Bartik instrument is used.

It is worth noting that the flattening of the Phillips curve that is implied by the ψ estimates in the model with two-way fixed effects is similar in magnitude to what we recover from a conventional aggregate Phillips curve fit to quarterly data, *so long as* we account for the shift in the inflation process that occurred in the mid-1990s. Prior to the mid-1990s, inflation dynamics were essentially $I(1)$, implying that inflation was characterized by an "accelerationist" specification during this period. Subsequently—and at least until the pandemic-related inflation surge—inflation became mean-reverting around a stable stochastic trend.[26] Simple quarterly Phillips curves that account for this shift in the inflation process imply a slope of 0.225 prior to the mid-1990s with a subsequent decline to 0.026.[27] These point estimates are very similar to the ones we obtain for ψ pre- and post-1990, which in turn suggests that the flattening of the Phillips curve documented in aggregate data is also being captured here. (Note that this interpretation differs from the one given by Hazell et al., who argue that the apparent flattening of the aggregate Phillips curve is an artifact of not controlling for inflation expectations.)

[26] See chapter 6 of Rudd (2024) for a full discussion.

[27] The aggregate quarterly models use an unemployment gap (defined using CBO's noncyclical unemployment rate) and relative import prices, and measure inflation as the annualized log-difference in the core CPI excluding housing. (We exclude housing to better match the inflation measure used in the state-level regressions and to avoid the effect of the change in CPI housing-cost measurement in the early 1980s.) The first model relates the first-difference of inflation to import prices and the gap and is fit from 1978:Q1 to 1991:Q4; the second model relates the level of inflation to three own lags, the gap, and the import price term, and is fit from 1995:Q1 to 2017:Q4. (We start in 1995 because inflation becomes mean reverting around 1995, following a persistent reduction that took place in the wake of the 1990–1991 recession.)

Table 4: Phillips Curve Slope Pre- and Post-1990

	Time FE, lag UR IV		**Time FE, Bartik IV**	
	Pre-1990	Post-1990	Pre-1990	Post-1990
	(1)	(2)	(3)	(4)
A. Unemployment rate				
Sum (κ)	0.011	0.004	0.011***	0.005*
	(0.008)	(0.003)	(0.002)	(0.002)
Eq. 6.4 (ψ)	0.208*	0.072	0.423	0.342**
	(0.119)	(0.063)	(0.333)	(0.169)
B. Unemployment gap				
Sum (κ)	0.016	0.002	0.021***	0.009
	(0.015)	(0.005)	(0.002)	(0.006)
Eq. 6.4 (ψ)	0.240*	0.017	0.467	0.651*
	(0.134)	(0.074)	(0.315)	(0.338)
N	788	3,672	387	3,672

Note: All regressions include state fixed effects. Standard errors in parentheses. * $p < 0.10$, ** $p < 0.05$, *** $p < 0.01$.

The preceding analysis has two important implications for the identification of the Phillips curve using state-level data. To begin with, because state-level U-stars exhibit meaningful time variation and substantial heterogeneity across states, the assumption that a state-level U-star is constant or closely aligned with an aggregate estimate is likely to be a poor one (by extension, two-way fixed effects will be unable to control for the heterogeneity in state-level U-stars over time or at a particular point in time). Second, the slope estimates from the forward-looking Phillips curve specification appear to reflect a correlation between state-specific natural rates and nontradables inflation rather than a relation between inflation and cyclical movements in unemployment. By extension, the large and statistically significant correlation between inflation and demand-driven variation in the lagged unemployment rate or unemployment gap is consistent with the standard description of the Phillips curve as a relation between labor-market slack and inflation, as opposed to a new-Keynesian interpretation in which the unemployment rate acts as a proxy for expectations of future costs.

6.2 Discussion of the structural model

The finding that the discounted forward sum of unemployment gaps in equation (6.1) plays little to no role in inflation determination is in line with earlier tests of the new-Keynesian Phillips curve using aggregate data. Rudd and Whelan (2005) proposed testing the basic new-Keynesian Phillips curve,

$$\pi_t = \beta E_t \pi_{t+1} + \kappa x_t, \tag{6.5}$$

where x_t denotes a measure of excess demand or cost pressures such as an unemployment or output gap, by solving it forward K periods to yield

$$\pi_t = \kappa E_t \sum_{i=0}^{K} x_{t+i} + \beta^{K+1} E_t \pi_{t+K+1}. \tag{6.6}$$

(Note that this solution is exact and does not suffer from truncation error, in contrast to the finite-sum approximation used by Hazell et al., 2020.) Equation (6.6) can then be estimated by GMM under the assumption that the realized future value of a variable will equal its time-t expectation plus an unforecastable (rational) expectational error; alternatively, VAR-based forecasts of x_{t+i}

can be generated and used to assess the model's ability to track inflation.[28] Tests of equation (6.6) using aggregate data typically found little support for the model, in that the forward sum had little to no ability to explain actual inflation.[29]

The results that we obtain from state-level data can be viewed as confirming the new-Keynesian model's inability to provide a good description of inflation dynamics. The estimates of κ that we found using unemployment-rate gaps as the driving variable x_t were not only small, but were consistently statistically insignificant, implying that the model's prediction that forward-looking behavior should dominate price setting finds no support in the data.

Tests of equation (6.6) also found that the new-Keynesian model was unable to explain the significant role played by lagged inflation in empirical inflation equations prior to the mid-1990s. This latter fact is directly relevant to the main argument of Hazell et al.'s paper. Hazell et al. document that their estimated model explains almost none of the variation in nonhousing inflation, and use their finding of a flat Phillips curve to argue that the Volcker disinflation of the 1980s was mostly the result of a shift in long-run inflation expectations as opposed to the rise in unemployment that was induced by tight monetary policy.[30] But the real reason that the model cannot fit the 1980s well is because the forward sum of equation (6.6) cannot account for the persistence in inflation that made the Volcker disinflation so costly in terms of unemployment.

We might also be surprised at Hazell et al.'s claim that long-term inflation expectations matter in the context of the new-Keynesian Phillips curve. Equation (6.5) involves a short-term expectation, and while the closed-form solution of the model (6.6) involves a forward sum that goes to infinity as K does, the expectation of that forward sum *is* the (short-term) expectation of next period's inflation rate. Moreover, allowing for nonzero trend inflation in a Calvo model significantly changes the nature of the price-setting problem (and the model's solution) so that the resulting model looks very different from a simpler version like (6.5).[31] More broadly, Werning

[28]As Rudd and Whelan (2005) discuss, equation (6.6) does not suffer from problems that make instrumental variables estimates of equation (6.5) unreliable. In addition, when this approach is applied to "hybrid" new-Keynesian models (where lagged inflation is included on the right-hand-side of equation 6.5), GMM estimation is less likely to suffer from the weak-instrument problems that attend direct tests of the hybrid model. (The fact that this is true actually provides additional evidence against the new-Keynesian Phillips curve, since tests of equations like 6.5 and 6.6 should be identical if the model is correct.)

[29]See Rudd and Whelan (2007) for a summary.

[30]The inability of their model to explain nonhousing price inflation is documented in their appendix figure C.3.

[31]See Ascari and Sbordone (2014).

(2022) examined the role of short- versus long-term expectations in the context of a general class of sticky-price models (albeit models in which the effects of nonzero trend inflation aren't considered). He argues that short-run inflation expectations are more important, in the sense that the influence of long-term expectations goes to zero as the long term gets longer; specifically, his result shows that the influence of $E_t\pi_{t+i}$ goes to zero as i gets large.[32]

These considerations suggest that finding a role for long-run expectations in canonical sticky-price models would be harder than one might think.[33] However, Hazell et al. claim that it's actually a straightforward undertaking. They start with the basic new-Keynesian Phillips curve,

$$\pi_t = \beta E_t \pi_{t+1} - \kappa \left(u_t - u_t^n \right) + \nu_t, \tag{6.7}$$

where $(u_t - u_t^n)$ is the unemployment gap (u^n is the natural rate) and ν_t captures other inflation shocks. The closed-form solution of the model can be written as

$$\pi_t = -\kappa E_t \sum_{j=0}^{\infty} \beta^j \left(u_{t+j} - u_{t+j}^n \right) + v_t, \tag{6.8}$$

where v_t collects the expected future discounted sum of the ν terms,

$$v_t = E_t \sum_{j=0}^{\infty} \beta^j \nu_{t+j} \tag{6.9}$$

(typically values of ν after time t are assumed to have an unconditional mean of zero, though they don't have to). But Hazell et al. instead solve the model to yield the equivalent expression

$$\pi_t = -\kappa E_t \sum_{j=0}^{\infty} \beta^j u_{t+j} + \omega_t, \tag{6.10}$$

[32]That finding doesn't quite rule out a role for long-run expectations, because what Werning refers to as "[long-run] expectations" are better thought of as "far-future expectations." In particular, his result is still consistent with an expectation of inflation over some longish horizon T, for example $\frac{1}{T} E_t \sum_{i=1}^{T} \pi_{t+i}$, having an important effect on current inflation. Moreover, long-term expectations will remain an important influence on inflation if short-term expectations are formed as the sum of a long-run (trend) component and a transitory component. But Werning's result does contradict the solution that Hazell et al. propose.

[33]Even allowing for a time-varying inflation trend in a canonical sticky-price model, as is done by Ascari and Sbordone (2014), causes the model to deliver patently counterfactual predictions (in particular, that the Phillips curve should be steepest in low-inflation periods like the 2000s, or that inflation persistence should be lowest in high-inflation periods like the 1970s)—see Rudd (2022) for a discussion.

where ω_t collects the expected discounted forward sum of the u^n and ν terms,

$$\omega_t = E_t \sum_{j=0}^{\infty} \beta^j (\kappa u^n_{t+j} + \nu_{t+j}). \tag{6.11}$$

They then define the "transitory" component of unemployment, $\tilde{u}_t$, as

$$\tilde{u}_t = u_t - E_t u_{t+\infty}. \tag{6.12}$$

Adding and subtracting $\frac{\kappa}{1-\beta} E_t u_{t+\infty}$ on the right side of equation (6.10) and noting that

$$-\frac{\kappa}{1-\beta} E_t u_{t+\infty} = E_t \pi_{t+\infty}, \tag{6.13}$$

lets us rewrite the equation in terms of $\tilde{u}$ as

$$\pi_t = -\kappa E_t \sum_{j=0}^{\infty} \beta^j \tilde{u}_{t+j} + E_t \pi_{t+\infty} + \omega_t. \tag{6.14}$$

Hazell et al. claim that the presence of the $E_t \pi_{t+\infty}$ term in equation (6.14), which enters the equation with a coefficient of one, demonstrates the importance of long-run expectations.

This solution is puzzling when we compare it with equation (6.6). As that equation shows, if inflation is bounded, then the terminal inflation term $\beta^{K+1} E_t \pi_{t+K+1}$ should go to zero as K goes to infinity; that's the reason that a terminal inflation term isn't present in equations (6.8) or (6.10) and it's also the reason that a rational-expectations solution exists. So why does a $E_t \pi_{t+\infty}$ term appear in equation (6.14)?

The puzzle is resolved when we see that the solution proposed by Hazell et al. is either vacuous or leads to inconsistencies. As was noted in the derivation to equation (6.14), all we are doing is adding and subtracting the same term $E_t \pi_{t+\infty} = \frac{-\kappa}{1-\beta} E_t u_{t+\infty}$ on the right-hand side of the equation, and we assume that the public's expectations respect this consistency relation (equation 6.13). Hence, if people's expectation $E_t \pi_{t+\infty}$ were to rise (say) by a percentage point, they should revise their expectation for $E_t u_{t+\infty}$ by $-(1-\beta)/\kappa$. But that implies no change to the right-hand side of equation (6.14), and so no change in inflation, for the same expected sequence of current and future actual unemployment rates $E_t u_{t+j}$. And that in turn implies that inflation will not converge to the new $E_t\pi_{t+\infty}$ and the unemployment rate will not converge to the new $E_t u_{t+\infty}$, which violates the definition of these terms and also implies that the unconditional mean of $\tilde{u}$ will not be zero. (This last point implies that the solution Hazell et al. obtain when they assume $\beta = 1$ is incorrect.)

We also run into problems if we assume that $E_t\pi_{t+\infty}$ and $E_t u_{t+\infty}$ are free to change independently, so that equation (6.13) doesn't have to hold. If we raise u_{t+j} and $E_t u_{t+\infty}$ by the same amount in every period, inflation will be unchanged according to equation (6.14). So we get the same inflation rate even though the sequence of unemployment gaps $u_{t+j} - u^n_{t+j}$ is different in the two cases, which obviously violates equation (6.8).[34] And there is another, common-sense reason to be skeptical of the implications of Hazell et al.'s expression (6.14) if $E_t\pi_{t+\infty}$ is allowed to vary independently. Similar to Werning (2022), $E_t\pi_{t+\infty}$ is an expectation of *far-future* inflation rather than long-term inflation expectations as they are typically thought of (and that Hazell et al. use in their empirical work with aggregate data). It seems *a priori* implausible that a revision to the expectation of the rate of inflation in the very far future would have an immediate effect on current inflation, but that is what equation (6.14) implies.[35]

7 Conclusion

This paper estimates state-level trend unemployment rates using a duration-structure model that exploits information in unemployment inflows and duration-dependent outflows. Applying the framework of Ahn (2023) to all 50 U.S. states and the District of Columbia reveals substantial heterogeneity in trend U-stars across regions, particularly in the component of U-star that reflects

[34] A more contrived example assumes that the natural rate u^n permanently changes by some amount, with the effect on current inflation exactly offset in this case by a suitable one-time change in $E_t\pi_{t+\infty}$ and where the sequence of $u_{t+j} - E_t u_{t+\infty}$ terms is kept the same. That again implies that inflation will not converge to $E_t\pi_{t+\infty}$. Note also that in the degenerate case when the policymaker sets its target for π^* and u^* in a manner that is consistent with the long-run Phillips curve tradeoff $u^* = (1-\beta)\pi^*/\kappa$ and agents correctly expect $E_t\pi_{t+\infty} = \pi^*$ and $E_t u_{t+\infty} = u^*$, then we can't say that expectations are free variables—they are tied down by the policymaker. (In a fully specified model, if $E_t\pi^* \neq \pi^*$ and $E_t u^* \neq u^*$ but expectations still respect the long-run Phillips curve tradeoff, then individuals' resulting misperception of the policymaker's targets acts like a shock to the policy rule—see Rudd and Whelan, 2003.)

[35] Relatedly, if the new-Keynesian model is specified with the assumption that $\beta = 1$ (which is sometimes done to ensure that the model doesn't imply a long-run level tradeoff between inflation and real activity), it implies that the terminal inflation term in equation (6.6) won't vanish, again leading to the prediction that economic developments expected to occur thousands of years from now can have an immediate, one-for-one effect on current inflation.

long-term (or structural) unemployment. Agricultural states exhibit relatively small structural unemployment shares, while Rust Belt and several Sun Belt states display elevated long-term unemployment, highlighting persistent regional differences in labor-market functioning. We also find that the secular decline in trend U-star at the national level has not been broad-based, with U-stars in roughly half of the states showing little or no decline. Although cross-state dispersion has narrowed over time, this convergence is driven mainly by the short-term component, while heterogeneity in long-term unemployment remains pronounced.

Using these estimates, we revisit recent research that has used state-level data to estimate the slope of the Phillips curve. Once the heterogeneous behavior of trend U-star across states is accounted for and the unemployment rate is replaced by the unemployment gap, the slope of the forward-looking Phillips curve becomes statistically insignificant, even when state and time fixed effects are controlled for. This result suggests that previous state-level estimates that find a significant relationship between unemployment and inflation in the context of a new-Keynesian model largely reflect comovement between inflation and slow-moving components of trend unemployment, rather than a relationship between inflation and cyclical movements in labor-market slack. The results also imply that the forward-looking new-Keynesian Phillips curve provides as poor a characterization of state-level inflation dynamics as it does of aggregate inflation.

Overall, our findings underscore the importance of accounting for regional heterogeneity in the natural rate when measuring labor-market slack and estimating the Phillips curve on regional data, with obvious implications for both empirical modeling and the design of stabilization policies.

(a) CONNECTICUT

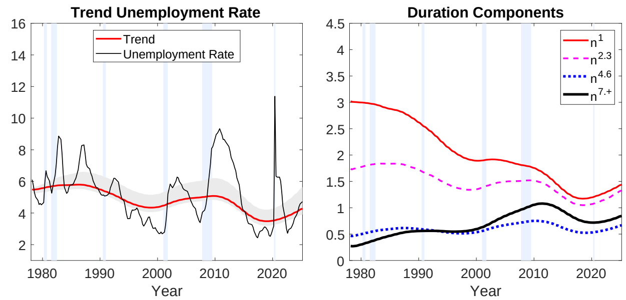

(b) MAINE

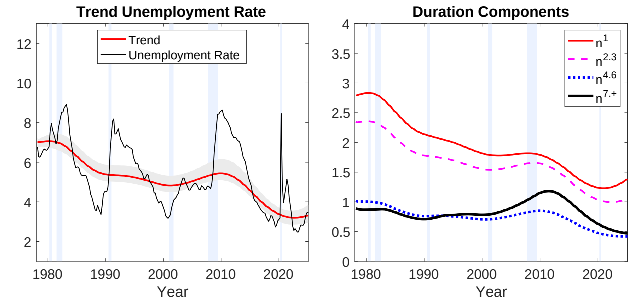

(c) MASSACHUSETTS

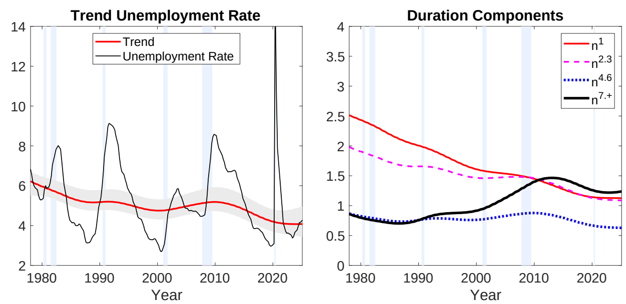

(d) NEW HAMPSHIRE

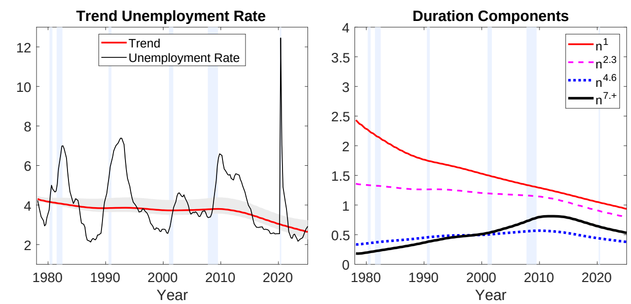

(e) RHODE ISLAND

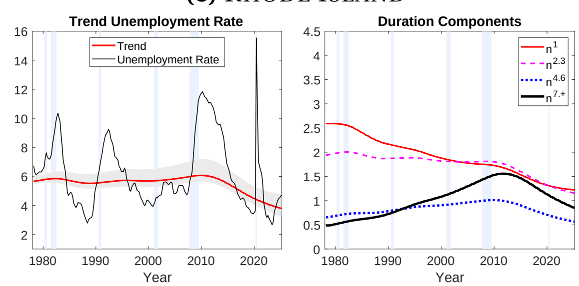

(f) VERMONT

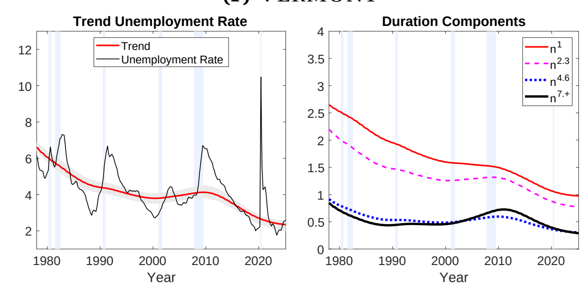

Figure 7: THE FIRST DISTRICT

Notes to figure: For each state, the left panel displays the trend U-star (red line) and its 68 percent posterior interval (grey area) along with the state' unemployment rate (black line). The right panel displays the duration components of the trend U-star: 1 month (red); 2-3 months (dashed magenta); 4-6 months (dotted blue); 7+ months (black). **Source:** Authors' calculation.

(a) NEW YORK

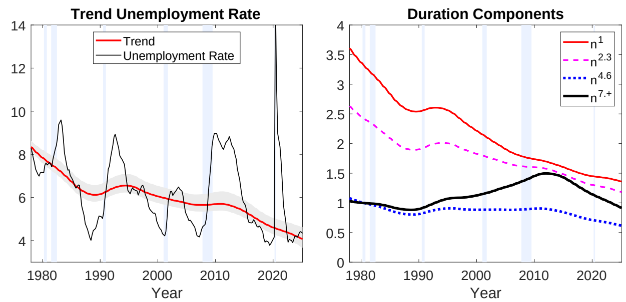

(b) NEW JERSEY

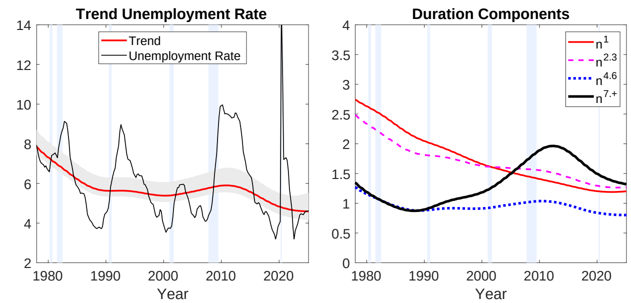

(c) CONNECTICUT

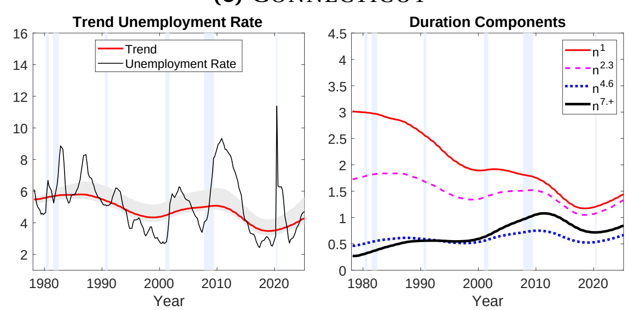

Figure 8: THE SECOND DISTRICT

Notes to figure: For each state, the left panel displays the trend U-star (red line) and its 68 percent posterior interval (grey area) along with the state' unemployment rate (black line). The right panel displays the duration components of the trend U-star: 1 month (red); 2-3 months (dashed magenta); 4-6 months (dotted blue); 7+ months (black). **Source:** Authors' calculation.

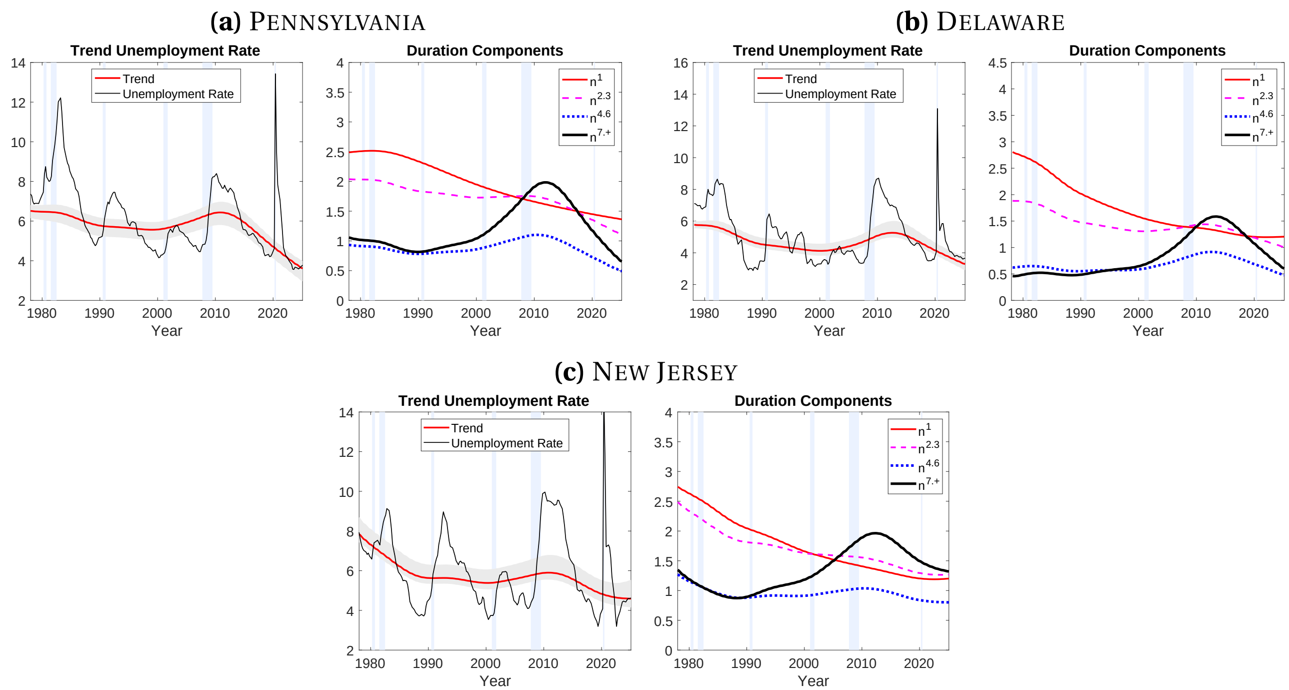

Figure 9: THE THIRD DISTRICT

Notes to figure: For each state, the left panel displays the trend U-star (red line) and its 68 percent posterior interval (grey area) along with the state' unemployment rate (black line). The right panel displays the duration components of the trend U-star: 1 month (red); 2-3 months (dashed magenta); 4-6 months (dotted blue); 7+ months (black). **Source:** Authors' calculation.

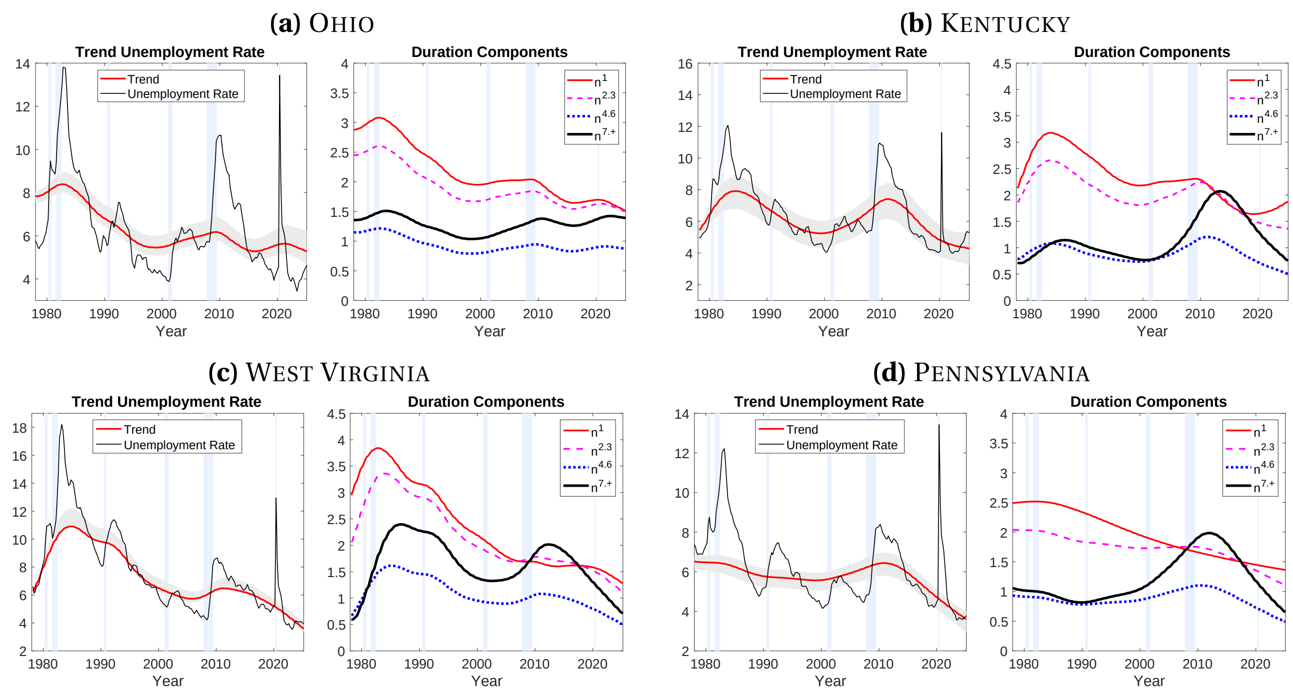

Figure 10: THE FOURTH DISTRICT

Notes to figure: For each state, the left panel displays the trend U-star (red line) and its 68 percent posterior interval (grey area) along with the state' unemployment rate (black line). The right panel displays the duration components of the trend U-star: 1 month (red); 2-3 months (dashed magenta); 4-6 months (dotted blue); 7+ months (black). **Source:** Authors' calculation.

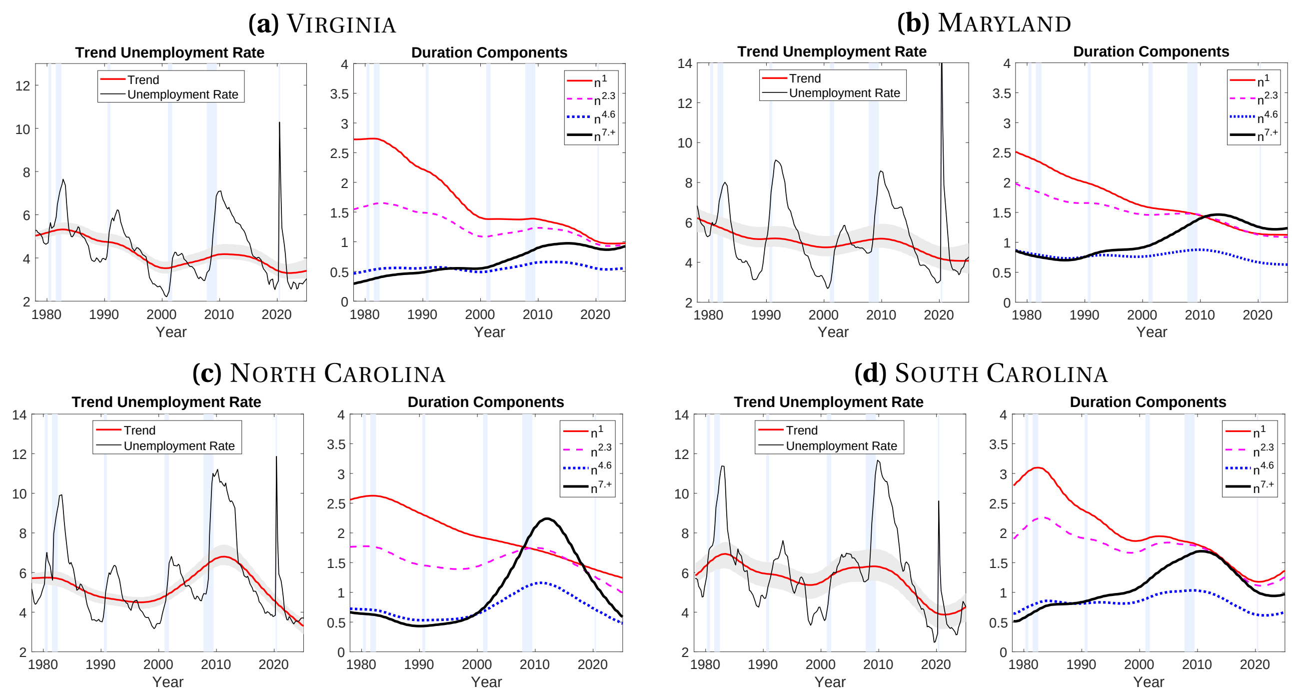

Figure 11: The Fifth District

Notes to figure: For each state, the left panel displays the trend U-star (red line) and its 68 percent posterior interval (grey area) along with the state' unemployment rate (black line). The right panel displays the duration components of the trend U-star: 1 month (red); 2-3 months (dashed magenta); 4-6 months (dotted blue); 7+ months (black). **Source:** Authors' calculation.

(a) ALABAMA

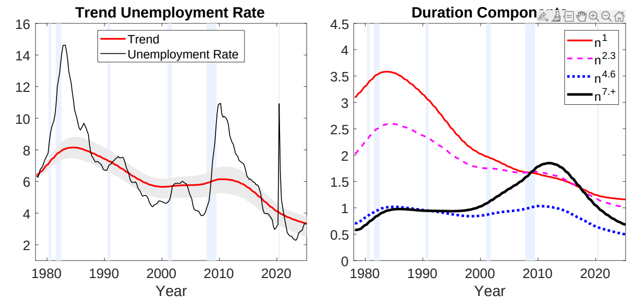

(b) FLORIDA

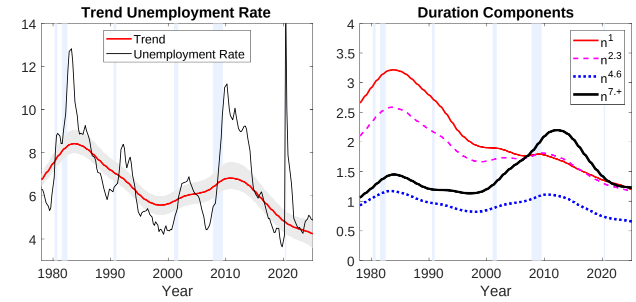

(c) GEORGIA

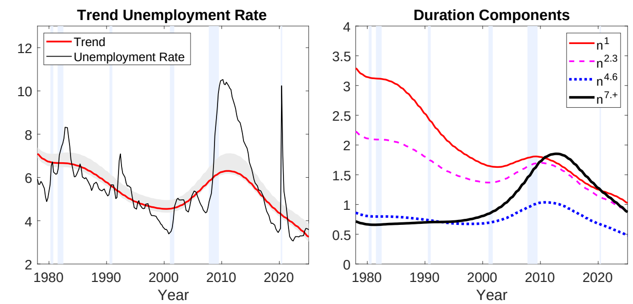

Figure 12: THE SIXTH DISTRICT

Notes to figure: For each state, the left panel displays the trend U-star (red line) and its 68 percent posterior interval (grey area) along with the state' unemployment rate (black line). The right panel displays the duration components of the trend U-star: 1 month (red); 2-3 months (dashed magenta); 4-6 months (dotted blue); 7+ months (black). **Source:** Authors' calculation.

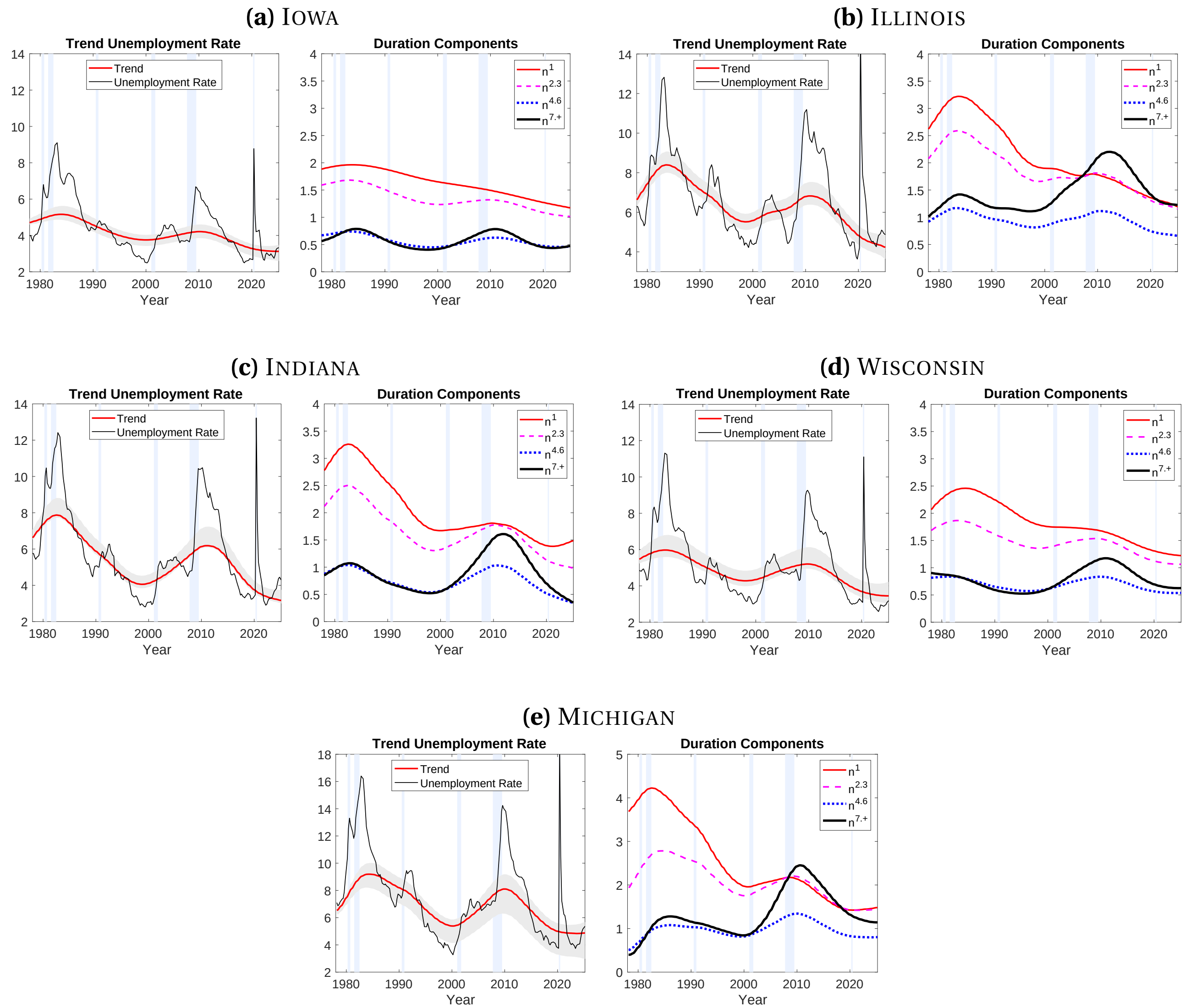

Figure 13: The Seventh District

Notes to figure: For each state, the left panel displays the trend U-star (red line) and its 68 percent posterior interval (grey area) along with the state' unemployment rate (black line). The right panel displays the duration components of the trend U-star: 1 month (red); 2-3 months (dashed magenta); 4-6 months (dotted blue); 7+ months (black). **Source:** Authors' calculation.

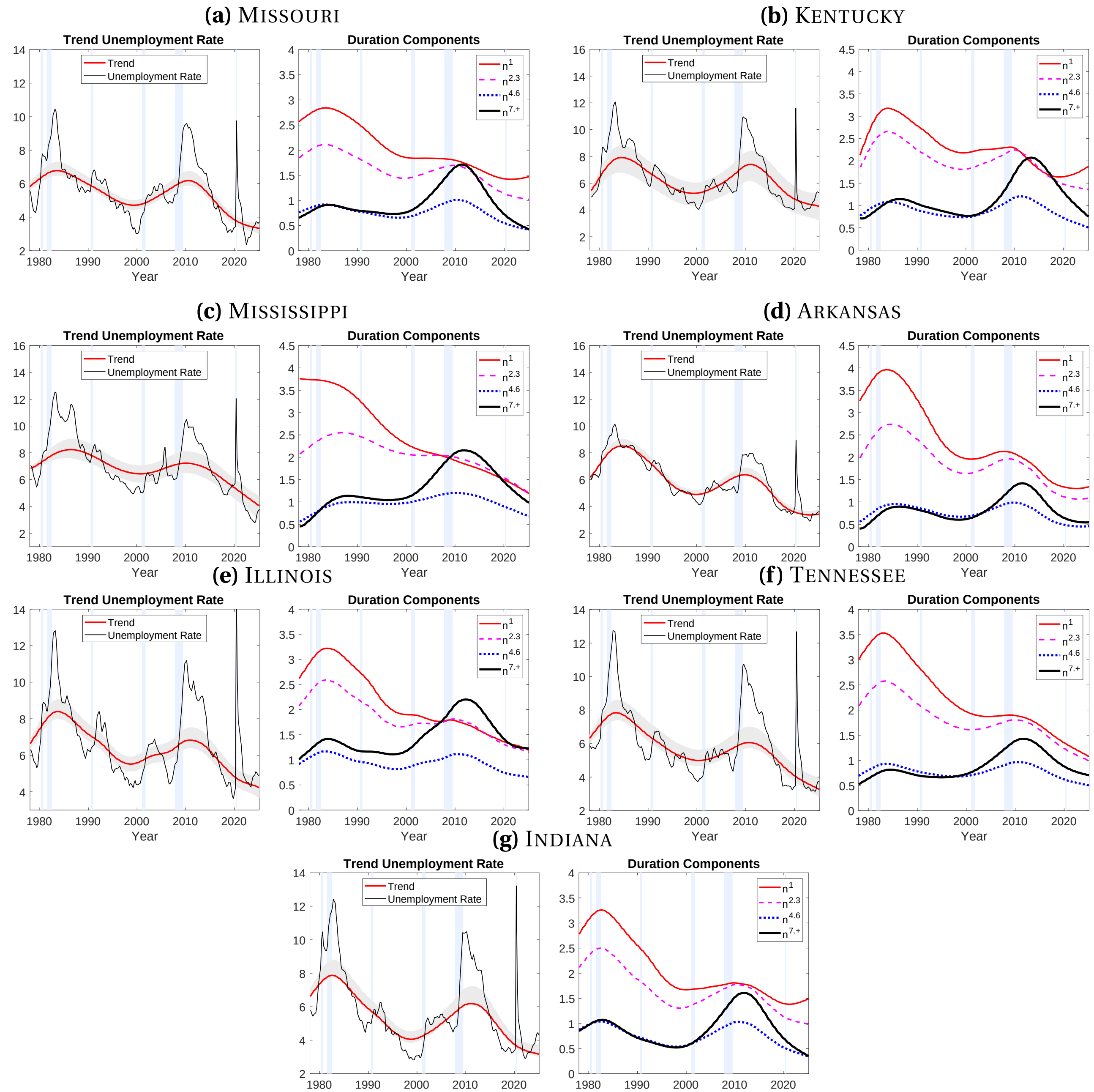

Figure 14: The Eighth District

Notes to figure: For each state, the left panel displays the trend U-star (red line) and its 68 percent posterior interval (grey area) along with the state' unemployment rate (black line). The right panel displays the duration components of the trend U-star: 1 month (red); 2-3 months (dashed magenta); 4-6 months (dotted blue); 7+ months (black). **Source:** Authors' calculation.

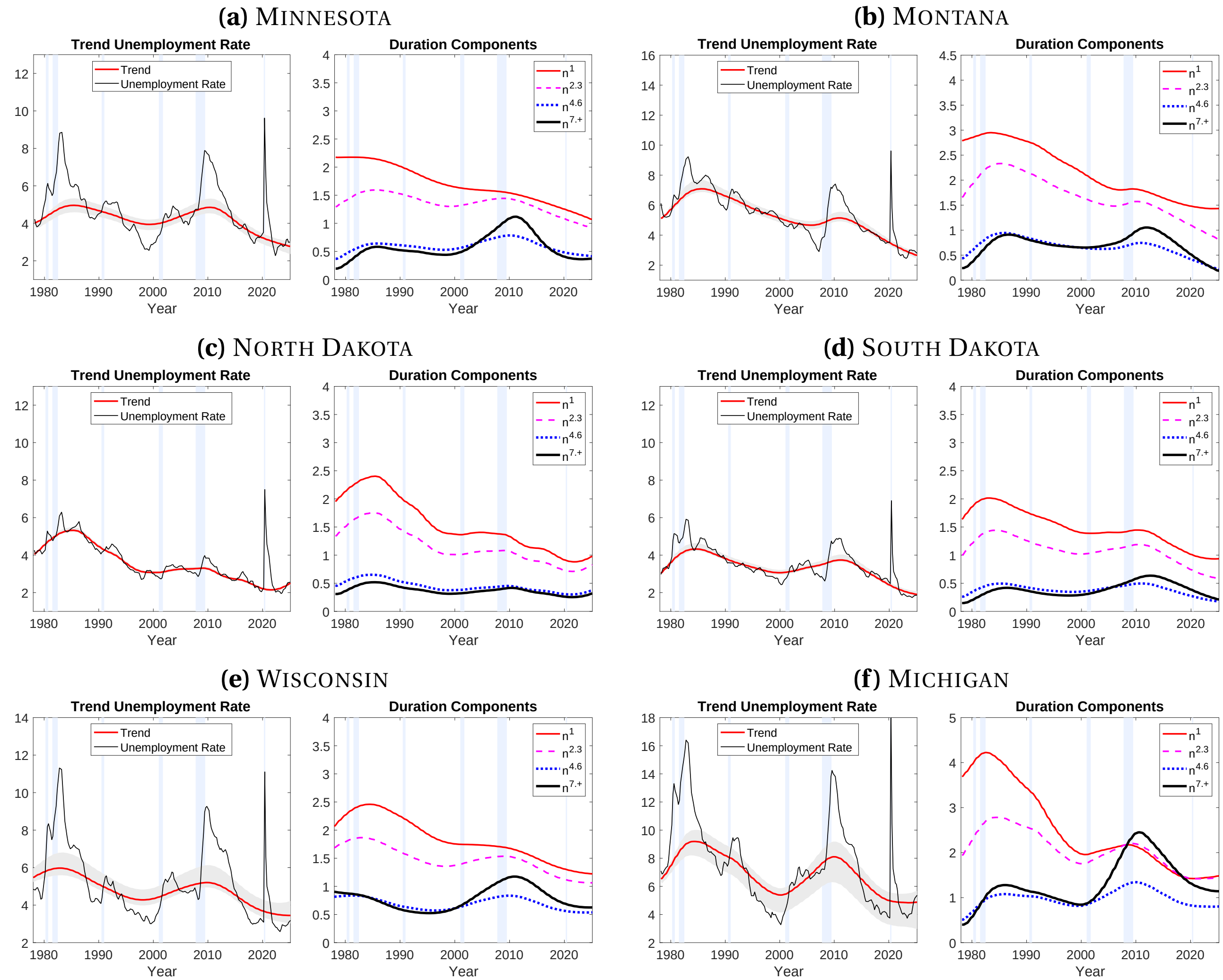

Figure 15: The Ninth District

Notes to figure: For each state, the left panel displays the trend U-star (red line) and its 68 percent posterior interval (grey area) along with the state' unemployment rate (black line). The right panel displays the duration components of the trend U-star: 1 month (red); 2-3 months (dashed magenta); 4-6 months (dotted blue); 7+ months (black). **Source:** Authors' calculation.

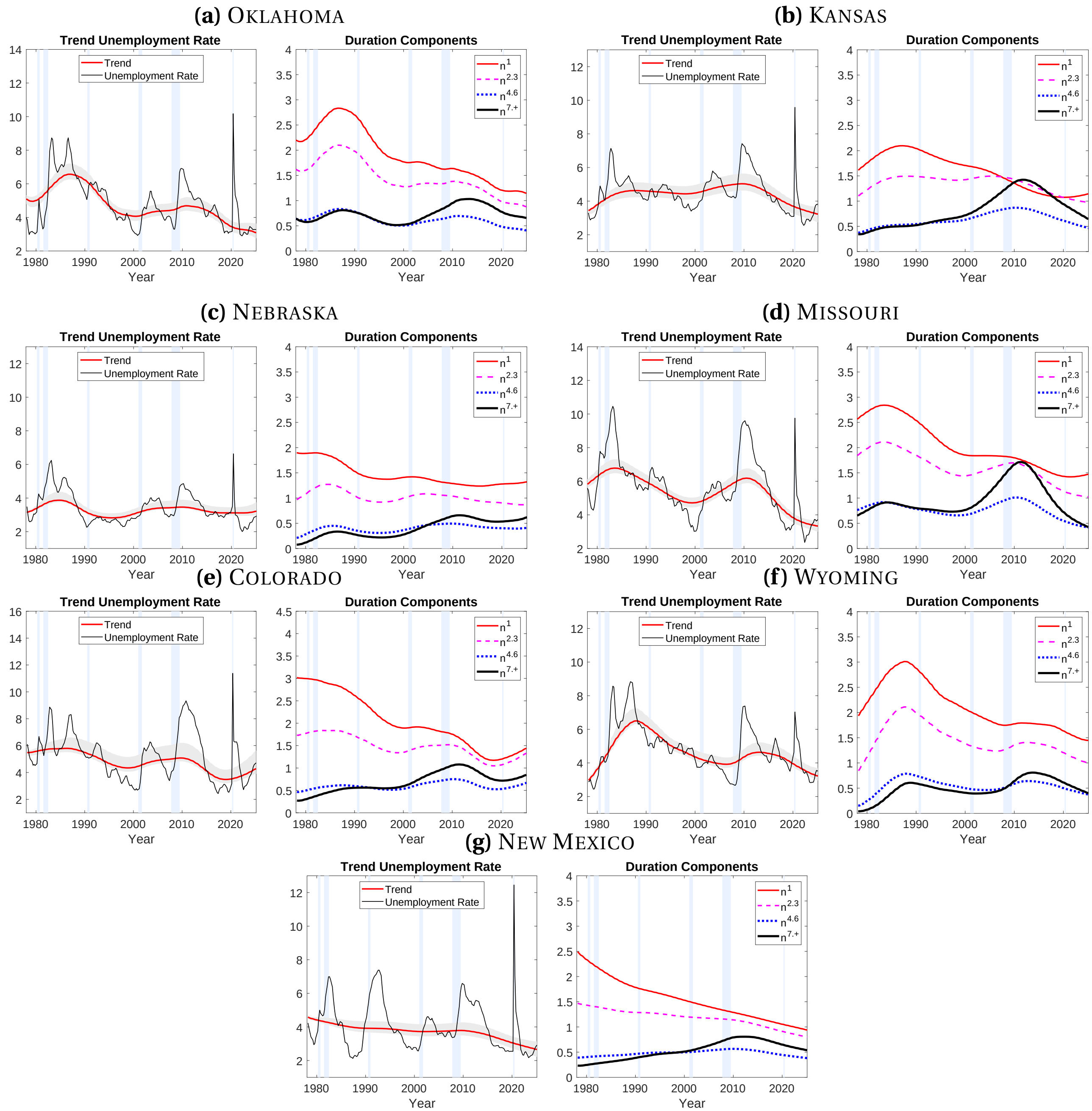

Figure 16: THE TENTH DISTRICT

Notes to figure: For each state, the left panel displays the trend U-star (red line) and its 68 percent posterior interval (grey area) along with the state' unemployment rate (black line). The right panel displays the duration components of the trend U-star: 1 month (red); 2-3 months (dashed magenta); 4-6 months (dotted blue); 7+ months (black). **Source:** Authors' calculation.

(a) TEXAS

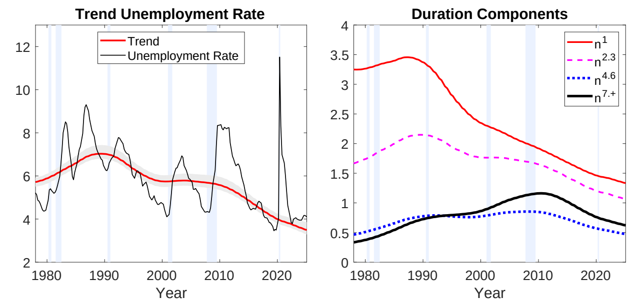

(b) LOUISIANA

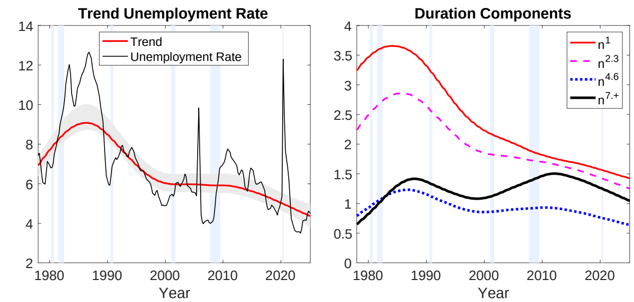

(c) NEW MEXICO

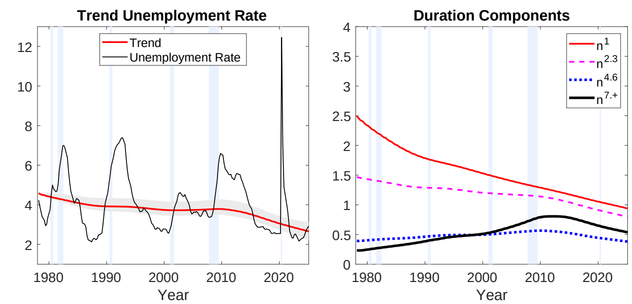

Figure 17: THE ELEVENTH DISTRICT

Notes to figure: For each state, the left panel displays the trend U-star (red line) and its 68 percent posterior interval (grey area) along with the state' unemployment rate (black line). The right panel displays the duration components of the trend U-star: 1 month (red); 2-3 months (dashed magenta); 4-6 months (dotted blue); 7+ months (black). **Source:** Authors' calculation.

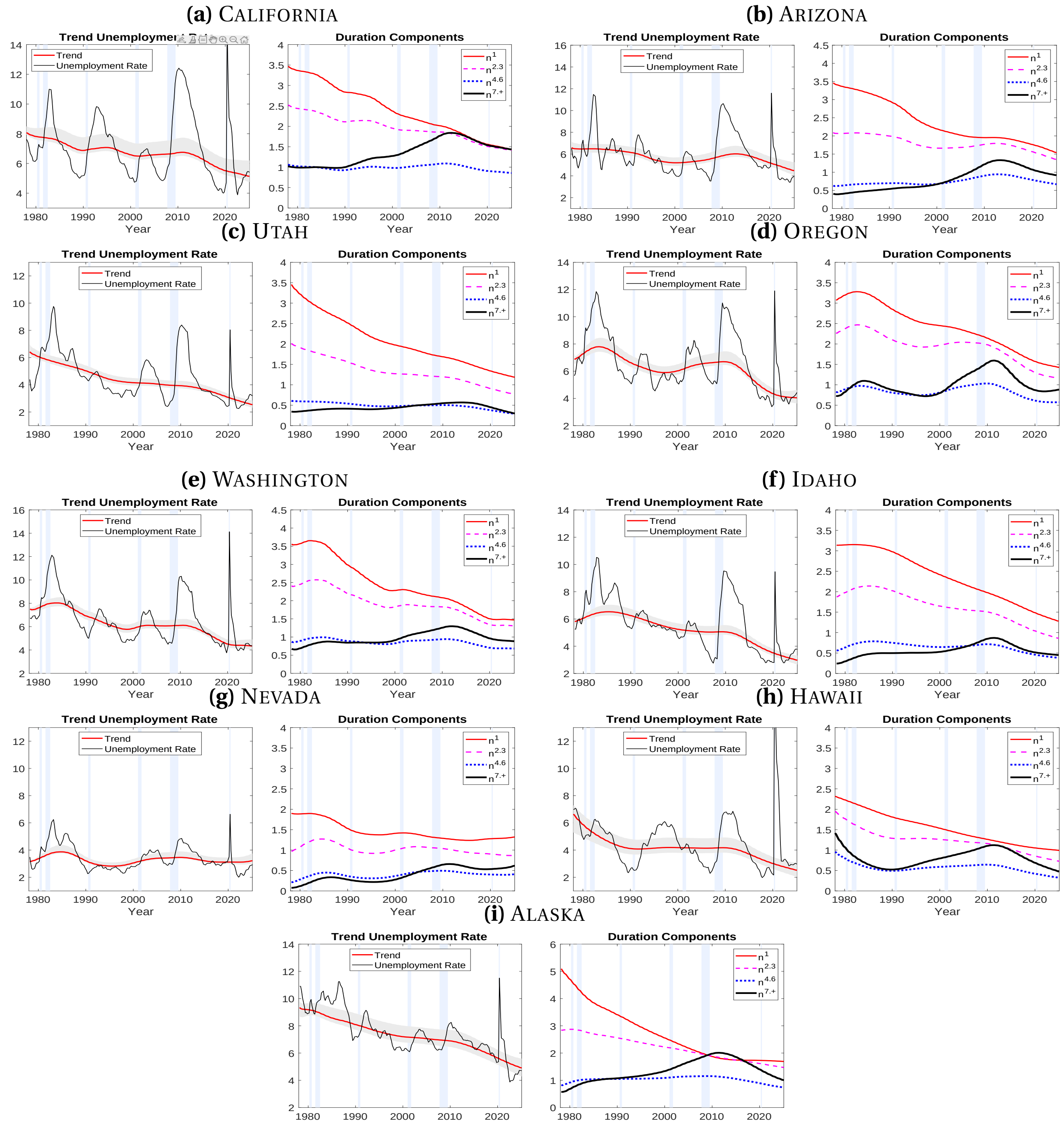

Figure 18: The Twelfth District

Notes to figure: For each state, the left panel displays the trend U-star (red line) and its 68 percent posterior interval (grey area) along with the state' unemployment rate (black line). The right panel displays the duration components of the trend U-star: 1 month (red); 2-3 months (dashed magenta); 4-6 months (dotted blue); 7+ months (black). **Source:** Authors' calculation.

References

Aaronson, Stephanie R, Mary C Daly, William L Wascher, and David W Wilcox, "Okun revisited: Who benefits most from a strong economy?," *Brookings Papers on Economic Activity*, 2019, *2019* (1), 333–404.

Ahn, Hie Joo, "Duration structure of unemployment hazards and the trend unemployment rate," *Journal of Economic Dynamics and Control*, 2023, *151*, 104664.

_ **and Jeremy B. Rudd**, "(Re-)Connecting Inflation and the Labor Market: A Tale of Two Curves," Finance and Economics Discussion Series 2024-050, Board of Governors of the Federal Reserve System (U.S.) July 2024.

Ascari, Guido and Argia M. Sbordone, "The Macroeconomics of Trend Inflation," *Journal of Economic Literature*, September 2014, *52* (3), 679–739.

Barnichon, Regis and Geert Mesters, "On the Demographic Adjustment of Unemployment," *The Review of Economics and Statistics*, 05 2018, *100* (2), 219–231.

Blanchard, Olivier Jean and Lawrence F. Katz, "Regional Evolutions," *Brookings Papers on Economic Activity*, 1992, *23* (1), 1–76.

Cajner, Tomaz, John Coglianese, and Joshua Montes, "The Long-Lived Cyclicality of the Labor Force Participation Rate," *The Review of Economics and Statistics*, 2025.

Chan, Joshua, Gary Koop, Dale J. Poirier, and Justin L. Tobias, *Bayesian Econometric Methods* number 9781108437493. In 'Cambridge Books.', Cambridge University Press, 2019.

Chodorow-Reich, Gabriel and Johannes Wieland, "Secular Labor Reallocation and Business Cycles," *Journal of Political Economy*, 2020, *128* (6), 2245–2287.

Crump, Richard K., Stefano Eusepi, Marc Giannoni, and Ayşegül Şahin, "A Unified Approach to Measuring u^*," NBER Working Papers 25930, National Bureau of Economic Research, Inc June 2019.

_ **,** _ **,** _ **, and** _ , "The Unemployment–Inflation Trade-off Revisited," *Journal of Monetary Economics*, 2024, *141*, 1–25.

Fitzgerald, Terry J., Callum Jones, Mariano Kulish, and Juan Pablo Nicolini, "Is There a Stable Relationship between Unemployment and Future Inflation?," Staff Report 614, Federal Reserve Bank of Minneapolis October 2020.

Fleischman, Charles A. and John M. Roberts, "From many series, one cycle: improved estimates of the business cycle from a multivariate unobserved components model," Finance and Economics Discussion Series 2011-46, Board of Governors of the Federal Reserve System (U.S.) 2011.

Forni, Mario and Marco Lippi, *Aggregation and the Microfoundations of Dynamic Macroeconomics*, Oxford University Press, 1997.

Grant, Angelia L. and Joshua C.C. Chan, "Reconciling output gaps: Unobserved components model and Hodrick–Prescott filter," *Journal of Economic Dynamics and Control*, 2017, *75*, 114 – 121.

Hall, Robert E and Marianna Kudlyak, “The Active Role of the Natural Rate of Unemployment,” Working Paper 31848, National Bureau of Economic Research November 2023.

Hazell, Jonathon, Juan Herreño, Emi Nakamura, and Jón Steinsson, “The Slope of the Phillips Curve: Evidence from U.S. States,” Working Paper 28005, National Bureau of Economic Research October 2020.

Hornstein, Andreas, “Accounting for unemployment: the long and short of it,” Working Paper 12-07, Federal Reserve Bank of Richmond 2012.

_ **and Marianna Kudlyak**, “Aggregate Labor Force Participation and Unemployment and Demographic Trends,” Working Paper Series 2019-7, Federal Reserve Bank of San Francisco February 2019.

_ **and** _ , “Trends in Labor Force Participation and Unemployment, 1976-2024,” Working Paper 2026-11, Federal Reserve Bank of San Francisco 5 2026.

Jo, Yoon Joo and Sarah Zubairy, “State-Dependent Government Spending Multipliers: Downward Nominal Wage Rigidity and Sources of Business Cycle Fluctuations,” *American Economic Journal: Macroeconomics*, January 2025, *17* (1), 379–413.

Lenza, Michele and Giorgio E. Primiceri, “How to estimate a vector autoregression after March 2020,” *Journal of Applied Econometrics*, 2022, *37* (4), 688–699.

McLeay, Michael and Silvana Tenreyro, “Optimal Inflation and the Identification of the Phillips Curve,” *NBER Macroeconomics Annual*, 2020, *34*, 199–255.

Nakamura, Emi and Jón Steinsson, “Fiscal Stimulus in a Monetary Union: Evidence from US Regions,” *American Economic Review*, March 2014, *104* (3), 753–92.

Ng, Serena, “Modeling Macroeconomic Variations After COVID-19,” Papers 2103.02732, arXiv.org March 2021.

Rudd, Jeremy, “Why do we think that inflation expectations matter for inflation? (And should we?),” *Review of Keynesian Economics*, 2022, *10* (1), 25–45.

_ **and Karl Whelan**, “Inflation Targets, Credibility, and Persistence in a Simple Sticky-Price Framework,” Finance and Economics Discussion Series 2003-043, Board of Governors of the Federal Reserve System (U.S.) 2003.

_ **and** _ , “New tests of the new-Keynesian Phillips curve,” *Journal of Monetary Economics*, 2005, *52* (6), 1167–1181.

_ **and** _ , “Modeling Inflation Dynamics: A Critical Review of Recent Research,” *Journal of Money, Credit and Banking*, 2007, *39* (s1), 155–170.

Rudd, Jeremy B., *A Practical Guide to Macroeconomics*, Cambridge University Press, 2024.

Stock, James H. and Mark W. Watson, “Median unbiased estimation of coefficient variance in a time-varying parameter model,” *Journal of the American Statistical Association*, March 1998, *93* (441), 349–358.

Tasci, Murat, “The ins and outs of unemployment in the long run: unemployment flows and the natural rate,” Working Papers 1224, Federal Reserve Bank of Cleveland 2012.

Werning, Ivan, “Expectations and the Rate of Inflation,” NBER Working Papers 30260, National Bureau of Economic Research Jul 2022.

A Priors

A.1 Trend–cycle model

For each series of length T, let y_t denote the (quarterly, time-aggregated) observation. The model is the unobserved-components specification

$$y_t = \tau_t + c_t, \tag{A.1}$$

$$\Delta^2\tau_t = \tau_t - 2\tau_{t-1} + \tau_{t-2} = u_t, \qquad u_t \sim (0, \sigma_\tau^2), \tag{A.2}$$

$$c_t = \phi_1 c_{t-1} + \phi_2 c_{t-2} + \varepsilon_t, \qquad \varepsilon_t \sim (0, \sigma_c^2), \tag{A.3}$$

for $t = 1, \ldots, T$, with $u_t \perp \varepsilon_s$ for all t, s. The trend τ_t follows an I(2) process so that its first difference—the local growth rate—evolves as a random walk; this is the standard "smooth trend" specification of Harvey (1989) and underlies the Chan–Grant style sampler used here. The cycle c_t follows a stationary AR(2) process whose roots are restricted to lie inside the unit circle.

Stacking (A.2) for $t = 1, \ldots, T$ yields

$$H_2\boldsymbol{\tau} = \alpha_{\tau_0} + \boldsymbol{u}, \qquad \boldsymbol{u} \sim (\mathbf{0}, \sigma_\tau^2 I_T),$$

where H_2 is the second-difference matrix and α_{τ_0} collects the initial conditions (τ_0, τ_{-1}). Stacking (A.3) similarly yields

$$H_\phi(y - \boldsymbol{\tau}) = \boldsymbol{\varepsilon}, \qquad \boldsymbol{\varepsilon} \sim (\mathbf{0}, \sigma_c^2 I_T),$$

with H_ϕ the lower-triangular AR(2) matrix built from $\phi = (\phi_1, \phi_2)'$. The two unknown initial trend values $\boldsymbol{\tau}_0 \equiv (\tau_0, \tau_{-1})'$ are treated as parameters and sampled from their full conditional distribution, exactly as in (A.8) below.

A.2 Prior specification

The unknown parameters are $\boldsymbol{\theta} = (\phi_1, \phi_2, \sigma_c^2, \sigma_\tau^2, \tau_0, \tau_{-1})$. Priors are independent across blocks:

$$p(\boldsymbol{\theta}) \;=\; p(\phi)\, p(\sigma_c^2)\, p(\sigma_\tau^2)\, p(\boldsymbol{\tau}_0).$$

A.2.1 AR(2) cycle coefficients ϕ

The autoregressive coefficients are given a bivariate Gaussian prior truncated to the stationary region:

$$\phi \;\sim\; \big(\phi_0,\, V_\phi\big)\, \mathbf{1}\{\phi \in S\}. \tag{A.4}$$

The prior mean ϕ_0 encodes the prior belief that the cyclical component exhibits the positively autocorrelated, hump-shaped impulse response typical of business-cycle dynamics in unemployment-related series. The value across states and series is $\phi_0 = (1.3, -0.7)'$. The prior precision V_ϕ^{-1} is set to I_2 (unit precision) for most series; for $j = 1$ it is loosened to $10^{-3} I_2$ in many states (a near-flat prior over ϕ). The exact value of V_ϕ^{-1} for each state and series is reported in Tables A.1–A.5.

A.2.2 Stationarity restriction

The indicator $\mathbf{1}\{\phi \in S\}$ in (A.4) restricts ϕ to the AR(2) stationarity triangle. Operationally, the sampler accepts a candidate draw ϕ^c only if

$$\phi_1^c + \phi_2^c < 0.99, \qquad \phi_2^c - \phi_1^c < 0.99, \qquad \phi_2^c > -0.99, \tag{A.5}$$

which is the standard set of inequalities defining the interior of the stationarity region (with a small margin so that draws on the boundary are excluded). Rejected candidates leave ϕ unchanged at its previous value. This restriction is identical across all states and all series.

A.2.3 Cycle innovation variance σ_c^2

The cycle innovation variance is given a conjugate inverse-gamma prior:

$$\sigma_c^2 \sim \big(\nu_c, S_c\big), \tag{A.6}$$

implying the full conditional

$$\sigma_c^2 \mid \cdot \sim \Big(\nu_c + \tfrac{T}{2},\ S_c + \tfrac{1}{2}(c - X_\phi \phi)'(c - X_\phi \phi)\Big).$$

Hyperparameters (ν_c, S_c) are calibrated separately for each series and each state; see Tables A.1–A.5. Series for which a tight prior is appropriate (notably the duration parameter β_0 ($j = 2$), where $(\nu_c, S_c) = (10^{-6}, 10^{-6})$ across all states) use very small values, yielding a near-improper prior on σ_c^2. The labor force series uses larger values in those states for which the cycle component is non-negligible.

A.2.4 Trend innovation variance σ_τ^2

Following Chan and Grant (2017) and the bounded prior approach of Frisch–Waugh-style decompositions, the trend innovation variance is given a uniform prior on a bounded interval:

$$\sigma_\tau^2 \sim \left(0, \overline{\sigma}_\tau^2\right), \tag{A.7}$$

with the upper bound $\overline{\sigma}_\tau^2$ chosen series by series and state by state. The full conditional density is

$$p\left(\sigma_\tau^2 \mid \cdot\right) \propto (\sigma_\tau^2)^{-T/2} \exp\left\{-\frac{1}{2\sigma_\tau^2} \sum_{t=2}^{T} (\Delta\tau_t - \Delta\tau_{t-1})^2\right\} \mathbf{1}\left\{0 < \sigma_\tau^2 < \overline{\sigma}_\tau^2\right\},$$

which is sampled via a discretized grid (500 grid points, with end-points jittered to avoid placing mass on the boundary). The tight upper bound plays the role of a smoothness restriction on the trend: It precludes large random shifts in trend growth and disciplines the trend–cycle decomposition in the absence of strong informational content from the data alone. The values of $\overline{\sigma}_\tau^2$ used for each state and series are reported in Tables A.1–A.5.

A.2.5 Initial trend conditions

The pair of pre-sample trend values $\boldsymbol{\tau}_0 = (\tau_0, \tau_{-1})'$ is given a Gaussian prior

$$\boldsymbol{\tau}_0 \sim \left(a_0, B_0\right). \tag{A.8}$$

For the inflow rate and the three duration-distribution parameters ($j = 1, \ldots, 4$), the prior mean is

$$a_0 = \left(\bar{y}, \bar{y}\right)' + \delta_j \cdot \mathbf{1}_2,$$

where $\bar{y}$ is the sample mean of the series over the available pre-COVID sample and δ_j is a small series- and state-specific shift used to nudge the initial trend toward economically plausible levels. For the labor force series, the prior mean is $a_0 = (y_1, y_1)'$, the first observed value of the series. The prior covariance B_0 is diagonal with magnitude 10, 100, or 1,000 depending on the state and series; see Tables A.1–A.5.

A.2.6 Sampler initialization

Throughout, the Markov chain is initialized at $\phi^{(0)} = \phi_0$, $\sigma_c^{2(0)} = \nu_c$, $\sigma_\tau^{2(0)} = \overline{\sigma}_\tau^2$, and $\boldsymbol{\tau}_0^{(0)} = a_0$. The sampler is run for $N_{\text{sim}} = 10{,}000$ post-burn-in iterations after a burn-in of 1,000, and posterior summaries are based on the resulting draws.

A.3 State-level hyperparameter values

Tables A.1–A.5 report the full set of hyperparameters used for each of the 51 states for each of the five series, namely the unemployment inflow rate ($j = 1$), the three duration-distribution parameters β_0, β_1, β_2 ($j = 2, 3, 4$), and the labor force. The columns are: δ_j (the shift in the prior mean of $\boldsymbol{\tau}_0$ for that series), B_0 (the prior covariance of $\boldsymbol{\tau}_0$), ϕ_0 (the prior mean of the AR(2) coefficients), V_ϕ^{-1} (the prior precision of ϕ), ν_c and S_c (the inverse-gamma hyperparameters for σ_c^2), and $\overline{\sigma}_\tau^2$ (the upper bound of the uniform prior on σ_τ^2).

B Factor Estimates

Figures B.1 – B.6 display each state's factor estimates and their trends. For each state, the upper left panel shows the estimated inflows, the upper right panel β_0, the lower left β_1, and the lower right panel β_2. The black lines are the factor estimates, the solid blue lines are the posterior means of trend estimates, and the dashed blue lines are the 68 percent posterior intervals.

Table A.1: HYPERPARAMETERS FOR THE UNEMPLOYMENT INFLOW RATE ($j = 1$) BY STATE. δ_j IS THE SHIFT APPLIED TO THE PRIOR MEAN: $a_0 = (\bar{y}, \bar{y})' + \delta_j \cdot \mathbf{1}_2$. ν_c, S_c ARE THE INVERSE-GAMMA SHAPE AND SCALE; $\overline{\sigma}^2_\tau$ IS THE UPPER BOUND OF THE UNIFORM PRIOR ON THE TREND INNOVATION VARIANCE.

State	δ_j	B_0	ϕ_0	V_ϕ^{-1}	ν_c	S_c	$\overline{\sigma}^2_\tau$	State	δ_j	B_0	ϕ_0	V_ϕ^{-1}	ν_c	S_c	$\overline{\sigma}^2_\tau$
AK	-0.1	$100\,I_2$	$(1.3,-0.7)$	I_2	10^{-4}	10^{-4}	10^{-5}	MT	$+0.2$	$100\,I_2$	$(1.3,-0.7)$	$10^{-3}\,I_2$	10^{-4}	10^{-4}	10^{-5}
AL	-0.1	$100\,I_2$	$(1.3,-0.7)$	$10^{-3}\,I_2$	10^{-4}	10^{-4}	10^{-5}	NC	-0.2	$100\,I_2$	$(1.3,-0.7)$	$10^{-3}\,I_2$	10^{-4}	10^{-5}	2×10^{-6}
AR	$+0.1$	$100\,I_2$	$(1.3,-0.7)$	$10^{-3}\,I_2$	10^{-4}	10^{-4}	5×10^{-7}	ND	$+0.2$	$100\,I_2$	$(1.3,-0.7)$	$10^{-3}\,I_2$	10^{-4}	10^{-4}	10^{-5}
AZ	-0.1	$100\,I_2$	$(1.3,-0.7)$	$10^{-3}\,I_2$	10^{-4}	10^{-4}	2×10^{-6}	NE	-0.1	$100\,I_2$	$(1.3,-0.7)$	$10^{-3}\,I_2$	10^{-4}	10^{-4}	2×10^{-5}
CA	0	$100\,I_2$	$(1.3,-0.7)$	I_2	10^{-1}	10^{-1}	10^{-4}	NH	$+0.1$	$100\,I_2$	$(1.3,-0.7)$	$10^{-3}\,I_2$	10^{-4}	10^{-4}	5×10^{-7}
CO	-0.1	$100\,I_2$	$(1.3,-0.7)$	$10^{-3}\,I_2$	10^{-4}	10^{-5}	5×10^{-6}	NJ	-0.2	$100\,I_2$	$(1.3,-0.7)$	$10^{-3}\,I_2$	10^{-4}	10^{-5}	2×10^{-6}
CT	-0.4	$100\,I_2$	$(1.3,-0.7)$	$10^{-3}\,I_2$	10^{-4}	10^{-4}	2×10^{-6}	NM	$+0.1$	$100\,I_2$	$(1.3,-0.7)$	I_2	10^{-4}	10^{-4}	10^{-4}
DC	-0.5	$100\,I_2$	$(1.3,-0.7)$	$10^{-3}\,I_2$	10^{-4}	10^{-4}	10^{-5}	NV	-0.5	$100\,I_2$	$(1.3,-0.7)$	$10^{-3}\,I_2$	10^{-4}	10^{-4}	10^{-5}
DE	-0.1	$100\,I_2$	$(1.3,-0.7)$	$10^{-3}\,I_2$	10^{-4}	10^{-4}	2×10^{-6}	NY	0	$100\,I_2$	$(1.3,-0.7)$	$10^{-3}\,I_2$	10^{-4}	10^{-4}	5×10^{-5}
FL	0	$100\,I_2$	$(1.3,-0.7)$	$10^{-3}\,I_2$	10^{-4}	10^{-4}	5×10^{-5}	OH	0	$10\,I_2$	$(1.3,-0.7)$	$10^{-3}\,I_2$	10^{-4}	10^{-4}	5×10^{-5}
GA	-0.2	$100\,I_2$	$(1.3,-0.7)$	$10^{-3}\,I_2$	10^{-4}	10^{-4}	10^{-5}	OK	-0.2	$100\,I_2$	$(1.3,-0.7)$	$10^{-3}\,I_2$	10^{-4}	10^{-5}	5×10^{-6}
HI	-0.35	$100\,I_2$	$(1.3,-0.7)$	$10^{-3}\,I_2$	10^{-4}	10^{-5}	2×10^{-6}	OR	$+0.1$	$100\,I_2$	$(1.3,-0.7)$	$10^{-3}\,I_2$	10^{-4}	10^{-4}	10^{-6}
IA	$+0.2$	$10\,I_2$	$(1.3,-0.7)$	$10^{-3}\,I_2$	10^{-4}	10^{-4}	10^{-5}	PA	-0.2	$100\,I_2$	$(1.3,-0.7)$	$10^{-3}\,I_2$	10^{-4}	10^{-5}	2×10^{-6}
ID	-0.1	$100\,I_2$	$(1.3,-0.7)$	$10^{-3}\,I_2$	10^{-4}	10^{-4}	2×10^{-6}	RI	$+0.2$	$100\,I_2$	$(1.3,-0.7)$	$10^{-3}\,I_2$	10^{-4}	10^{-4}	10^{-5}
IL	0	$10\,I_2$	$(1.3,-0.7)$	$10^{-3}\,I_2$	10^{-4}	10^{-4}	5×10^{-5}	SC	0	$100\,I_2$	$(1.3,-0.7)$	$10^{-3}\,I_2$	10^{-4}	10^{-4}	5×10^{-6}
IN	-0.1	$100\,I_2$	$(1.3,-0.7)$	$10^{-3}\,I_2$	10^{-4}	10^{-4}	10^{-5}	SD	$+0.3$	$100\,I_2$	$(1.3,-0.7)$	$10^{-3}\,I_2$	10^{-4}	10^{-4}	5×10^{-6}
KS	$+1$	$100\,I_2$	$(1.3,-0.7)$	$10^{-3}\,I_2$	10^{-4}	10^{-4}	3×10^{-5}	TN	-0.1	$100\,I_2$	$(1.3,-0.7)$	$10^{-3}\,I_2$	10^{-4}	10^{-5}	5×10^{-6}
KY	$+0.1$	$100\,I_2$	$(1.3,-0.7)$	I_2	10^{-5}	10^{-5}	10^{-5}	TX	0	$10\,I_2$	$(1.3,-0.7)$	$10^{-3}\,I_2$	10^{-4}	10^{-4}	5×10^{-5}
LA	-0.2	$100\,I_2$	$(1.3,-0.7)$	$10^{-3}\,I_2$	10^{-4}	10^{-5}	2×10^{-6}	UT	0	$100\,I_2$	$(1.3,-0.7)$	$10^{-3}\,I_2$	10^{-4}	10^{-4}	5×10^{-6}
MA	-0.2	$100\,I_2$	$(1.3,-0.7)$	$10^{-3}\,I_2$	10^{-4}	10^{-5}	2×10^{-6}	VA	0	$100\,I_2$	$(1.3,-0.7)$	$10^{-3}\,I_2$	10^{-4}	10^{-4}	10^{-5}
MD	0	$100\,I_2$	$(1.3,-0.7)$	$10^{-3}\,I_2$	10^{-4}	10^{-4}	10^{-6}	VT	-0.2	$100\,I_2$	$(1.3,-0.7)$	$10^{-3}\,I_2$	10^{-4}	10^{-5}	2×10^{-6}
ME	0	$100\,I_2$	$(1.3,-0.7)$	$10^{-3}\,I_2$	10^{-4}	10^{-4}	2×10^{-5}	WA	$+0.3$	$100\,I_2$	$(1.3,-0.7)$	$10^{-3}\,I_2$	10^{-4}	10^{-4}	5×10^{-6}
MI	$+0.2$	$100\,I_2$	$(1.3,-0.7)$	$10^{-3}\,I_2$	10^{-4}	10^{-4}	5×10^{-5}	WI	-0.2	$100\,I_2$	$(1.3,-0.7)$	$10^{-3}\,I_2$	10^{-4}	10^{-5}	2×10^{-6}
MN	$+0.1$	$100\,I_2$	$(1.3,-0.7)$	$10^{-3}\,I_2$	10^{-4}	10^{-4}	5×10^{-7}	WV	$+0.2$	$100\,I_2$	$(1.3,-0.7)$	$10^{-3}\,I_2$	10^{-4}	10^{-4}	10^{-4}
MO	-0.2	$100\,I_2$	$(1.3,-0.7)$	$10^{-3}\,I_2$	10^{-4}	10^{-5}	2×10^{-6}	WY	0	$100\,I_2$	$(1.3,-0.7)$	$10^{-3}\,I_2$	10^{-4}	10^{-4}	5×10^{-6}
MS	$+0.1$	$100\,I_2$	$(1.3,-0.7)$	$10^{-3}\,I_2$	10^{-4}	10^{-4}	5×10^{-7}								

Table A.2: HYPERPARAMETERS FOR THE DURATION-DISTRIBUTION PARAMETER β_0 ($j = 2$) BY STATE.

State	δ_j	B_0	ϕ_0	V_ϕ^{-1}	ν_c	S_c	$\overline{\sigma}_\tau^2$	State	δ_j	B_0	ϕ_0	V_ϕ^{-1}	ν_c	S_c	$\overline{\sigma}_\tau^2$
AK	-0.2	$100\,I_2$	$(1.3,-0.7)$	I_2	10^{-4}	10^{-4}	10^{-5}	MT	-0.2	$100\,I_2$	$(1.3,-0.7)$	I_2	10^{-6}	10^{-6}	6.25×10^{-6}
AL	-0.1	$100\,I_2$	$(1.3,-0.7)$	I_2	10^{-6}	10^{-6}	6.25×10^{-6}	NC	$+0.3$	$100\,I_2$	$(1.3,-0.7)$	I_2	10^{-6}	10^{-6}	6.25×10^{-6}
AR	-0.1	$100\,I_2$	$(1.3,-0.7)$	I_2	10^{-6}	10^{-6}	6.25×10^{-6}	ND	-0.2	$100\,I_2$	$(1.3,-0.7)$	I_2	10^{-6}	10^{-6}	2.25×10^{-6}
AZ	-0.1	$100\,I_2$	$(1.3,-0.7)$	I_2	10^{-6}	10^{-6}	6.25×10^{-6}	NE	-0.1	$100\,I_2$	$(1.3,-0.7)$	I_2	10^{-6}	10^{-6}	6.25×10^{-6}
CA	$+0.3$	$100\,I_2$	$(1.3,-0.7)$	I_2	10^{-6}	10^{-6}	6.25×10^{-6}	NH	-0.1	$100\,I_2$	$(1.3,-0.7)$	I_2	10^{-6}	10^{-6}	6.25×10^{-6}
CO	$+0.3$	$100\,I_2$	$(1.3,-0.7)$	I_2	10^{-6}	10^{-6}	6.25×10^{-6}	NJ	$+0.3$	$100\,I_2$	$(1.3,-0.7)$	I_2	10^{-6}	10^{-6}	6.25×10^{-6}
CT	$+0.5$	$100\,I_2$	$(1.3,-0.7)$	I_2	10^{-6}	10^{-6}	6.25×10^{-6}	NM	-0.4	$100\,I_2$	$(1.3,-0.7)$	I_2	10^{-6}	10^{-6}	6.25×10^{-6}
DC	$+0.5$	$100\,I_2$	$(1.3,-0.7)$	I_2	10^{-6}	10^{-6}	2.25×10^{-6}	NV	$+0.1$	$100\,I_2$	$(1.3,-0.7)$	I_2	10^{-6}	10^{-6}	10^{-5}
DE	-0.1	$100\,I_2$	$(1.3,-0.7)$	I_2	10^{-6}	10^{-6}	6.25×10^{-6}	NY	$+0.3$	$100\,I_2$	$(1.3,-0.7)$	I_2	10^{-6}	10^{-6}	2.25×10^{-6}
FL	$+0.3$	$100\,I_2$	$(1.3,-0.7)$	I_2	10^{-6}	10^{-6}	2.25×10^{-6}	OH	-0.3	$10\,I_2$	$(1.3,-0.7)$	I_2	10^{-6}	10^{-6}	5×10^{-7}
GA	$+0.3$	$100\,I_2$	$(1.3,-0.7)$	I_2	10^{-6}	10^{-6}	2.25×10^{-6}	OK	$+0.3$	$100\,I_2$	$(1.3,-0.7)$	I_2	10^{-6}	10^{-6}	6.25×10^{-6}
HI	$+0.3$	$100\,I_2$	$(1.3,-0.7)$	I_2	10^{-6}	10^{-6}	6.25×10^{-6}	OR	-0.1	$100\,I_2$	$(1.3,-0.7)$	I_2	10^{-6}	10^{-6}	6.25×10^{-6}
IA	-0.1	$10\,I_2$	$(1.3,-0.7)$	I_2	10^{-6}	10^{-6}	6.25×10^{-6}	PA	$+0.3$	$100\,I_2$	$(1.3,-0.7)$	I_2	10^{-6}	10^{-6}	10^{-6}
ID	-0.2	$100\,I_2$	$(1.3,-0.7)$	I_2	10^{-6}	10^{-6}	6.25×10^{-6}	RI	-0.3	$100\,I_2$	$(1.3,-0.7)$	I_2	10^{-6}	10^{-6}	2.25×10^{-6}
IL	-0.3	$10\,I_2$	$(1.3,-0.7)$	I_2	10^{-6}	10^{-6}	6.25×10^{-6}	SC	-0.3	$100\,I_2$	$(1.3,-0.7)$	I_2	10^{-6}	10^{-6}	2.25×10^{-6}
IN	$+0.5$	$100\,I_2$	$(1.3,-0.7)$	I_2	10^{-6}	10^{-6}	6.25×10^{-6}	SD	-0.4	$100\,I_2$	$(1.3,-0.7)$	I_2	10^{-6}	10^{-6}	2.25×10^{-6}
KS	-0.2	$100\,I_2$	$(1.3,-0.7)$	I_2	10^{-6}	10^{-6}	6.25×10^{-6}	TN	$+0.3$	$100\,I_2$	$(1.3,-0.7)$	I_2	10^{-6}	10^{-6}	6.25×10^{-6}
KY	-0.1	$100\,I_2$	$(1.3,-0.7)$	I_2	10^{-6}	10^{-6}	6.25×10^{-6}	TX	$+0.3$	$10\,I_2$	$(1.3,-0.7)$	I_2	10^{-6}	10^{-6}	2.25×10^{-6}
LA	$+0.3$	$100\,I_2$	$(1.3,-0.7)$	I_2	10^{-6}	10^{-6}	6.25×10^{-6}	UT	-0.4	$100\,I_2$	$(1.3,-0.7)$	I_2	10^{-6}	10^{-6}	2.25×10^{-6}
MA	$+0.3$	$100\,I_2$	$(1.3,-0.7)$	I_2	10^{-6}	10^{-6}	6.25×10^{-6}	VA	$+0.3$	$100\,I_2$	$(1.3,-0.7)$	I_2	10^{-6}	10^{-6}	2.25×10^{-6}
MD	-0.3	$100\,I_2$	$(1.3,-0.7)$	I_2	10^{-6}	10^{-6}	6.25×10^{-6}	VT	$+0.3$	$100\,I_2$	$(1.3,-0.7)$	I_2	10^{-6}	10^{-6}	6.25×10^{-6}
ME	$+0.1$	$100\,I_2$	$(1.3,-0.7)$	I_2	10^{-6}	10^{-6}	6.25×10^{-6}	WA	-0.4	$100\,I_2$	$(1.3,-0.7)$	I_2	10^{-6}	10^{-6}	2.25×10^{-6}
MI	-0.2	$100\,I_2$	$(1.3,-0.7)$	I_2	10^{-6}	10^{-6}	6.25×10^{-6}	WI	$+0.3$	$100\,I_2$	$(1.3,-0.7)$	I_2	10^{-6}	10^{-6}	6.25×10^{-6}
MN	-0.1	$100\,I_2$	$(1.3,-0.7)$	I_2	10^{-6}	10^{-6}	6.25×10^{-6}	WV	-0.2	$100\,I_2$	$(1.3,-0.7)$	I_2	10^{-6}	10^{-6}	5×10^{-6}
MO	$+0.3$	$100\,I_2$	$(1.3,-0.7)$	I_2	10^{-6}	10^{-6}	6.25×10^{-6}	WY	-0.4	$100\,I_2$	$(1.3,-0.7)$	I_2	10^{-6}	10^{-6}	2.5×10^{-5}
MS	-0.1	$100\,I_2$	$(1.3,-0.7)$	I_2	10^{-6}	10^{-6}	6.25×10^{-6}								

Table A.3: HYPERPARAMETERS FOR THE DURATION-DISTRIBUTION PARAMETER β_1 ($j = 3$) BY STATE.

State	δ_j	B_0	ϕ_0	V_ϕ^{-1}	ν_c	S_c	$\overline{\sigma}_\tau^2$	State	δ_j	B_0	ϕ_0	V_ϕ^{-1}	ν_c	S_c	$\overline{\sigma}_\tau^2$
AK	0	$100\,I_2$	$(1.3,-0.7)$	I_2	1	10^{-3}	10^{-6}	MT	0	$100\,I_2$	$(1.3,-0.7)$	I_2	1	10^{-3}	10^{-6}
AL	0	$100\,I_2$	$(1.3,-0.7)$	I_2	1	10^{-3}	10^{-6}	NC	0	$100\,I_2$	$(1.3,-0.7)$	I_2	1	10^{-3}	10^{-6}
AR	0	$100\,I_2$	$(1.3,-0.7)$	I_2	1	10^{-3}	10^{-6}	ND	0	$100\,I_2$	$(1.3,-0.7)$	I_2	10^{-3}	10^{-3}	10^{-6}
AZ	0	$100\,I_2$	$(1.3,-0.7)$	I_2	1	10^{-3}	10^{-6}	NE	0	$100\,I_2$	$(1.3,-0.7)$	I_2	1	10^{-3}	10^{-6}
CA	-0.1	$100\,I_2$	$(1.3,-0.7)$	I_2	1	10^{-3}	2×10^{-6}	NH	0	$100\,I_2$	$(1.3,-0.7)$	I_2	1	10^{-3}	10^{-6}
CO	0	$100\,I_2$	$(1.3,-0.7)$	I_2	1	10^{-3}	10^{-6}	NJ	0	$100\,I_2$	$(1.3,-0.7)$	I_2	1	10^{-3}	10^{-6}
CT	-0.2	$100\,I_2$	$(1.3,-0.7)$	I_2	1	10^{-3}	2×10^{-6}	NM	0	$100\,I_2$	$(1.3,-0.7)$	I_2	1	10^{-3}	10^{-6}
DC	-0.2	$100\,I_2$	$(1.3,-0.7)$	I_2	1	10^{-3}	2×10^{-6}	NV	-0.1	$100\,I_2$	$(1.3,-0.7)$	I_2	1	10^{-3}	10^{-6}
DE	0	$100\,I_2$	$(1.3,-0.7)$	I_2	1	10^{-3}	10^{-6}	NY	0	$100\,I_2$	$(1.3,-0.7)$	I_2	1	10^{-3}	10^{-6}
FL	0	$100\,I_2$	$(1.3,-0.7)$	I_2	1	10^{-3}	2×10^{-6}	OH	-0.2	$10\,I_2$	$(1.3,-0.7)$	I_2	1	10^{-3}	2×10^{-6}
GA	0	$100\,I_2$	$(1.3,-0.7)$	I_2	1	10^{-3}	2×10^{-6}	OK	0	$100\,I_2$	$(1.3,-0.7)$	I_2	1	10^{-3}	10^{-6}
HI	0	$100\,I_2$	$(1.3,-0.7)$	I_2	1	10^{-3}	10^{-6}	OR	0	$100\,I_2$	$(1.3,-0.7)$	I_2	1	10^{-3}	10^{-6}
IA	-0.3	$10\,I_2$	$(1.3,-0.7)$	I_2	1	10^{-3}	2×10^{-6}	PA	0	$100\,I_2$	$(1.3,-0.7)$	I_2	1	10^{-3}	10^{-6}
ID	0	$100\,I_2$	$(1.3,-0.7)$	I_2	1	10^{-3}	10^{-6}	RI	0	$100\,I_2$	$(1.3,-0.7)$	I_2	10^{-3}	10^{-3}	10^{-6}
IL	-0.2	$10\,I_2$	$(1.25,-0.3)$	I_2	1	10^{-3}	2×10^{-6}	SC	0	$100\,I_2$	$(1.3,-0.7)$	I_2	10^{-3}	10^{-3}	10^{-6}
IN	-0.2	$100\,I_2$	$(1.3,-0.7)$	I_2	1	10^{-3}	10^{-6}	SD	0	$100\,I_2$	$(1.3,-0.7)$	I_2	10^{-3}	10^{-3}	10^{-6}
KS	-0.3	$100\,I_2$	$(1.3,-0.7)$	I_2	1	10^{-3}	10^{-6}	TN	0	$100\,I_2$	$(1.3,-0.7)$	I_2	1	10^{-3}	10^{-6}
KY	0	$100\,I_2$	$(1.3,-0.7)$	I_2	1	10^{-3}	10^{-6}	TX	0	$10\,I_2$	$(1.3,-0.7)$	I_2	1	10^{-3}	2×10^{-6}
LA	0	$100\,I_2$	$(1.3,-0.7)$	I_2	1	10^{-3}	10^{-6}	UT	0	$100\,I_2$	$(1.3,-0.7)$	I_2	10^{-3}	10^{-3}	10^{-6}
MA	0	$100\,I_2$	$(1.3,-0.7)$	I_2	1	10^{-3}	10^{-6}	VA	0	$100\,I_2$	$(1.3,-0.7)$	I_2	1	10^{-3}	2×10^{-6}
MD	-0.1	$100\,I_2$	$(1.3,-0.7)$	I_2	1	10^{-3}	10^{-6}	VT	0	$100\,I_2$	$(1.3,-0.7)$	I_2	1	10^{-3}	10^{-6}
ME	-0.2	$100\,I_2$	$(1.3,-0.7)$	I_2	1	10^{-3}	10^{-6}	WA	0	$100\,I_2$	$(1.3,-0.7)$	I_2	10^{-3}	10^{-3}	10^{-6}
MI	0	$100\,I_2$	$(1.3,-0.7)$	I_2	1	10^{-3}	10^{-6}	WI	0	$100\,I_2$	$(1.3,-0.7)$	I_2	1	10^{-3}	10^{-6}
MN	0	$100\,I_2$	$(1.3,-0.7)$	I_2	1	10^{-3}	10^{-6}	WV	0	$100\,I_2$	$(1.3,-0.7)$	I_2	10^{-3}	10^{-3}	10^{-6}
MO	0	$100\,I_2$	$(1.3,-0.7)$	I_2	1	10^{-3}	10^{-6}	WY	0	$100\,I_2$	$(1.3,-0.7)$	I_2	10^{-3}	10^{-3}	10^{-6}
MS	0	$100\,I_2$	$(1.3,-0.7)$	I_2	1	10^{-3}	10^{-6}								

Table A.4: Hyperparameters for the duration-distribution parameter β_2 ($j = 4$) by state.

State	δ_j	B_0	ϕ_0	V_ϕ^{-1}	ν_c	S_c	$\overline{\sigma}_\tau^2$	State	δ_j	B_0	ϕ_0	V_ϕ^{-1}	ν_c	S_c	$\overline{\sigma}_\tau^2$
AK	-1	$100\,I_2$	$(1.3,-0.7)$	I_2	10^{-2}	10^{-3}	10^{-4}	MT	-1	$100\,I_2$	$(1.3,-0.7)$	I_2	10^{-2}	10^{-3}	10^{-3}
AL	-1	$100\,I_2$	$(1.3,-0.7)$	I_2	10^{-2}	10^{-3}	10^{-4}	NC	$+0.5$	$100\,I_2$	$(1.3,-0.7)$	I_2	10^{-4}	10^{-4}	10^{-5}
AR	-1	$100\,I_2$	$(1.3,-0.7)$	I_2	10^{-2}	10^{-3}	10^{-3}	ND	-1	$100\,I_2$	$(1.3,-0.7)$	I_2	10^{-3}	10^{-3}	10^{-5}
AZ	-1	$100\,I_2$	$(1.3,-0.7)$	I_2	10^{-2}	10^{-3}	10^{-4}	NE	-1	$100\,I_2$	$(1.3,-0.7)$	I_2	10^{-2}	10^{-3}	10^{-3}
CA	$+0.5$	$100\,I_2$	$(1.3,-0.7)$	I_2	10^{-4}	10^{-4}	10^{-5}	NH	-1	$100\,I_2$	$(1.3,-0.7)$	I_2	10^{-2}	10^{-3}	10^{-3}
CO	$+0.5$	$100\,I_2$	$(1.3,-0.7)$	I_2	10^{-4}	10^{-4}	10^{-4}	NJ	$+0.5$	$100\,I_2$	$(1.3,-0.7)$	I_2	10^{-4}	10^{-4}	10^{-5}
CT	$+0.5$	$100\,I_2$	$(1.3,-0.7)$	I_2	10^{-4}	10^{-4}	10^{-5}	NM	-1	$100\,I_2$	$(1.3,-0.7)$	I_2	10^{-2}	10^{-3}	10^{-3}
DC	$+2$	$100\,I_2$	$(1.3,-0.7)$	I_2	10^{-4}	10^{-4}	5×10^{-5}	NV	-1	$100\,I_2$	$(1.3,-0.7)$	I_2	10^{-2}	10^{-3}	5×10^{-5}
DE	-1	$100\,I_2$	$(1.3,-0.7)$	I_2	10^{-2}	10^{-3}	10^{-4}	NY	$+0.5$	$100\,I_2$	$(1.3,-0.7)$	I_2	10^{-4}	10^{-4}	10^{-5}
FL	$+0.5$	$100\,I_2$	$(1.3,-0.7)$	I_2	10^{-4}	10^{-4}	10^{-5}	OH	0	$10\,I_2$	$(1.3,-0.7)$	I_2	10^{-4}	10^{-4}	10^{-5}
GA	$+0.5$	$100\,I_2$	$(1.3,-0.7)$	I_2	10^{-4}	10^{-4}	10^{-5}	OK	$+1$	$100\,I_2$	$(1.3,-0.7)$	I_2	10^{-4}	10^{-4}	5×10^{-5}
HI	$+1$	$100\,I_2$	$(1.3,-0.7)$	I_2	10^{-4}	10^{-4}	10^{-5}	OR	-1	$100\,I_2$	$(1.3,-0.7)$	I_2	10^{-2}	10^{-3}	10^{-3}
IA	-2	$10\,I_2$	$(1.3,-0.7)$	I_2	10^{-4}	10^{-4}	10^{-3}	PA	$+0.5$	$100\,I_2$	$(1.3,-0.7)$	I_2	10^{-4}	10^{-4}	10^{-4}
ID	-1	$100\,I_2$	$(1.3,-0.7)$	I_2	10^{-2}	10^{-3}	10^{-4}	RI	-1	$100\,I_2$	$(1.3,-0.7)$	I_2	10^{-3}	10^{-3}	10^{-4}
IL	0	$10\,I_2$	$(1.25,-0.3)$	I_2	10^{-4}	10^{-4}	10^{-5}	SC	-1	$100\,I_2$	$(1.3,-0.7)$	I_2	10^{-3}	10^{-3}	10^{-4}
IN	$+0.5$	$100\,I_2$	$(1.3,-0.7)$	I_2	10^{-4}	10^{-4}	10^{-5}	SD	-1	$100\,I_2$	$(1.3,-0.7)$	I_2	10^{-3}	10^{-3}	10^{-4}
KS	-1	$100\,I_2$	$(1.3,-0.7)$	I_2	10^{-2}	10^{-3}	10^{-3}	TN	$+0.5$	$100\,I_2$	$(1.3,-0.7)$	I_2	10^{-4}	10^{-4}	10^{-5}
KY	-1	$100\,I_2$	$(1.3,-0.7)$	I_2	10^{-2}	10^{-3}	5×10^{-4}	TX	$+1.5$	$10\,I_2$	$(1.3,-0.7)$	I_2	10^{-4}	10^{-4}	10^{-5}
LA	$+0.5$	$100\,I_2$	$(1.3,-0.7)$	I_2	10^{-4}	10^{-4}	10^{-5}	UT	-1	$100\,I_2$	$(1.3,-0.7)$	I_2	10^{-3}	10^{-3}	10^{-4}
MA	$+0.5$	$100\,I_2$	$(1.3,-0.7)$	I_2	10^{-4}	10^{-4}	10^{-5}	VA	$+0.5$	$100\,I_2$	$(1.3,-0.7)$	I_2	10^{-4}	10^{-4}	10^{-5}
MD	-1	$100\,I_2$	$(1.3,-0.7)$	I_2	10^{-2}	10^{-3}	10^{-3}	VT	$+0.5$	$100\,I_2$	$(1.3,-0.7)$	I_2	10^{-4}	10^{-4}	10^{-5}
ME	-1	$100\,I_2$	$(1.3,-0.7)$	I_2	10^{-2}	10^{-3}	10^{-3}	WA	-1	$100\,I_2$	$(1.3,-0.7)$	I_2	10^{-3}	10^{-3}	10^{-4}
MI	-1	$100\,I_2$	$(1.3,-0.7)$	I_2	10^{-2}	10^{-3}	10^{-3}	WI	$+0.5$	$100\,I_2$	$(1.3,-0.7)$	I_2	10^{-4}	10^{-4}	10^{-5}
MN	-1	$100\,I_2$	$(1.3,-0.7)$	I_2	10^{-2}	10^{-3}	10^{-3}	WV	-1	$100\,I_2$	$(1.3,-0.7)$	I_2	10^{-3}	10^{-3}	10^{-4}
MO	$+0.5$	$100\,I_2$	$(1.3,-0.7)$	I_2	10^{-4}	10^{-4}	10^{-5}	WY	-1	$100\,I_2$	$(1.3,-0.7)$	I_2	10^{-3}	10^{-3}	10^{-4}
MS	-1	$100\,I_2$	$(1.3,-0.7)$	I_2	10^{-2}	10^{-3}	10^{-3}								

Table A.5: Hyperparameters for the labor force series by state. $a_0 = (y_1, y_1)'$ for all states.

State	B_0	ϕ_0	V_ϕ^{-1}	ν_c	S_c	$\overline{\sigma}_\tau^2$	State	B_0	ϕ_0	V_ϕ^{-1}	ν_c	S_c	$\overline{\sigma}_\tau^2$
AK	$100\,I_2$	$(1.3,-0.7)$	I_2	10^{-1}	5×10^{-2}	10^{-4}	MT	$1000\,I_2$	$(1.3,-0.7)$	I_2	10^{-2}	10^{-3}	10^{-3}
AL	$100\,I_2$	$(1.3,-0.7)$	I_2	10^{-1}	5×10^{-2}	10^{-3}	NC	$100\,I_2$	$(1.3,-0.7)$	I_2	10^{-2}	10^{-2}	2×10^{-4}
AR	$1000\,I_2$	$(1.3,-0.7)$	I_2	10^{-2}	10^{-3}	10^{-5}	ND	$1000\,I_2$	$(1.3,-0.7)$	I_2	10^{-2}	10^{-3}	10^{-3}
AZ	$100\,I_2$	$(1.3,-0.7)$	I_2	10^{-1}	5×10^{-2}	10^{-3}	NE	$1000\,I_2$	$(1.3,-0.7)$	I_2	10^{-2}	10^{-3}	10^{-3}
CA	$100\,I_2$	$(1.3,-0.7)$	I_2	3	5×10^{-1}	10^{-1}	NH	$1000\,I_2$	$(1.3,-0.7)$	I_2	10^{-2}	10^{-3}	10^{-3}
CO	$100\,I_2$	$(1.3,-0.7)$	I_2	10^{-2}	10^{-2}	2×10^{-4}	NJ	$100\,I_2$	$(1.3,-0.7)$	I_2	10^{-2}	10^{-2}	2×10^{-4}
CT	$100\,I_2$	$(1.3,-0.7)$	I_2	10^{-1}	10^{-2}	10^{-4}	NM	$1000\,I_2$	$(1.3,-0.7)$	I_2	10^{-2}	10^{-3}	10^{-3}
DC	$100\,I_2$	$(1.3,-0.7)$	I_2	10^{-1}	10^{-2}	10^{-3}	NV	$1000\,I_2$	$(1.3,-0.7)$	I_2	10^{-2}	10^{-3}	5×10^{-3}
DE	$100\,I_2$	$(1.3,-0.7)$	I_2	10^{-1}	5×10^{-2}	10^{-3}	NY	$100\,I_2$	$(1.3,-0.7)$	I_2	3	5×10^{-1}	10^{-1}
FL	$100\,I_2$	$(1.3,-0.7)$	I_2	3	5×10^{-1}	10^{-1}	OH	$100\,I_2$	$(1.3,-0.7)$	I_2	10^{-1}	10^{-1}	10^{-3}
GA	$100\,I_2$	$(1.3,-0.7)$	I_2	10^{-2}	10^{-3}	2×10^{-3}	OK	$100\,I_2$	$(1.3,-0.7)$	I_2	10^{-2}	10^{-2}	2×10^{-4}
HI	$100\,I_2$	$(1.3,-0.7)$	I_2	10^{-2}	10^{-2}	2×10^{-4}	OR	$1000\,I_2$	$(1.3,-0.7)$	I_2	10^{-2}	10^{-3}	10^{-4}
IA	$100\,I_2$	$(1.3,-0.7)$	I_2	10^{-1}	10^{-2}	10^{-3}	PA	$100\,I_2$	$(1.3,-0.7)$	I_2	10^{-2}	10^{-2}	2×10^{-4}
ID	$100\,I_2$	$(1.3,-0.7)$	I_2	10^{-1}	5×10^{-2}	10^{-3}	RI	$1000\,I_2$	$(1.3,-0.7)$	I_2	10^{-2}	10^{-3}	10^{-3}
IL	$100\,I_2$	$(1.3,-0.7)$	I_2	10^{-1}	5×10^{-2}	10^{-3}	SC	$1000\,I_2$	$(1.3,-0.7)$	I_2	10^{-2}	10^{-3}	10^{-3}
IN	$100\,I_2$	$(1.3,-0.7)$	I_2	10^{-1}	5×10^{-2}	10^{-3}	SD	$1000\,I_2$	$(1.3,-0.7)$	I_2	10^{-2}	10^{-3}	10^{-4}
KS	$1000\,I_2$	$(1.3,-0.7)$	I_2	10^{-2}	10^{-3}	10^{-5}	TN	$100\,I_2$	$(1.3,-0.7)$	I_2	10^{-2}	10^{-2}	2×10^{-4}
KY	$1000\,I_2$	$(1.3,-0.7)$	I_2	10^{-2}	10^{-3}	10^{-5}	TX	$100\,I_2$	$(1.3,-0.7)$	I_2	3	5×10^{-1}	10^{-1}
LA	$100\,I_2$	$(1.3,-0.7)$	I_2	10^{-2}	10^{-2}	2×10^{-4}	UT	$1000\,I_2$	$(1.3,-0.7)$	I_2	10^{-2}	10^{-3}	10^{-2}
MA	$100\,I_2$	$(1.3,-0.7)$	I_2	10^{-2}	10^{-2}	2×10^{-4}	VA	$100\,I_2$	$(1.3,-0.7)$	I_2	5×10^{-1}	5×10^{-2}	10^{-3}
MD	$1000\,I_2$	$(1.3,-0.7)$	I_2	10^{-2}	10^{-3}	10^{-3}	VT	$100\,I_2$	$(1.3,-0.7)$	I_2	10^{-2}	10^{-2}	2×10^{-4}
ME	$1000\,I_2$	$(1.3,-0.7)$	I_2	10^{-2}	10^{-3}	10^{-5}	WA	$1000\,I_2$	$(1.3,-0.7)$	I_2	10^{-2}	10^{-3}	2×10^{-3}
MI	$10\,I_2$	$(1.3,-0.7)$	I_2	10^{-3}	10^{-3}	5×10^{-3}	WI	$100\,I_2$	$(1.3,-0.7)$	I_2	10^{-2}	10^{-2}	2×10^{-4}
MN	$1000\,I_2$	$(1.3,-0.7)$	I_2	10^{-2}	10^{-3}	10^{-4}	WV	$100\,I_2$	$(1.3,-0.7)$	I_2	10^{-3}	10^{-4}	10^{-3}
MO	$100\,I_2$	$(1.3,-0.7)$	I_2	10^{-2}	10^{-2}	2×10^{-4}	WY	$1000\,I_2$	$(1.3,-0.7)$	I_2	10^{-2}	10^{-3}	10^{-3}
MS	$1000\,I_2$	$(1.3,-0.7)$	I_2	10^{-2}	10^{-3}	10^{-4}							

Figure B.1: FACTOR ESTIMATES (1)

(a) ALASKA

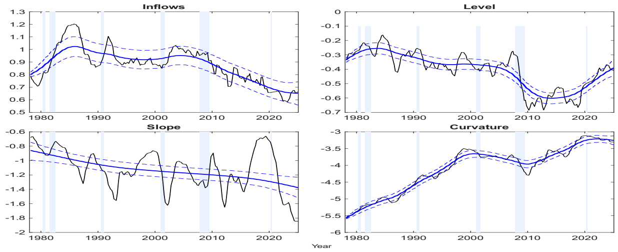

(b) ALABAMA

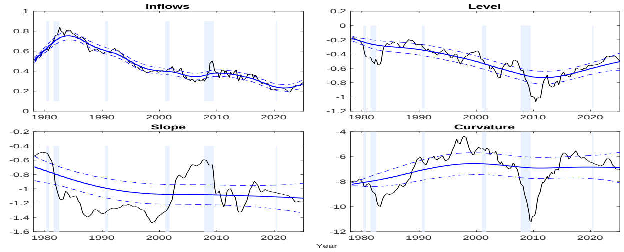

(c) ARKANSAS

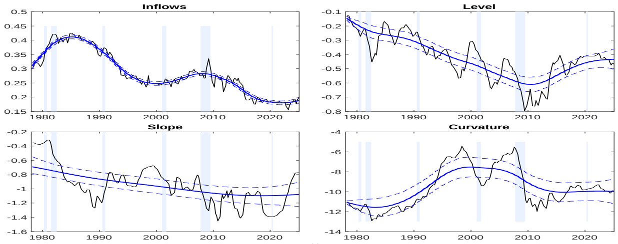

(d) ARIZONA

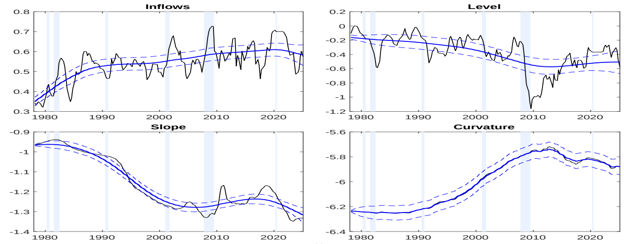

(e) CALIFORNIA

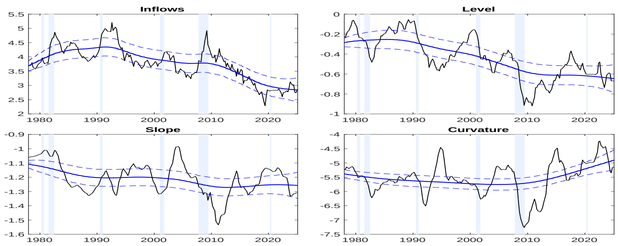

(f) COLORADO

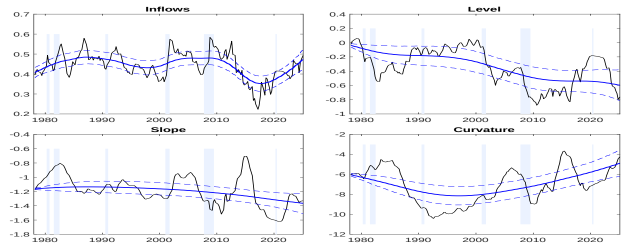

(g) CONNECTICUT

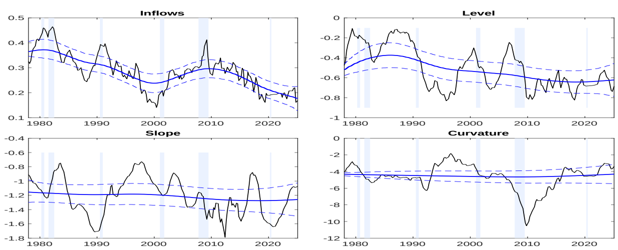

(h) DISTRICT OF COLUMBIA

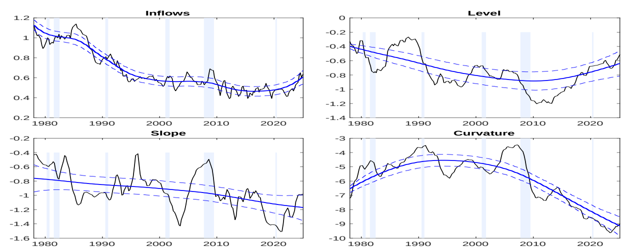

(i) DELAWARE

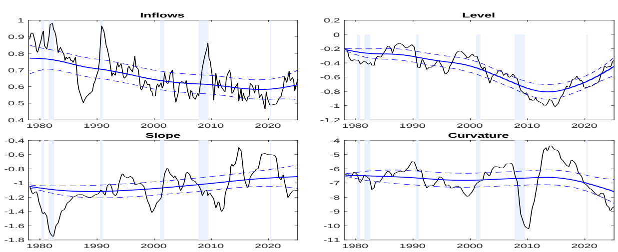

(j) FLORIDA

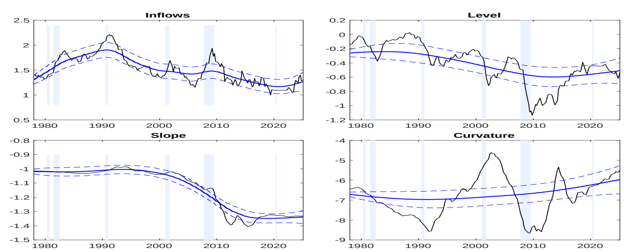

Notes to Figure B.1: For each state, the inflows are displayed in the upper left panel, β_0 in the upper right panel, β_1 in the lower left panel, β_2 in the lower right panel. The black lines are the factor estimates, the solid blue lines are the posterior means of trend estimates, and the dashed blue lines are the 68 percent posterior intervals. Shaded areas are NBER recessions. **Source:** Authors' calculation.

Figure B.2: FACTOR ESTIMATES (2)

(a) GEORGIA

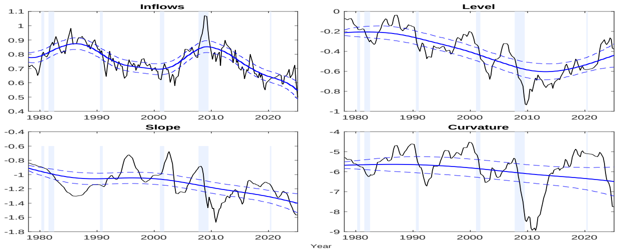

(b) HAWAII

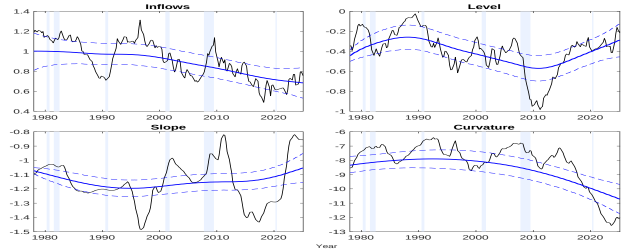

(c) IOWA

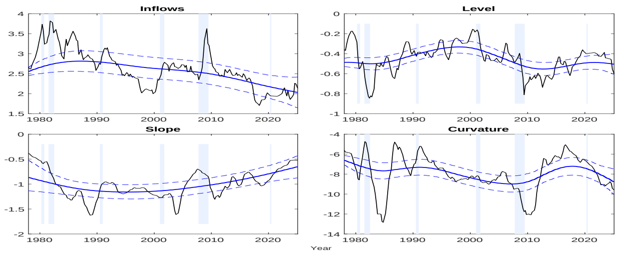

(d) IDAHO

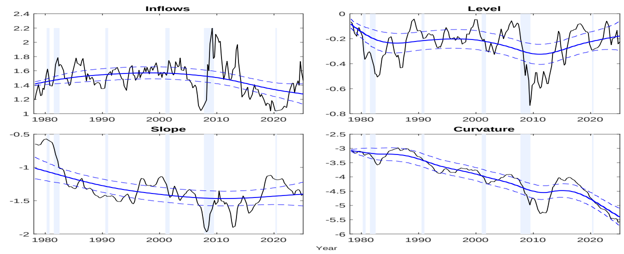

(e) ILLINOIS

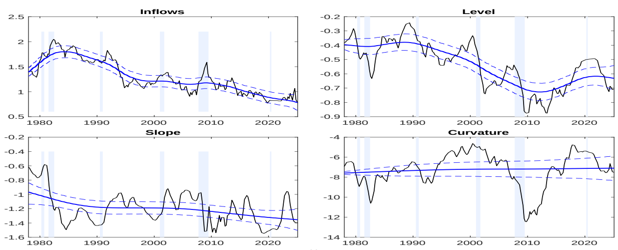

(f) INDIANA

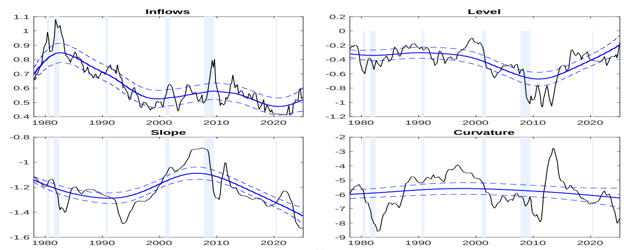

(g) KANSAS

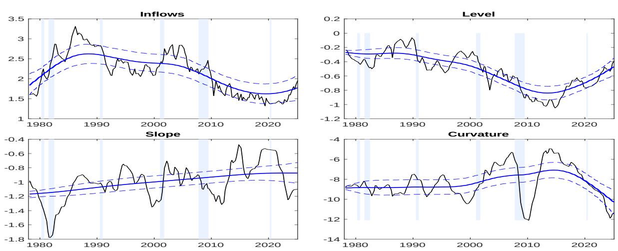

(h) KENTUCKY

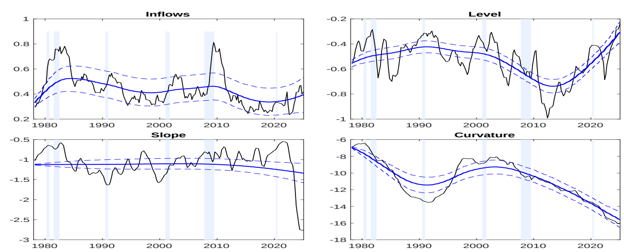

(i) LOUISIANA

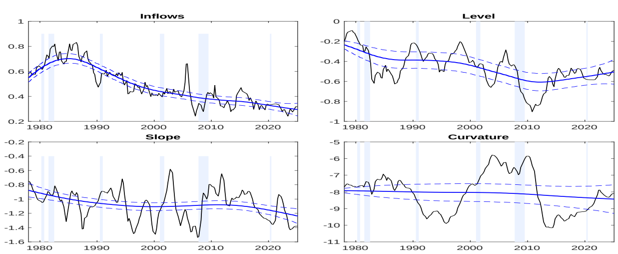

(j) MASSACHUSETTS

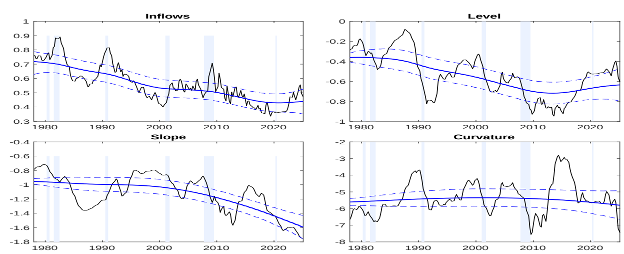

Notes to Figure B.2: For each state, the inflows are displayed in the upper left panel, β_0 in the upper right panel, β_1 in the lower left panel, β_2 in the lower right panel. The black lines are the factor estimates, the solid blue lines are the posterior means of trend estimates, and the dashed blue lines are the 68 percent posterior intervals. Shaded areas are NBER recessions. **Source:** Authors' calculation.

Figure B.3: FACTOR ESTIMATES (3)

(a) MARYLAND

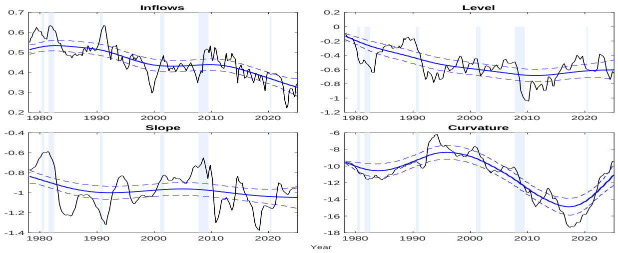

(b) MAINE

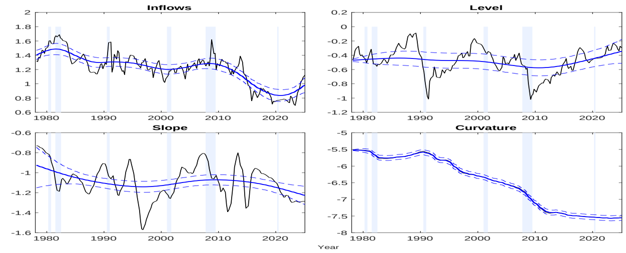

(c) MICHIGAN

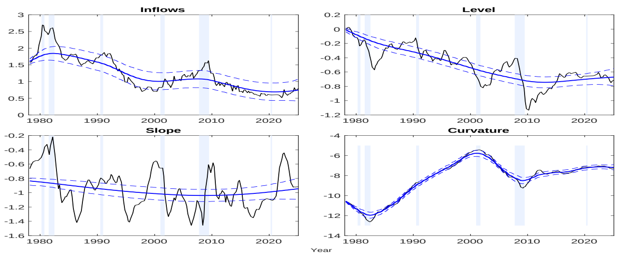

(d) MINNESOTA

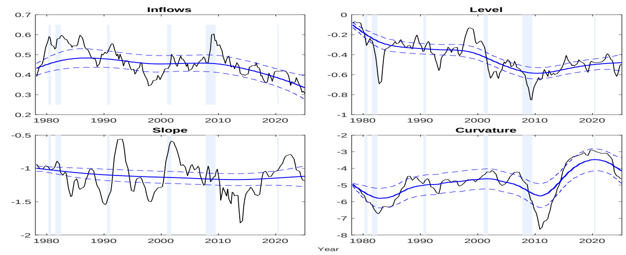

(e) MISSOURI

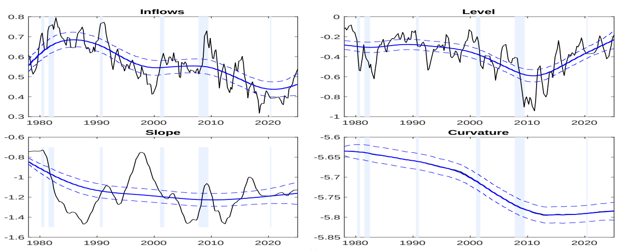

(f) MISSISSIPPI

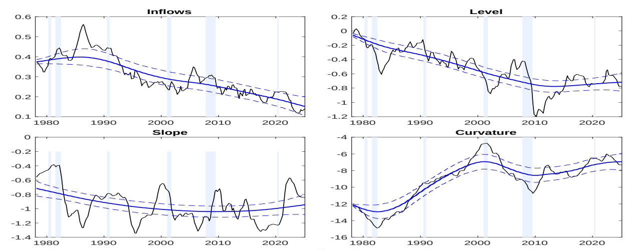

(g) MONTANA

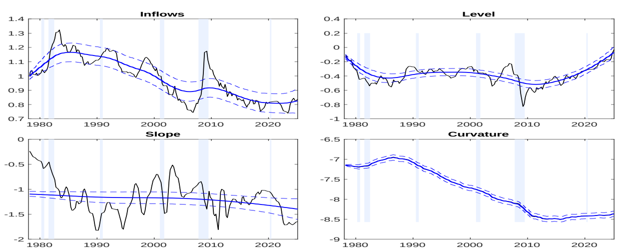

(h) NORTH CAROLINA

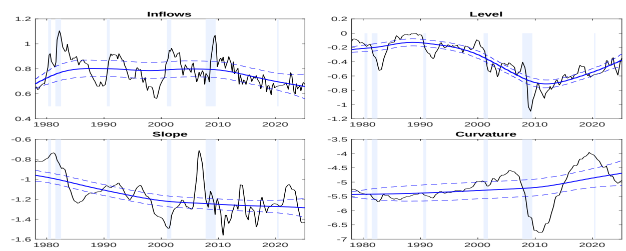

(i) NORTH DAKOTA

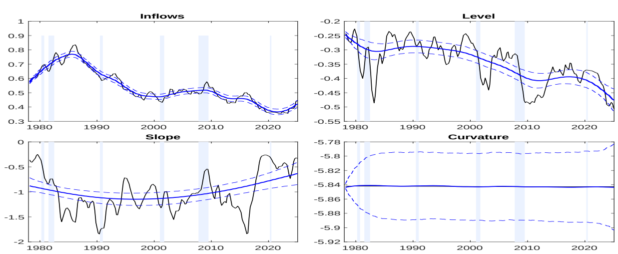

(j) NEBRASKA

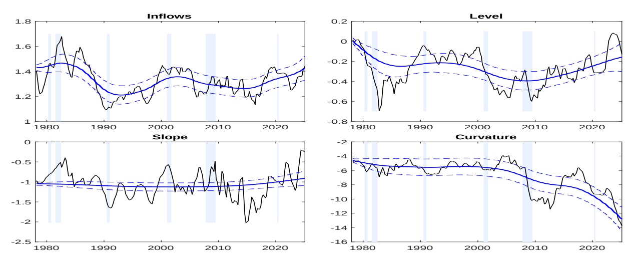

Notes to Figure B.3: For each state, the inflows are displayed in the upper left panel, β_0 in the upper right panel, β_1 in the lower left panel, β_2 in the lower right panel. The black lines are the factor estimates, the solid blue lines are the posterior means of trend estimates, and the dashed blue lines are the 68 percent posterior intervals. Shaded areas are NBER recessions. **Source:** Authors' calculation.

Figure B.4: FACTOR ESTIMATES (4)

(a) NEW HAMPSHIRE

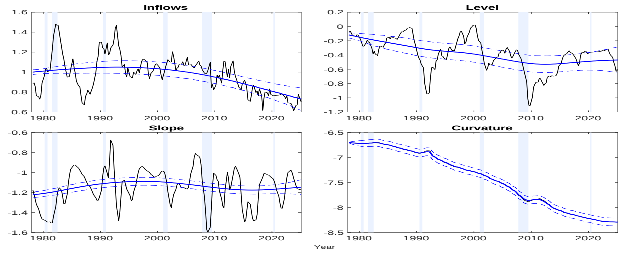

(b) NEW JERSEY

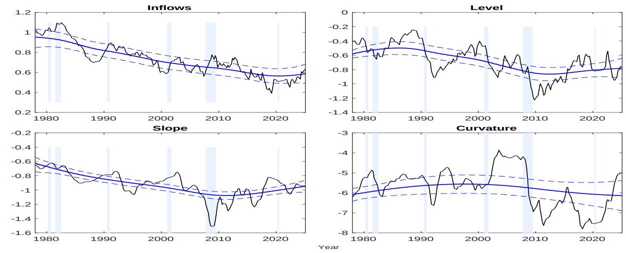

(c) NEW MEXICO

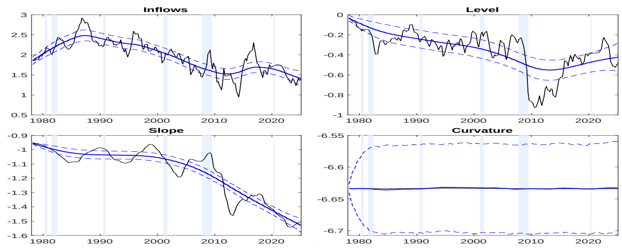

(d) NEVADA

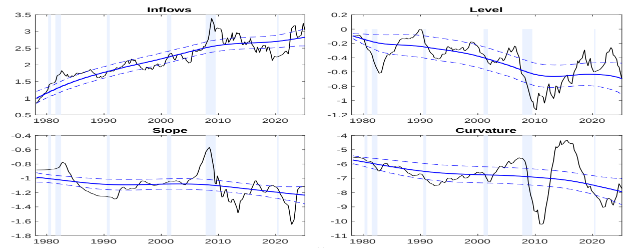

(e) NEW YORK

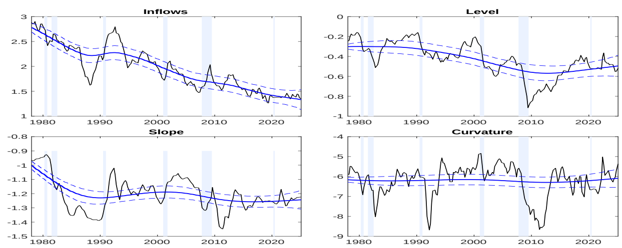

(f) OHIO

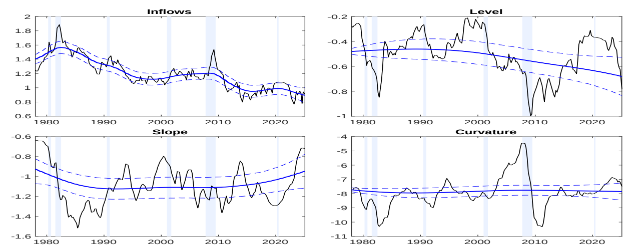

(g) OKLAHOMA

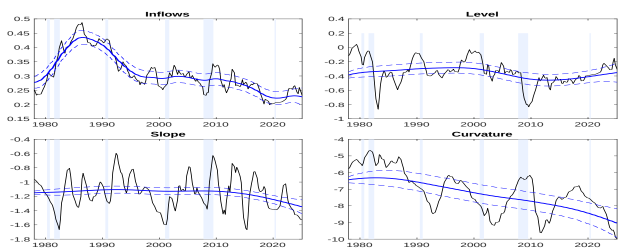

(h) OREGON

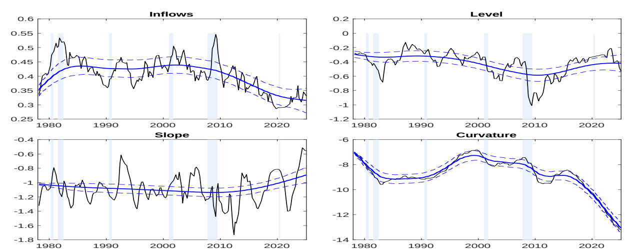

(i) PENNSYLVANIA

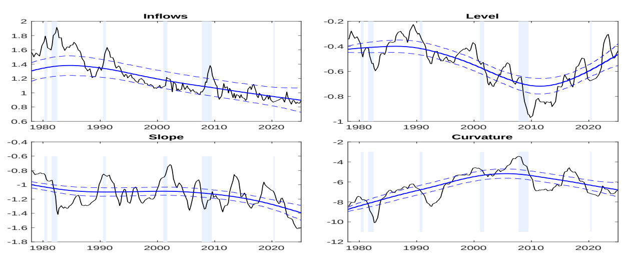

(j) RHODE ISLAND

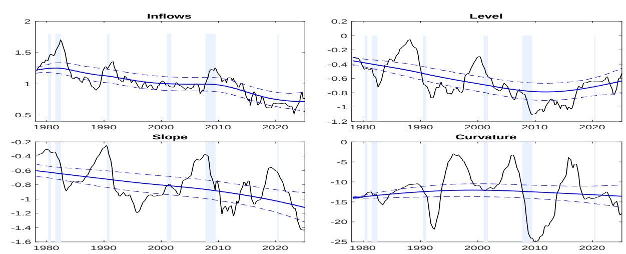

Notes to Figure B.4: For each state, the inflows are displayed in the upper left panel, β_0 in the upper right panel, β_1 in the lower left panel, β_2 in the lower right panel. The black lines are the factor estimates, the solid blue lines are the posterior means of trend estimates, and the dashed blue lines are the 68 percent posterior intervals. Shaded areas are NBER recessions. **Source:** Authors' calculation.

Figure B.5: FACTOR ESTIMATES (5)

(a) SOUTH CAROLINA

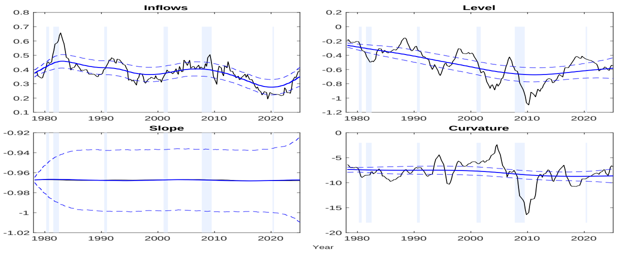

(b) SOUTH DAKOTA

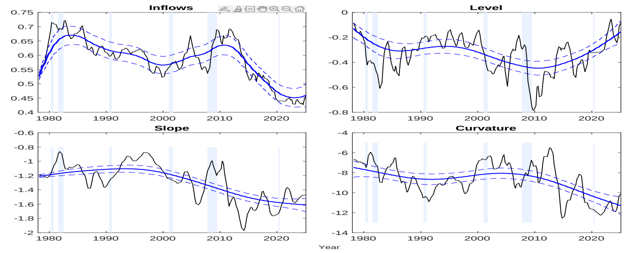

(c) TENNESSEE

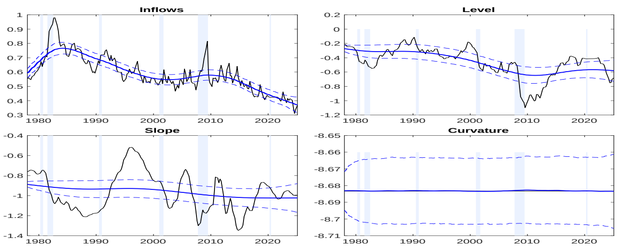

(d) TEXAS

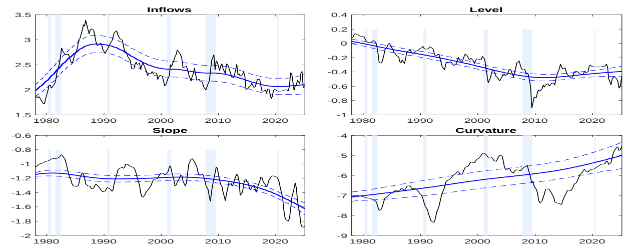

(e) UTAH

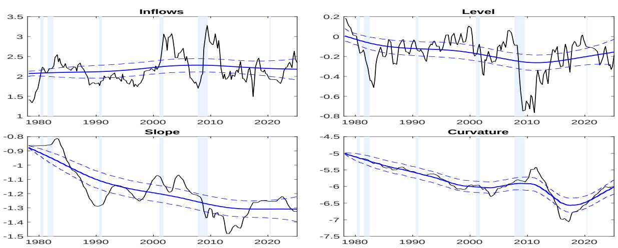

(f) VIRGINIA

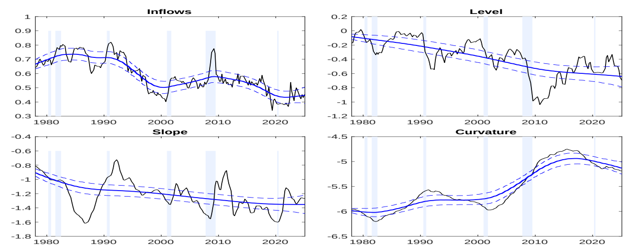

(g) VERMONT

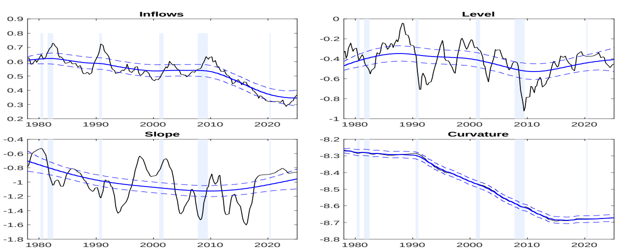

(h) WASHINGTON

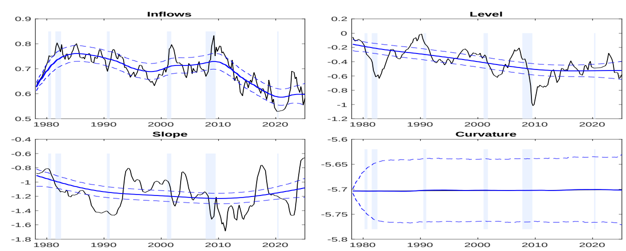

(i) WISCONSIN

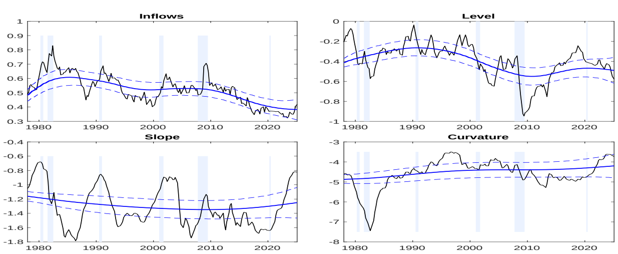

(j) WEST VIRGINIA

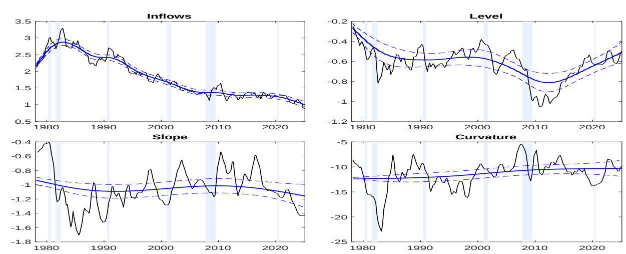

Notes to Figure B.5: For each state, the inflows are displayed in the upper left panel, β_0 in the upper right panel, β_1 in the lower left panel, β_2 in the lower right panel. The black lines are the factor estimates, the solid blue lines are the posterior means of trend estimates, and the dashed blue lines are the 68 percent posterior intervals. Shaded areas are NBER recessions. **Source:** Authors' calculation.

Figure B.6: FACTOR ESTIMATES (6)

(a) WYOMING

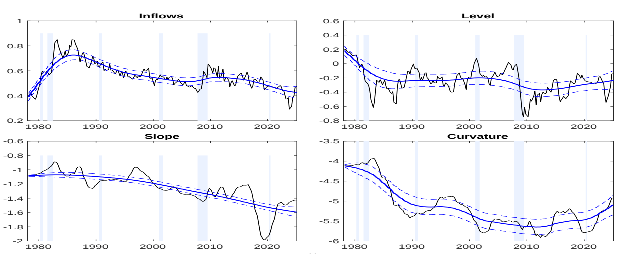

Notes to Figure B.6: For each state, the inflows are displayed in the upper left panel, β_0 in the upper right panel, β_1 in the lower left panel, β_2 in the lower right panel. The black lines are the factor estimates, the solid blue lines are the posterior means of trend estimates, and the dashed blue lines are the 68 percent posterior intervals. Shaded areas are NBER recessions. **Source:** Authors' calculation.